AEDC-TR-72-32

cy 4

CLUSTER FORMATION IN FREE-JET EXPANSIONS

A. B. Bailey, M. R. Busby, and R. Dawbarn
ARO, Inc.

April 1972

Approved for public release; distribution unlimited.

VON KÁRMÁN GAS DYNAMICS FACILITY
ARNOLD ENGINEERING DEVELOPMENT CENTER
AIR FORCE SYSTEMS COMMAND
ARNOLD AIR FORCE STATION, TENNESSEE

NOTICES

When U. S. Government drawings specifications, or other data are used for any purpose other than a definitely related Government procurement operation, the Government thereby incurs no responsibility nor any obligation whatsoever, and the fact that the Government may have formulated, furnished, or in any way supplied the said drawings, specifications, or other data, is not to be regarded by implication or otherwise, or in any manner licensing the holder or any other person or corporation, or conveying any rights or permission to manufacture, use, or sell any patented invention that may in any way be related thereto.

Qualified users may obtain copies of this report from the Defense Documentation Center.

References to named commercial products in this report are not to be considered in any sense as an endorsement of the product by the United States Air Force or the Government.

CLUSTER FORMATION IN FREE-JET EXPANSIONS

A. B. Bailey, M. R. Busby, and R. Dawbarn
ARO, Inc.

FOREWORD

The research reported herein was sponsored by Air Force Cambridge Research Laboratories (AFCRL), Air Force Systems Command (AFSC), under Program Element 62101F.

The results presented were obtained by ARO, Inc. (a subsidiary of Sverdrup & Parcel and Associates, Inc.), contract operator of the Arnold Engineering Development Center (AEDC), Air Force Systems Command (AFSC), Arnold Air Force Station, Tennessee, under Contrace F40600-72-C-0003. This work was conducted from April 1970 to April 1971, under ARO Project Numbers SW5009 and VW5140. The manuscript was submitted for publication on December 2, 1971.

The authors wish to thank D. Golomb and R. E. Good of AFCRL for their technical assistance during the present tests and J. Benek for work on Project No. SW5009 which is reported herein.

This technical report has been reviewed and is approved.

Eules L. Hively
Research and Development
Division
Directorate of Technology

R. O. Dietz
Acting Director
Directorate of Technology

ABSTRACT

An aerodynamic molecular beam has been used in an attempt to develop criteria for the determination of the onset of condensation in free-jet expansions of various gases. Measurements have been made of the total, monomer, dimer, trimer, etc., beam intensity and velocity distribution as a function of source pressure for the following conditions: (1) sonic orifice diameters of 0.0147, 0.0386, and 0.1245 cm, (2) 15-deg semiangle conical nozzle with a 0.111-cm-diam throat, (3) source temperatures from 185 to 430°K, (4) source pressures ranging from 5 to 10,000 torr, (5) argon, nitrogen, nitric oxide, sulphur dioxide, carbon dioxide, and krypton, and (6) 22°K skimmer and collimator surfaces. The total and monomer beam intensities increased almost linearly with increasing source pressure up to a particular pressure. At this point the two beam intensities ceased to vary at the same rate. The pressure at which this occurred varied systematically with source temperature, pressure, and diameter according to the relation pd/T^2 = constant. For argon and nitrogen flows through sonic orifices, pd/T^2 equaled 1.7×10^{-4} and 3.6×10^{-4} torr-cm $(°K)^{-2}$, respectively. It is suggested that the pressure at which this deviation occurred is indicative of condensation in the free-jet expansion downstream from the sonic orifices. The variation of beam velocity with source pressure was characterized by an approximately constant value up to a particular pressure at which point it started to increase. In general, the pressure at which this occurred was approximately the same as that at which the total and monomer beam intensities started to deviate. For argon and nitrogen and a fixed orifice size, p/T^2 = constant at the point of velocity increase, whereas $pd/T^2 \neq$ constant. The dimer, trimer, etc., beam intensity variations with source pressure were characterized by the occurrence of a well-defined intensity peak at a particular source pressure. At these peaks, for a fixed orifice size p/T^2 = constant and p/T^4 = constant for argon and nitrogen, respectively. An investigation of the monomer and dimer mole fractions in a condensed beam revealed that the absolute values of these fractions can be affected by skimmer interaction.

CONTENTS

APPENDIX
ILLUSTRATIONS

Figure

NOMENCLATURE

A	Nozzle exit area
A*	Nozzle throat area
a	Lateral acceleration of the cluster
C_p	Specific heat at constant pressure
D	Distance from cluster beam to extractor plate
D_C	Dimer beam intensity - cold skimmer
D_W	Dimer beam intensity - warm skimmer
d	Beam orifice diameter
F	Lateral force on an ionized cluster
I_c	Total beam intensity - cold skimmer
I_w	Total beam intensity - warm skimmer
Kn	Knudsen number
L	Flight length from chopper to detector
ℓ	Diameter of orifice in extractor plate
M_c	Monomer beam intensity - cold skimmer
M_T	Terminal Mach number
M_w	Monomer beam intensity - warm skimmer
m	Mass of a molecule
N	Number of molecules in a cluster
$\dot{N}$	Total beam flux
n	Multiple ionization
p	Stagnation pressure
p′	Impact pressure
p_B	Beam pressure
p_{Bg}	Chamber pressure
p_{GE}	Total beam intensity as measured by miniature GE gage
q	Electron charge
T	Stagnation temperature

t	Time
t_m	Time of maximum signal
V	Field voltage
V_m	Velocity of maximum signal
v	Cluster velocity
x	Axial distance from plane of orifice or nozzle throat
ρ	Gas density

SECTION I
INTRODUCTION

When a jet expands into a high vacuum environment, condensation may occur, leading to the formation of molecular clusters which can lead to significant changes in the flow properties. The effects of these flow field changes are of importance in (1) the use of jet releases in upper atmosphere rocket sounding work and (2) the effect of the forces generated by molecular clusters when those clusters impinge on a body immersed in a rocket plume.

In the past 20 years aerodynamic molecular beams have been used to study condensation phenomena in free-jet expansions. Many facilities of this type exist. References 1 and 2 give a representative description of their basic operational characteristics. Some of the many measurements that have been made in free-jet expansions are (1) total beam intensity, (2) individual mass beam intensity, (3) velocity of the individual masses, and (4) the determination of the size of the molecular clusters. Some characteristics of the above measurements have been suggested as indicators of varying degrees of condensation.

Bier and Hagena (Ref. 3) proposed that either the maximum or minimum of the total beam intensity versus source pressure (Fig. 1, Appendix) indicates the onset of condensation. Ruby (Ref. 1), Brown and Heald (Ref. 4), Govers et al. (Ref. 5), and Bossel (Ref. 6) have demonstrated that such maxima and minima were not necessarily associated with condensation but could be explained in terms of beam-skimmer interaction effects. Bier and Hagena recognized the existence of the skimmer interaction effect and employed the additional criterion that the beam velocity should also have maxima and minima at these pressures. As a result of their studies Bier and Hagena suggested that these extrema could be correlated in terms of the parameter pd.

Ruby, et al. (Refs. 1 and 2) and Golomb et al. (Ref. 7) made measurements of the dimer, trimer, tetramer, etc., beam intensities. The individual mass beam intensity measurements were characterized by a sharply defined peak. They found that the pressure at which this peak occurred could also be correlated in terms of pd.

As a result of some preliminary work in the present study, it was concluded that the pressure at which the dimer beam intensity peaked could be affected by (1) skimmer interaction, (2) source diameter and roughness, and (3) lack of control of source temperature.

The foregoing discussion has been concerned primarily with the determination of condensation as it occurs in free-jet expansions. Aerodynamicists have been interested in the onset of condensation in supersonic and hypersonic wind tunnel nozzles for the last 30 years. Several techniques have been developed to determine the onset of condensation in these flows. The technique that can most readily be applied to the study of free-jet expansions is the measurement of stream impact pressure. Many investigations have been made of wind tunnel flows (Refs. 8 and 9), and some condensation criteria have been established.

In the present report, impact pressure measurements that were made in the expanding flow from a conical nozzle are compared with mass spectrometer measurements made in the same flow. This will enable a direct comparison of the macroscopic and molecular properties of the flow. The basic purpose of this investigation is to determine the parameters which affect the onset of condensation in the expanding flow of various gases.

SECTION II
APPARATUS

2.1 AERODYNAMIC MOLECULAR BEAM SYSTEM

The AEDC Aerodynamic Molecular Beam System (Fig. 2) is a 3-1/2-ft-diam, 6-1/2-ft-long stainless steel chamber divided into three sections by two removable bulkheads. Vacuum conditions are produced by oil diffusion pumps and 77°K liquid-nitrogen and 22°K gaseous-helium cryoliners. This pumping system produces base pressures of 10^{-8} torr and maintains pressures of 1×10^{-4}, 1×10^{-7}, and 3×10^{-8} torr in the source, collimation, and test chambers, respectively, during testing.

For Ruby, et al. (Ref. 2) the molecular beam was produced using a 2.54-cm 22°K skimmer and a 0.4-cm collimating orifice. A more detailed description of this system is contained in Refs. 1 and 2.

For the present series of tests some modifications were made to the system to give a greater degree of operational flexibility. A schematic of the modified molecular beam system is shown in Fig. 3.

2.2 BEAM SOURCE

A schematic of the molecular beam source is shown in Fig. 4. The test gas flows through the center tube which vents into a settling chamber

prior to passing through the orifice under test. The heating (or cooling) fluid passes through two tubes concentric with the gas supply tube. The source is approximately 4 ft long, which, together with the settling chamber, should give the test gas sufficient time to accommodate to the temperature of the circulating fluid. The temperature of the source gas is measured with a copper-constantan thermocouple located at the upstream end of the settling chamber. Temperatures in the range 180 to 430°K are achieved as follows:

1. For temperatures from 180 to 250°K, liquid nitrogen is circulated through a reservoir containing Freon MF®. The nitrogen flow rate is adjusted such that the desired temperature is achieved in the Freon which is then pumped through the source.
2. For 280 to 300°K, water is pumped through the source.
3. For 350 to 430°K, gaseous nitrogen is passed through a resistance-heated stainless steel tube and then through the source.

The source can be removed without bringing the test chamber to atmospheric pressure. It is retracted until the front of the source clears the gate valve which is then closed and the source removed. When the source is replaced the volume of gas trapped between the gate valve and the O-ring seal is pumped out with an auxiliary vacuum pump before opening the gate valve. The integrity of the O-ring seal is preserved over the temperature range of these tests by pumping on the annular volume that surrounds the heating (or cooling) fluid tubes.

The thin wall stainless steel bellows (Fig. 3) permits the source to be moved in the vertical and horizontal planes. The source is adjusted until the beam intensity as measured by the miniature General Electric (GE) ionization gage is a maximum. At this point it is assumed that the source is correctly aligned with the skimmer and collimator.

The orifices were made in 0.005-cm stainless steel shim stock silver-soldered to the orifice insert (Fig. 4). Various diameter orifices were then cut in the stainless steel using an Elox® process. Examination of these orifices showed that they were not smooth and circular. A honing and polishing procedure has been developed to improve the quality of orifices formed in this manner. Photographs of the orifices before and after polishing are shown in Figs. 5a through d. These photographs indicate that after polishing the orifices are reasonably smooth and circular. The three orifices used in the present series of tests had diameters of 0.0147, 0.0386, and 0.1245 cm.

In addition to these sonic orifices a 15-deg semiangle conical nozzle having a throat diameter of 0.111 cm and an exit to throat area ratio of 36.3 was used.

The cryogenically cooled skimmer used by Ruby, et al. (Ref. 2) significantly reduced the skimmer interaction effect, and the resulting beam intensity versus pressure variation was closer to the ideal intensity variation shown in Fig. 1. At the higher source pressures there was still a break in the intensity pressure variation which was thought to have resulted from a scattering problem at the warm conical collimator. The warm conical collimator was replaced by a 14.5-cm-diam, 22°K-cooled collimator with a 0.4-cm orifice (Fig. 6).

In order to reduce the gas load in the collimation section of the chamber, the 2.54-cm-diam skimmer used by Ruby, et al. (Ref. 1) was modified such that the orifice was reduced to 1.27-cm diameter and had the same form as that of the collimator shown in Fig. 6.

2.3 DETECTOR SYSTEMS

2.3.1 Total Beam Intensity Detector System

The total incident beam intensity was measured with a miniature ionization gage positioned on the beam centerline. For these measurements the normal 2.54-cm-diam opening of this gage was reduced to 0.6 cm as shown in Fig. 7. This reduction in opening served to (1) increase the sensitivity of the gage to directed gas flows and (2) ensure that molecular clusters are broken up by wall collisions and that a gage response is obtained before the molecules escape.

2.3.2 Modulated Beam Detector

The modulated beam detection system consists of (1) a mechanical beam chopper, (2) a quadrupole mass spectrometer (2 to 600 amu), and (3) a lock-in (narrow bandpass) amplifier. A schematic of the system is shown in Fig. 8, and a detailed description is given in Ref. 10.

The collimated molecular beam is chopped into pulses by a slotted rotating wheel. The wheel is driven by a small two-phase vacuum-rated synchronous motor at approximately 75 Hz. A photoetching technique was used to make 20 equally spaced 1.9- by 0.16-cm slots in the 0.005-cm-thick stainless steel wheel. The beam to be chopped by the wheel is defined by a 0.16- by 0.16-cm orifice in a 0.005-cm-thick stainless steel plate located upstream of the wheel. After the beam has

been chopped, the pulses fly through the ionization region of the mass spectrometer. An ionized sample of the beam is deflected into the quadrupole section which is tuned to a particular mass number. The resulting ion current is amplified by an electron multiplier which sends a pulsed signal to the lock-in amplifier, which acts as a bandpass amplifier centered on the chopper frequency. A light and photocell detector, mounted at the chopper wheel, provide the chopping frequency to the amplifier and keep it synchronized with the actual molecular beam modulation frequency. The lock-in amplifier increases the signal-to-noise ratio by amplifying only those signals having the proper frequency and phase with respect to the reference signal from the photocell. This amplified signal, recorded on a voltmeter, is a measure of the intensity of the mass number under investigation.

2.3.3 Velocity Distribution Detection System

A detailed description of this system is contained in Ref. 11. The components of the system are shown schematically in Fig. 9. After the collimated beam passes through the chopper wheel, the molecules spread according to their velocity distribution. The beam then passes through the ionizing section of the mass spectrometer. The spectrometer operates as a flow density detector and measures the local particle density as a function of time. The local density in the ion source is directly proportional to the arrival rate of the molecules and inversely proportional to their velocity.

The quadrupole section is tuned to the mass number of interest, and the resulting ion current is amplified by the electron multiplier. A Field Effect Transistor (FET) emitter follower circuit is mounted directly on the quadrupole tube inside the vacuum chamber. This FET emitter follower acts as a buffer or impedance-matching device between the required high amplifier input impedance at the electron multiplier output and the low impedance required for the coaxial cables which lead out of the chamber.

A time reference for the spectrometer output is provided by the light-photocell arrangement shown in Fig. 9. The mass spectrometer signal represents the molecular arrival rate, which is time dependent, referenced to a particular "start time" plus the random noise of the background gas. The "start time" is the time the chopper shutter opens. The signal is then processed in the waveform eductor which is basically a device for extracting a weak signal from a high noise background. In the present application the resulting output from the waveform eductor is recorded by photographing the oscilloscope trace.

As a matter of practical interest the two systems described in this and the preceding section differ only in the electronics after the ionized beam has passed through the electron multiplier section. These circuit changes are made outside the test chamber. This has the advantage that it is no longer necessary (as it has been to this time, cf., Ref. 2) to bring the test chamber to atmospheric pressure to change from the Modulated Beam Detector mode to the Velocity Distribution mode.

2.3.4 Impact Pressure Measurement

As noted in Section I, one of the conventional methods for determining the onset of condensation in wind-tunnel flows has been the measurement of impact pressure as a function of source temperature at a fixed source pressure. In the present series of tests an impact probe made from 0.08-cm-diam stainless steel tube was attached to a push-pull feedthrough in the top of the chamber. This permitted the probe to be located in the orifice (or nozzle) flow field. The source-probe distance could be varied by moving the source axially. A 300-torr absolute MKS Baratron® transducer was used to measure impact pressure.

2.3.5 Electrostatic and Magnetic Deflection Technique for Cluster Size Determination

This technique has been used by Hagena et al. (Ref. 12) and is described by Bauchert and Hagena (Ref. 13). A schematic of the system used in the present investigation is shown in Fig. 10. The molecular beam is modulated by the rotating chopper wheel, and the resulting pulsed beam is then ionized in the mass spectrometer head. The resulting ions then pass through the magnetic or electric field to the electron multiplier provided their kinetic energy per unit charge is large enough to overcome either of these deflection fields. From a knowledge of the field strength and the velocity of the molecules it is possible to assign a mass to the molecules which give rise to the electron multiplier signal.

SECTION III
EXPERIMENTAL PROCEDURES

The basic experimental procedures followed in this investigation were similar to those described in detail in Refs. 1 and 2. Brief mention will be made of some of the modifications that were made in these procedures.

Basically, five sets of measurements were made:

1. beam intensity measurements of monomer, dimer, trimer, etc., cluster ions
2. incident beam velocity distribution
3. total beam intensity
4. impact pressure
5. electrostatic and magnetic beam deflection.

These measurements were made at the following test conditions: (1) source pressures varying from 5 to 10,000 torr, (2) source temperatures ranging from 185 to 430°K, (3) sonic orifice diameters of 0.0147, 0.0386, and 0.1245 cm, (4) a 15-deg semiangle conical nozzle having a 0.111-cm-diam throat and an exit-to-throat area ratio of 36.3, and (5) argon, nitrogen, nitric oxide, sulphur dioxide, carbon dioxide, and krypton gases.

For some of the test conditions the upper source pressure was determined by the pumping capacity in the collimation and test chambers. In general, this limit was reached for the largest orifice and the nozzle. Another limit was set by the fact that the gas addition system was limited to pressures of 10,000 torr. This was a limiting operational characteristic for the smallest orifice.

The nondimensionalized source-to-skimmer distances for the 0.0147-, 0.0386-, 0.1245-, and 0.111-cm-diam sources were approximately 1500, 590, and 630 source diameters, respectively. With the exception of the smaller orifice these distances were consistent with those used by Ruby et al. (Ref. 2). The rationale for the present investigation was not to establish the optimum nozzle skimmer separation distance for each orifice but rather to vary the pressure, temperature, and source gas at a fixed source-to-skimmer distance.

For the initial series of tests, the source pressures were measured with aneroid-type dial gages; i. e., (1) for pressures from 5 to 800 torr, a Wallace and Tiernan gage was used which has a quoted accuracy of ±1 torr; (2) for the range from 500 to 5000 torr, a Kollsman gage with a quoted accuracy of ±10 torr was used; and (3) for the range from 5000 to 10,000 torr, a dial gage having an accuracy of ±500 torr was used. In the final phases of this study, another gas addition system was installed where the source pressure was measured with two Consolidated Electrodynamics Corporation Electromanometers®. The range of these instruments is (1) 5 to 800 torr with an accuracy of ±1 torr and (2) 800 to

8000 torr with an accuracy of ±8 torr. One of the significant advantages of these pressure transducers as opposed to the aneroid gages is their shorter response time to pressure changes and a consequent reduction in the time required to change source flow conditions.

Individual mass beam intensity measurements were obtained with the modulated beam detection system. In measurements of this type the mass spectrometer was tuned to the mass number of interest and the output voltage was monitored as the source pressure was incrementally increased. All external spectrometer settings were held constant during these runs. Normally, the extractor, focus, and ion energy voltages are held constant at 10, 135, and 22 v, respectively, and the emission current and electron energy are held at 0.2 ma and 90 v, respectively. The electron multiplier voltage was varied from 1500 to 3000 v, depending upon the strength of the signal; i. e., for the low signal levels typically encountered when making measurements of the dimer, trimer, tetramer, etc., beam intensity, the electron multiplier amplification was increased by raising the voltage to 3000 v.

The effects of varying the emission current, electron energy, and high voltage levels upon the mass spectrometer output are summarized in Figs. 11a through d.

In a number of the tests made during the present study the mass spectrometer was modified such that it was able to measure the integrated signal of all those clusters having a mass in the range from 2 to 600. This total beam intensity (i. e., 2 to 600 amu) would be compared with the total beam intensity measurement made with the GE gage.

For measurements of incident beam velocity, the mass spectrometer was tuned to the mass number of interest and the signal was then correctly phased. In the present study it was decided that the velocity of interest was that which occurred at the time of maximum output signal. To calculate this velocity it is necessary to know (1) the flight distance and (2) the total flight time. Throughout the present series of tests the flight distance was held at 25.75 cm. The total time of flight is comprised of a consideration of (1) the shutter opening time, which can be calculated from a knowledge of the chopper diameter and the slot width and (2) the time between the photocell output and the output of the first waveform eductor module. This time interval was measured to an accuracy of 1.0 μsec with a 10-MHz Beckman counter, (3) the total sweep time of the waveform eductor also measured to an accuracy of 1 μsec with a Beckman counter, and (4) the flight time in the mass spectrometer itself (this has been derived for various mass numbers in earlier experiments, e. g., Ref. 2).

SECTION IV
RESULTS AND DISCUSSION

4.1 TOTAL BEAM INTENSITY MEASUREMENTS

It was noted earlier that prior to the use of cryogenically cooled skimmers the total beam intensity varied in the manner shown in Fig. 1. Benek (Ref. 14) presents some experimental results which demonstrate the effect of various types of skimmers upon the total beam intensity (Fig. 12). Benek shows from theoretical considerations that the beam intensity can be affected by the molecules reflected by the skimmer. Kogan (Ref. 15, p. 493) indicates that the ideal skimmer would be one which would absorb all the impinging molecules, i. e., a suitable cryogenic surface.

In the present investigation the skimmer and collimator were both 22°K pumping surfaces. These temperatures were sufficiently low to pump the gases being used in the present investigation. In particular, it was assumed that room temperature carbon dioxide would be totally cryopumped by the surfaces. If this true, why wouldn't CO_2 follow the curve longer?

The variation of the total beam intensity with source pressure for carbon dioxide is shown in Fig. 13. For source pressures of less than 150 torr, the total beam intensity variation with source pressure is in agreement with the ideal variation shown in Fig. 1. For source pressures greater than 150 torr, the total beam intensity increases at a lesser rate than the ideal. For source pressures greater than 2000 torr, it appears to resume the ideal rate of increase. The effects of various degrees of skimmer interaction are demonstrated by comparing the present data with those of Brown and Heald (Ref. 4) in Fig. 13. It is of interest to note that there is a marked similarity in the form of the argon and carbon dioxide total beam intensity measurements shown in Figs. 12 and 13.

Total beam intensity measurements for carbon dioxide, argon, and nitrogen are compared in Fig. 14. A consideration of these data indicates that for each of these gases there is a source pressure above which the total beam intensity ceases to increase at the ideal rate.

If this break in the total beam intensity curve resulted from a breakdown in the pumping of the cryogenically cooled skimmer and/or collimator, it would be expected to do so at a particular heat load or gas flow rate. Because of the similarity in the density of these gases, a similar gas flow rate would correspond to approximately the same

source pressure for each gas (ignoring for the moment the differences in the ratio of specific heats). Because the break in the total beam intensity occurs at widely different source pressures for the different gases, it is unlikely that there was a breakdown in the pumping of the skimmer and/or collimator surfaces. Thus, for these three gases it seems reasonable to suggest that the break in the total beam intensity resulted from a change in the flow characteristics in the free-jet expansion.

The total beam intensity as measured by the miniature GE gage is a measure of the free-stream impact pressure which is related to ρv^2. For the continuum flow regime, it has been shown in Refs. 8, 9, and 16 that ρv^2 decreases with the onset of condensation. The similarity between these two events suggests that the total beam intensity decrease registered by the GE gage is also indicative of condensation.

The present data were analyzed to determine the effect of source temperature and diameter upon the pressure at which the break in the total beam intensity occurred. Some examples of the total and individual mass beam intensities measurements upon which this analysis was based are contained in Figs. 15a through i. The total beam intensity measurements for argon are summarized in Figs. 16a through c. In these curves (Fig. 16) the linear portions of the total beam intensity curves were arbitrarily matched in order to illustrate clearly the effect of source temperature upon the pressure at which the break in the total beam intensity occurred. These data are summarized in Fig. 17, where the product pd is plotted as a function of source temperature. A consideration of these data indicates that $pd/T^2 = 1.7 \times 10^{-4}$ torr cm $(°K)^{-2}$ for argon in the range of conditions covered.

4.2 COMPARISON OF TOTAL AND MONOMER BEAM INTENSITY MEASUREMENTS

Prior to condensation, the molecular beam is essentially a monomer beam. With the onset of condensation, clusters are formed from these monomers and the monomer concentration decreases. Thus, an alternative method of determining the onset of condensation would be to determine where the monomer and total beam intensity variations first start to deviate from one another. This should be a more desirable method for determining the onset of condensation since for some conditions (Fig. 15f) it was difficult to determine accurately where the break in the total beam intensity occurred.

The monomer and total beam intensity measurements were arbitrarily matched over the pressure range before the break in the total

beam intensity curve. The results of this matching for argon and nitrogen are shown in Figs. 18a through j. The pressure at which the total and monomer beam intensities first deviated is reasonably well defined. This pressure is plotted as a function of source temperature and diameter for argon and nitrogen in Figs. 19a and b. A consideration of these data indicates that (1) for sonic orifices, $pd/T^2 = 1.7 \times 10^{-4}$ and 3.6×10^{-4} torr cm $(°K)^{-2}$ for argon and nitrogen, respectively, and (2) for conical nozzles, $pd/T^2 = 8 \times 10^{-5}$ and 1.8×10^{-4} for argon and nitrogen, respectively. It is of interest to note that for argon flow through a sonic orifice the value of pd/T^2 is the same when based on the break in the total beam intensity variation and on the deviation of the monomer and total beam intensity variations. This also may be true of the other gases but the data are not as complete.

Daum and Gyarmathy (Ref. 8) have shown experimentally that the onset of condensation in nozzle flows is dependent upon the rate of expansion of the flow. This results from the fact that a finite time is required for the nucleation and growth process to take place. Data have been obtained (Ref. 8) which demonstrate that condensation occurs at lower degrees of supersaturation in contoured nozzles than in conical nozzles. The present data demonstrate these same characteristics in that condensation occurred at a lower source pressure for the conical nozzle than for the same size sonic orifice.

However, changes in sonic orifice diameter result in different rates of flow expansion which in turn should result in condensation onset at different values of the product pd. The present data for sonic orifices do not indicate any effect of orifice diameter (i. e., changes in rate of flow expansion) upon the product pd. This may be indicative of the fact that for the range of orifice sizes investigated herein condensation is not a strong function of orifice size. Therefore, caution should be exercised in any attempt to use the values of pd/T^2 to predict the onset of condensation at conditions that are significantly different from the present experimental test conditions.

As was discussed earlier, skimmer interaction can have a marked effect upon the form of the total beam intensity variation with source pressure. Similar effects were observed for the monomer beam intensity variation with source pressure. A comparison of some warm (Figs. 18f and g) and cold skimmer (Figs. 18c and d) tests indicates that the total and monomer beam intensities first deviated at somewhat higher pressure for the warm skimmer than with the cold skimmer. This may simply be indicative of the fact that the onset of this deviation was more difficult to define for the warm skimmer than it was for the cold skimmer.

4.3 VELOCITY CORRESPONDING TO THE TIME OF MAXIMUM SIGNAL

The energy equation for a perfect gas expanded to very low static temperatures is closely approximated by

$$C_p T = 1/2\ m\ V_m^2$$

Thermal speed is usually $|\vec{C}| = |\vec{c} - \vec{c}_0|$, cf p 319 of Vincenti & Kruger

Values of the thermal speed (V_m) for nitrogen and argon are given as a function of source temperature in Fig. 20.

It has been stated in Ref. 2 that the velocity corresponding to the time of maximum signal is an accurately determined experimental flow field property, and is defined as

$$V_m = \frac{L}{t_m}$$

where L is the flight distance and t_m is the time to the maximum signal. Furthermore, it has been assumed (Ref. 2) that this velocity is approximately equal to the mean thermal speed of the gas.

Figures 21a and b show some typical oscilloscope traces from which argon monomer and dimer velocity measurements have been derived. To illustrate the effects of source pressure on beam velocity and beam static pressure, these traces have been combined in Fig. 22. With increasing source pressure (1) the time to the maximum signal decreases, indicating an increase in the velocity, and (2) the width of the velocity distribution decreases, indicating a decrease in static temperature. (This is a direct result of the increase in the terminal Mach number that occurs with increasing pressure).

The velocities for argon and nitrogen are presented as a function of source pressure for various orifice diameters and gas temperatures in Figs. 23a through o. Figure 23a demonstrates the characteristic variation of velocity with source pressure. The bulk of the data shown in the subsequent figures exhibit these characteristics. For some cases this characteristic form (i. e., Fig. 23a) is not clearly defined (Figs. 23ℓ and p). In one case, Fig. 23q, a velocity variation with pressure is shown which appears to be inconsistent with the other data, Figs. 23a through p. At low pressures the gas velocity is constant and approximately equal to the thermal velocity determined from the thermocouple measured source temperature as shown in Fig. 20. A pressure is reached where the velocity begins to increase with further increases in source pressure. In some instances (Fig. 23f) at the highest pressures tested the velocity appears to achieve a constant value at a higher level than the thermal velocity.

A factor of some importance in determining that this characteristic velocity variation represents a change in the flow properties of the expanding gas is whether the temperature of the gas upstream of the orifice was constant. As noted earlier, the temperature of the inlet gas was monitored with a copper-constantan thermocouple located just upstream of the settling chamber. This thermocouple was monitored continuously, and in any one test run its temperature did not vary significantly (i. e., ±5°K). On the basis of these measurements, it can be assumed that the source temperature was held constant and that the velocity variations do represent changes that occur in the expanding flow. This is confirmed to some extent by the data shown in Fig. 23f. For this test the gas was held close to room temperature by circulating water through the source. The measured source temperature of 290°K (62°F) is a reasonable value for the temperature of the supply water. The room temperature in the test area was approximately 296°K (72°F). It can be seen from Fig. 23f and Fig. 20 that the velocity corresponds to a gas temperature of approximately 330°K (115°F) at 10,000 torr. Since there are no heat sources close to the molecular beam source that could give rise to temperature differences of this magnitude it has been concluded that (1) the constant temperature measured by the thermocouple does represent a constant temperature in the supply gas and (2) the increase in gas velocity represents a change in the characteristics of the expanding flow.

At room temperature, Ruby et al. (Ref. 2, Fig. 23d) have also obtained a velocity characteristic which indicates velocity changes of the type shown in Fig. 23f. However, the form of Ruby's velocity distributions (Ref. 2) at 100 and 600°K (Figs. 23c and g) was such that it was felt that some of the observed changes in gas velocity could have resulted from fluctuations in the source gas temperature. The 100°K data (Fig. 23e) indicate a considerably larger velocity increase than the room temperature data. The 600°K data indicate a decrease in velocity rather than an increase.

The pressure at which the velocity starts to increase is not sharply defined in Figs. 23a through q. To determine the pressure at which the velocity starts to increase, straight lines have been drawn through the data before and after the break. Where these two lines intersect has been taken to be representative of the pressure at which changes in the flow field properties occur.

These data are summarized in Fig. 24 where pd is plotted as a function of source temperature. It is apparent that p/T^2 is a constant, but pd/T^2 is no longer a constant. In general, the pressure at which the velocity increases is higher than that at which the monomer and

total beam intensity first deviate. Thus, while both events may be related to condensation it is not immediately obvious that they are directly related to one another.

It can be seen from Figs. 23d and q that the velocity appears to be affected by the type of skimmer used, i. e., warm conical skimmer or cryogenically cooled skimmer. The effect of the type of skimmer on the apparent beam velocity will be discussed in Section 4.8.

4.4 CLUSTER INTENSITY DATA

The dependence of cluster intensity upon source temperature, pressure, diameter, and shape is shown in Figs. 15a through h. It is apparent from a consideration of these data that there is a well-defined peak in the cluster beam intensity. Ruby (Ref. 1), Ruby et al. (Ref. 2), and Golomb et al. (Ref. 7), respectively, have suggested that the pressure at which the clusters peak is a function of the source diameter and temperature.

As noted in Section I it was considered that the pressure at which the peak occurs could be affected by (1) orifice roughness, (2) skimmer interaction, and (3) poor control of source temperature.

The degree of orifice roughness that can occur prior to polishing and honing is shown in Figs. 5a through d. Cluster beam intensity measurements have been made for both a smooth and a rough orifice in the present investigation. A comparison of these measurements is made in Fig. 25. It can be seen from these data that the peak in the dimer beam intensity is not significantly affected by the shape and roughness of the orifice. Also, the break in the total beam intensity is similarly unaffected by the orifice quality.

The effect of skimmer interaction upon the pressure at which the dimer beam intensity peaks is shown in Fig. 26. The net effect of this interaction is to shift the apparent peak to higher pressure than that for the no-interaction condition.

No direct experiments have been performed to evaluate the effect of poor source temperature control on cluster beam intensity measurements. However, the present investigation defines the effect of source temperature upon the location of the cluster beam intensity peak. Therefore, if the degree of uncertainty in the source temperature is known then the degree of uncertainty in the pressure at which the cluster beam intensity peaks can be determined.

The results of the present investigation for argon and nitrogen are summarized in Figs. 27a and b. A consideration of these data indicates that (1) for argon and nitrogen the pressure at which the cluster beam intensity peaks varies as T^2 and T^4, respectively, (2) for both these gases the term pd is not a constant at a fixed-source temperature.

In general, the peak in the dimer beam intensity is so well defined (Fig. 15b) that the pressure at which it occurs can be determined with a small degree of uncertainty. However, in the course of this investigation several dimer beam intensity curves had the form of those shown in Figs. 15a and h. It is apparent that for these cases there is more than one peak in the dimer beam intensity variation with pressure.

It was thought that a possible reason for these anomalous dimer beam intensity variations was that the mass spectrometer was misaligned. This possibility was considered because some of the velocity distribution data indicated that there might be some beam scattering in the mass spectrometer head. Normally, the velocity distribution traces were symmetrical (Fig. 21). However, in a few instances, traces of the type shown in Fig. 28 were obtained. It is suggested that the increase in the number of slower moving molecules indicated by these traces results from the molecular beam striking the mass spectrometer head.

The mass spectrometer was deliberately misaligned to produce velocity distributions of the type shown in Fig. 28. Measurements of total and individual mass beam intensity were then made (Fig. 15g). The mass spectrometer was then correctly aligned and similar measurements were made (Fig. 15f). It can be seen from these two sets of data that the effect of mass spectrometer misalignment is to modify the dimer beam intensity to such an extent that it is no longer possible to identify where the peak occurs in the dimer beam intensity. However, the form of the trimer, tetramer, beam intensities, although changed by mass spectrometer misalignment, still permits the clear definition of their peak location. The peaks observed with these higher number clusters occur at the same pressure both with and without mass spectrometer misalignment, and do not differ significantly from the pressure observed for the peak in the dimer beam intensity with a correctly aligned mass spectrometer. Therefore, the peak in cluster beam intensity has been defined by the peak in the trimer and tetramer distributions whenever there is a distortion in the dimer variation.

The two sets of data contained in Figs. 15f and g were obtained over such a small time interval that they can be compared absolutely. This comparison is made in Fig. 29. For pressures less than 100 torr,

the monomer beam intensity obtained with the misaligned mass spectrometer was 40 percent of that obtained with the correctly aligned mass spectrometer. For pressures greater than 600 torr, the monomer beam intensity obtained with the misaligned mass spectrometer exceeded that obtained with the correctly aligned mass spectrometer. This implies that a source of monomers has developed in order for this increase to occur. If it is assumed that for pressures greater than 100 torr the molecular beam consists of large molecular clusters, such clusters could be the source of monomers after they strike the mass-spectrometer head (when the mass spectrometer is misaligned). When this monomer beam intensity is matched to the total beam intensity, Fig. 29, it can be seen that the form of these two curves is in relatively good agreement. This suggests that after impact the large clusters break up into an almost wholly monomer beam.

In order to check on the validity of this suggestion, the following experiment was made with a carbon dioxide beam. Total and monomer beam intensity measurements for a 290°K carbon dioxide molecular beam were made (Fig. 30). As can be seen, the monomer and total beam intensity begin to deviate at pressures of approximately 150 torr. A flat, aluminum plate was mounted at an angle of 20 deg to the beam and the monomer beam intensity reflected normal to the plate was measured as a function of source pressure. It can be seen that the form of this monomer beam intensity variation is in good agreement with that of the total beam intensity. The significance of this result is that when the total cluster beam inpinges on a surface it breaks up into an essentially monomer reflected beam. This result is of some interest in that (1) it indicates that the total beam intensity as measured with the GE gage almost certainly has to be comprised of monomers since a single impact appears to break up the large clusters into monomers, and (2) Becker et al. (Refs. 17 and 18) have stated that nitrogen and helium clusters survive as clusters after impact, whereas the present data indicate that carbon dioxide clusters do not behave in this manner.

Implicit in the foregoing remarks is the assumption that large molecular clusters may be formed in a condensed molecular beam. Using a different experimental technique Hagena et al. (Ref. 12) have indicated that they have observed large molecular clusters in condensed beams. If large molecular clusters are formed in the condensed beam then problems can arise in the interpretation of individual mass beam intensity measurements as a result of the manner in which the molecular beam is sampled.

Assume that the molecular cluster is travelling at a uniform velocity in a uniform electric field (Fig. 31). If the cluster is singly

ionized as it enters this electric field it will be deflected towards the extractor plate. To travel through the orifice in the extractor plate and into the quadrupole section of the mass spectrometer it must travel the lateral distance D, while it travels axially a distance ℓ.

Force on the ionized cluster can be written as

$$F = \frac{nqV}{D}. \tag{1}$$

The acceleration towards the plate can be derived from

$$F = Nma. \tag{2}$$

From Eqs. (1) and (2) we can write acceleration as

$$a = \frac{nqV}{DNm} \tag{3}$$

The time for the cluster to travel the distance D and pass through the orifice is

$$t = \ell/v. \tag{4}$$

In time t the distance D is given by

$$D = 1/2\ at^2 \tag{5}$$

or

$$D = 1/2\ \frac{nqV}{DNm}\left(\frac{\ell}{v}\right)^2 \tag{6}$$

From Eq. (6)

$$N = 1/2\ \frac{nqV}{m}\left(\frac{\rho}{Dv}\right)^2 \tag{7}$$

The foregoing is an idealized description of the process taking place in the ionizing section of the mass spectrometer. This analysis is sufficiently realistic to permit an approximate estimate of the largest cluster that can be extracted from the beam.

It can be shown from a consideration of the mechanical and operational characteristics of the mass spectrometer that clusters as large as 100 to 1000 molecules may be deflected into the quadrupole section of the mass spectrometer. If on deflection any of these large clusters strike the mass spectrometer head they will be backscattered as an essentially monomer beam. If these debris monomers are still within the ionizing region of the mass spectrometer they will be ionized and deflected into the quadrupole section. In the breakup process it is possible that dimers, trimers, etc., are formed and these polymers can

be deflected into the quadrupole section. It is an hypothesis of Ref. 12 that clusters of 10^4, or greater, molecules are formed in a condensed beam. Such clusters cannot be deflected sufficiently to impact on the extractor plate of the mass spectrometer and this will mean that no monomers, dimers, trimers, etc., will be formed from these clusters.

This latter statement provides a possible explanation for the rapid decrease in dimer beam intensity at high source pressures (Fig. 15b). Also, the peak in the dimer beam intensity may be representative of the maximum size cluster that can be deflected into the quadrupole section of the mass spectrometer at particular operating conditions. Presumably, the pressure at which this peak occurs could be shifted by altering the extraction field voltage. To test this hypothesis, the ion energy (directly related to the field voltage) was doubled and as can be seen in Fig. 32 the peak in the dimer beam intensity shifted to a higher source pressure. This is a consistent result in that this higher field voltage can deflect a larger cluster into the quadrupole section of the mass spectrometer.

At this time it seems reasonable to suggest that the peak in the dimer beam intensity is indicative of the existence of massive condensation in the free-jet expansion. The conditions corresponding to this peak appear to be dependent, to some extent, upon the operational characteristics of the mass spectrometer (i. e., extractor field voltage).

From the foregoing discussion, the peak in the dimer intensity could have resulted from extracting at right angles to the molecular beam. If the mass spectrometer were mounted such that the condensed beam passed directly into the quadrupole section, the extraction problem encountered with the present mode of operation would have been avoided. Total monomer and dimer beam intensity measurements obtained with this mode of operation are compared with those obtained with the conventional mode of operation in Fig. 33a. The characteristic peak in the dimer beam intensity was not observed with this mode of operation. The dimer beam intensity is characterized by a rapid initial increase which is followed by a rate of increase consistent with that observed for the monomers.

The first opening in the mass spectrometer was larger (by a factor of approximately two) than the opening defining the beam entering the quadrupole section. This means that in the end-on mode a large portion of the clusters impinged directly on the extractor plate and was backscattered primarily as monomers.

This debris was then ionized and passed into the quadrupole section. If it is assumed that a portion of the monomer signal results from the breakup of large clusters this particular end-on mode of operation will always produce higher monomer intensity levels than the side-on mode which is extraction limited.

This experiment was repeated (Fig. 33b) using carbon dioxide as the test gas and in addition using a Bendix time-of-flight mass spectrometer in an end-on mode of operation. The monomer beam intensities obtained with this mass spectrometer are in good agreement with those of the quadrupole mass spectrometer operating in either mode. Peaks occurred in the dimer beam intensity for both the side-on and end-on modes of operation of the quadrupole mass spectrometer. No explanation can be offered at this time for these differences in the argon and carbon dioxide dimer intensity characteristics.

4.5 FREE-JET EXPANSIONS OF KRYPTON, NITRIC OXIDE, AND SULPHUR DIOXIDE

Measurements of total and individual mass beam intensity for the above gases are plotted in Figs. 34a through f.

The krypton data are compared with argon data obtained at similar test conditions in Fig. 34a. The monomer beam intensities for both gases are in good agreement. This agreement would be expected since both gases are monatomic and have similar vapor pressure characteristics. Since the molecular weight of krypton is twice that of argon the mass spectrometer will cease to extract krypton clusters at a lower pressure than for argon. This is a possible explanation for the fact that the peak in the dimer beam intensity occurs at a lower pressure for krypton than for argon.

The beam intensity measurements for nitric oxide are shown in Fig. 34b. Insufficient monomer data were obtained to define the pressure at which the monomer and total beam intensity first deviated. The dimer beam intensity peaked at a pressure of 1500 torr. Some similar measurements of dimer beam intensity (Ref. 7 and Figs. 34c, d, and e), made where there was a skimmer-interaction effect, indicate that the peak occurred at a pressure of 2000 torr for a 0.0343-cm-diam orifice. The fact that this pressure is greater than that obtained in the present investigation is in agreement with effect of skimmer interaction upon dimer beam intensity discussed earlier. It can be seen from the previous data (Figs. 34c through e) that the total and monomer beam intensities first deviated when $pd \approx 34$ torr cm. This is surprisingly

high when compared with the value of 34 torr cm obtained in the present study for nitrogen. Using the present data and assuming condensation to occur when the total flux curve first deviates from 45°, yields a value of pd ≈ 9 torr cm. This is more consistent with the expected behavior of NO from its known vapor pressure characteristics.

Dimer beam intensity measurements for sulphur dioxide (Fig. 34f) indicate that the peak value occurred at a pressure of 1100 torr.

4.6 CLUSTER SIZE DETERMINATION

For this particular test, molecular beam conditions were chosen such that the dimer beam intensity was at its maximum value. This condition was chosen in an attempt to determine if large molecular clusters were present in the beam.

At this test condition the secondary electron multiplier registered a signal with the mass spectrometer ionizing section turned on (Fig. 10). This signal disappeared when the mass spectrometer was turned off. With the mass spectrometer turned on the secondary electron multiplier signal disappeared when the source gas supply was shut off. These results suggest that the secondary electron multiplier signal resulted from ions formed in the mass spectrometer ionizing section.

A 500-v retarding field was applied to this ionized beam. No change was detected in the secondary electron multiplier signal. With a retarding field of this magnitude, clusters having a cluster-to-charge number ratio up to 700 should have been stopped and there should have been a reduction in the secondary electron multiplier signal. However, clusters up to this size may have already been deflected sufficiently in the ionizing section such that they did not pass into the secondary electron multiplier. A possible explanation for the secondary electron multiplier signal is that it was a measure of large clusters (>700) which were not deflected in the ionizing section of the mass spectrometer.

4.7 IMPACT PRESSURE MEASUREMENTS

The onset of condensation in wind tunnel nozzle flows can be determined from a study of impact pressure measurements (Refs. 8 and 9). The usual procedure is to fix a total pressure and monitor the impact pressure as the total temperature is decreased. Condensation is said to have occurred in the flow when the impact pressure changes from a constant value. The results of a set of measurements made in the

present investigation are shown in Fig. 35. Condensation onset was identified in a manner consistent with that used by Varwig and Mason (Ref. 9). From a knowledge of the impact pressure, stagnation pressure; and stagnation temperature at condensation onset, values of static temperature and pressure were calculated. These values are in good agreement with other experimental values of this type (Ref. 8 and Fig. 36). Thus, using conventional wind tunnel techniques, we have established that condensation occurred 2.54 cm downstream of the nozzle exit plane with a source temperature of 290°K and a source pressure of 800 torr.

For these source conditions the indications of the total and monomer beam intensity deviation, the velocity deviation, and peak in the dimer beam intensity are that some change in the expanding flow occurred at a lower source pressure. In comparing impact pressure measurements with the mass spectrometer data it must be remembered that one is a point measurement, whereas the other is an integrated measurement.
also are they not at different x locations?

If monomer total beam intensity deviations, velocity deviations, and dimer beam intensity peaks are indicative of condensation onset, then these impact pressure measurements appear to imply that condensation onset occurs well downstream of the nozzle throat. This suggestion is supported by some dimer beam intensity measurements made by Milne et al. (Ref. 19). As a result of their mass spectrometric studies they conclude that, "dimer is formed in appreciable quantities near the end of the expansion; in the ill-defined transition region to collisionless flow."

4.8 SKIMMER INTERACTION EFFECTS

Benek (Ref. 14) has reviewed many of the theoretical and experimental evaluations of the effect of skimmer interaction upon the total beam intensity. As a result of this review he formulated a model of the skimmer scattering process which appears to provide a reasonable prediction of the observed total beam intensity attenuation prior to the local minimum in the total beam intensity (Fig. 1). Implicit in this type of analysis is the assumption that the composition of the gas is not changed in the scattering process. That is to say the monomer, dimer, trimer, etc., mole fractions are constant values at a particular source pressure regardless of the degree of skimmer interaction.

Some measurements of total, monomer, and dimer beam intensity for warm and cold skimmers, discussed by Benek (Fig. 12 in Ref. 14), are reproduced in Figs. 37 and 38. At low source pressures

($p \lesssim 100$ torr) where skimmer interaction effects can be assumed to be small, the absolute values of total and monomer beam intensity as indicated by the GE gage and mass spectrometer are in good agreement. This suggests that it is reasonable to assume that absolute comparisons of total, monomer, and dimer beam intensities at the instrument location can be made, even when there has been some skimmer interaction (i. e., at higher source pressures $100 \lesssim p \lesssim 10,000$ torr).

Implicit in Benek's analysis is the assumption that the beam molecules and the molecules scattered from the skimmer are similar and are monomers. It is evident from a consideration of the individual mass beam intensity measurements for both the cold and warm skimmers and for source pressures less than 100 torr the beam is almost totally composed of monomers. It is for this reason that Benek's analysis predicts reasonable values of beam attenuation.

For pressures greater than 1000 torr the monomer beam intensity obtained with the warm skimmer decreased, whereas the total beam intensity increased. If the warm skimmer had not been affecting the molecular composition of the beam, then $M_w \times I_c/I_w$ would equal M_c. It can be seen from Fig. 37 that $M_w \times I_c/I_w$ is considerably less than M_c. This implies that the warm skimmer altered the composition of the beam. The mechanism of the interaction was such that it prevented the passage of monomers through the skimmer.

It is reasonable to assume that at pressures of 10,000 torr massive condensation had occurred and that the beam was composed of large molecular clusters. When large molecular clusters strike a surface, evidence exists (Fig. 30) to suggest that the resulting debris is mainly composed of monomers. Thus, when these large molecular clusters strike the lip of the warm skimmer large local monomer concentrations are formed. These background monomers will effectively attenuate the incident beam monomers. It is unlikely that these same background monomers will have a significant effect upon large molecular clusters.

The total beam intensity for the warm skimmer increased rapidly as the source pressure increased from 1000 to 10,000 torr. This variation can be explained in terms of clusters that grow in size with increasing source pressure. At 1000 torr the clusters were so small that the monomer background gas scattered them almost as effectively as it did the incident beam monomers. As the clusters grew in size the monomer background gas was a less effective scatterer and the total beam intensity increased rapidly.

The dimer intensity for the warm and cold skimmers was different for source pressures greater than 100 torr. It can be seen that $D_W \times I_C/I_W$ is in excellent agreement with D_C for source pressures less than 700 torr (Fig. 38). This is consistent with the corresponding monomer intensity measurements (Fig. 37). For pressures greater than 1000 torr, $D_W \times I_C/I_W$ is greater than D_C. This suggests that the dimer fraction has been affected by the skimming process. These results suggest that the dimer fraction increased while the monomer fraction decreased. No explanation for these apparently contradicting results can be offered at this time.

The preceding discussion suggests that (1) the mole fractions of monomers, dimers, trimers, etc. can be affected by the presence of a warm skimmer. Scattering at the skimmer entrance can effectively remove lighter species from the beam and (2) the local minimum in the total beam intensity curve is representative of a size of cluster that is too large to be significantly scattered by the monomer background gas. This minimum should be related to the occurrence of condensation in the free-jet expansion. However, considerable caution must be used in using this local minimum as an indicator of condensation onset. The reason for this being that Bier and Hagena (Ref. 3) have shown that for source-to-skimmer distances ranging from 10 to 70 orifice diameters the location of this minimum is a function of the separation distance.

It has been suggested earlier, as a result of the present work and that of Ref. 19, that condensation may occur far downstream of the orifice exit. If this is the case, then the possibility exists that at these relatively small-orifice skimmer separations the skimmer itself may directly affect the condensation process in the expansion. The measurements discussed by Benek (Ref. 14) for both the warm and cold skimmer were obtained with large-orifice skimmer separations (i. e., approximately 600-orifice diameters). For these conditions, the skimmer may be located such that it cannot affect the initial nucleation process in the free-jet expansion.

It has been shown in Figs. 23d and q that there is difference in the monomer velocity depending on whether a cryogenically cooled or warm conical skimmer is used. In general, on the basis of this limited data it can be seen that there is a greater variation in the velocity for the warm conical skimmer than for the cryogenically cooled skimmer. For these two test conditions the static temperature of the flow field was determined using a least-square technique (Ref. 1) to curve fit the velocity distribution data to a modified Maxwellian distribution function. These data are plotted in Fig. 39. It is obvious that there is a marked difference in the two sets of data when the source pressure is

approximately 2000 torr. At this source pressure, there is a sudden increase in the static temperature for the warm skimmer. It is suggested that this increase is a result of a scattering of the incident monomers by the background monomers that are formed by the impact of large clusters with the warm conical skimmer.

4.9 SUMMARY AND COMPARISON OF THE EXPERIMENTAL MEASUREMENTS

Based on the estimates of static temperature the terminal Mach number in the flow can be derived. Values of the terminal Mach number for the warm and cold skimmer are plotted in Fig. 40. It can be seen that for source pressures less than 200 torr the present data for warm and cold skimmers are in good agreement with each other and the measurements of Anderson et al. (Ref. 20). For source pressures greater than 200 torr the present data indicate a lower terminal Mach number than that predicted by an extrapolation of Ref. 20 data. This lower terminal Mach number corresponds to an increase in static temperature which is one of the indicators of condensation onset in classical condensation theory. This increase in static temperature should be associated with a decrease in flow velocity. If the velocity data of Fig. 23d are studied closely, it does appear that there may be a slight velocity decrease in the source pressure range from 100 to 300 torr. At a source temperature of 600°K, Fig. 23q, there is a well defined decrease in velocity at 1000 torr.

A comparison of all the experimental measurements for argon is made in Figs. 41a and b for two source temperatures. For a source temperature of 300°K, (1) the terminal Mach number deviates from Anderson et al. (Ref. 20) data at a pressure of 200 torr, (2) the dimer intensity is increasing rapidly at 150 torr, (3) the total beam intensity ceases to increase at the ideal rate for pressures greater than 100 torr, and (4) the total and monomer beam intensity start to deviate at pressures greater than 400 torr. If we accept the suggestion made in Section 4.4 that the dimer intensity results from the breakup of larger clusters in the mass spectrometer head, then the onset of condensation may be occurring at a source pressure of approximately 100 torr. A similar analysis of the data for a source temperature of 600°K (Fig. 41b) indicates that condensation may be occurring at source pressure of approximately 700 torr. Both these pressures are lower than that at which the monomer and total beam intensity variations first deviate which has been suggested as an indicator of condensation onset.

SECTION V
CONCLUSIONS

The present investigation has revealed that there are characteristic changes in the variations of the measured total monomer and dimer beam intensities and gas velocity with source pressure. These changes vary in a systematic manner with source, pressure, temperature, and diameter when a cryogenically (22°K) cooled skimmer and collimator are used to form the molecular beam. These results can be summarized as follows:

1. The total beam intensity increases directly with source pressure up to a particular pressure at which pressure it continues to increase at a less than ideal rate. For argon it has been shown that the pressure at which this break occurs in the total beam intensity is given by $pd/T^2 = 1.7 \times 10^{-4}$ torr cm $(°K)^{-2}$.

2. This break in the total beam intensity variation is accompanied by a similar break in the monomer beam intensity. The effect of the breaks in these two variations is such that the total and monomer beam intensities deviate. The pressure at which they start to deviate can be correlated in terms of pd/T^2 = constant. For argon and nitrogen flow values of 1.7×10^{-4} and 3.6×10^{-4} torr cm $(°K)^{-2}$, respectively, were found for flow through sonic orifices. Corresponding values of 8×10^{-5} and 1.8×10^{-4} torr cm $(°K)^{-2}$ were found for flow through conical nozzles. It is suggested that the deviation in the total and monomer beam intensities may be an indicator of condensation.

3. Beam velocity has an approximately constant value up to a particular pressure at which point it starts to increase. The pressure at which this deviation occurs cannot be correlated in terms of pd/T^2. However, for each orifice diameter p/T^2 has a constant value. More experimental data are needed to fully evaluate the significance of these velocity measurements.

4. The dimer, trimer, etc., intensity variations with source pressure are characterized by the existence of a well defined peak at a particular source pressure. In general, this peak occurs at higher source pressures

than do the characteristics mentioned in 1, 2, and 3 above. A completely satisfactory correlation of these well defined peaks, in terms of source temperature pressure and diameter, has not yet been obtained. An investigation of the monomer and dimer mole fractions in a condensed beam reveals that the absolute values of these fractions can be affected by skimmer interaction.

REFERENCES

1. Ruby, Earl C., Jr. "An Experimental Study of the Velocity Distribution and Relative Abundances of Argon Molecular Clusters in the Condensation Regions of a Free Jet." Masters Thesis, University of Tennessee, Knoxville, 1969.

2. Ruby, E. C., Brown, R. F., and Busby, M. R. "The Effects of Condensation on the Flow Field Properties in Free-Jet Expansions of Argon." AEDC-TR-70-142 (AD710616), August 1970.

3. Bier, K. and Hagena, O. "Optimum Conditions for Generating Supersonic Molecular Beams." Proceedings of the Fourth International Rarefied Gas Dynamics Symposium, Vol. 2, New York, Academic Press, 1966, pp. 260-278.

4. Brown, R. F. and Heald, J. H., Jr. "Background Gas Scattering and Skimmer Interaction Studies Using a Cryogenically Pumped Molecular Beam Generator." Proceedings of the Fifth International Rarefied Gas Dynamics Symposium, Vol. 2, New York, Academic Press, 1967, pp. 1407-1424.

5. Govers, T. R., Leroy, R. L., and Deckers, J. M. "The Concurrent Effects of Skimmer Interactions and Background Scattering on the Intensity of a Supersonic Molecular Beam." Proceedings of the Sixth International Rarefied Gas Dynamics Symposium, Vol. 2, New York, Academic Press, 1969, pp. 985-996.

6. Bossel, U. "Investigation of Skimmer Influences on the Production of Aerodynamically Intensified Molecular Beams." College of Engineering Report No. AS-68-6, University of California, Berkeley, August 1968.

7. Golomb, D., Good, R. E., and Brown, R. F. "Dimers and Clusters in Free Jets of Argon and Nitric Oxide." Journal of Chemical Physics, 52 (1970), p. 1545.

8. Daum, Fred L. and Gyarmathy, George. "Condensation of Air and Nitrogen in Hypersonic Wind Tunnels." AIAA Journal, Vol. 6, No. 3, March 1968, pp. 458-465.

9. Varwig, R. L. and Mason, S. B. "Condensation in a Contoured-Nozzle Shock Tunnel." AIAA Journal, Vol. 8, No. 10, October 1970, pp. 1900-1901.

10. Heald, J. H., Jr... "Performance of a Mass Spectrometric Modulated Beam Detector for Gas-Surface Interaction Measurements." AEDC-TR-67-35 (AD648984), Arnold Air Force Station, Tennessee, March 1967.

11. Powell, H. M. and Heald, J. H., Jr. "A System for the Measurement of Velocity Distributions of Molecular Beams." AEDC-TR-68-151 (AD675306), Arnold Air Force Station, Tennessee, September 1968.

12. Hagena, O. F., Obert,W., and Wedel, H. V. "Condensation in Supersonic Free Jets: Experiments with Different Gases and Nozzle Geometries." Euromech 13th Meeting on the Aerodynamics of Rarefied Gas Flows, National Physical Laboratory, Teddington, Middlesex, England, July 1969.

13. Bauchert, Jens and Hagena, Otto-Friedrich. "Massenbestimmung ionisierter Agglomerate in kondensierten Molekularstrahlen nach einer electrischen Gegenfeldmethod." Z. Naturforschg, 20a. 1135-1142 (1965).

14. Benek, J. A. "Prediction of Molecular Scattering Effects in Free-Jet Expansions." AEDC-TR-70-273 (AD717158), Arnold Air Force Station, Tennessee, January 1971.

15. Kogan, Mikhail N. "Rarefied Gas Dynamics." Plenum Press, New York, 1969, p. 493.

16. Haukohl, J. and Spradley, L. W. "Multi-Specie Condensation in Expanding Flows." Lockheed Missiles and Space Company, Huntsville, Alabama. NASA CR-102798, June 1970.

17. Becker, E. W., Klingelhofer, R., and Mayer, H. "Interaction of Nitrogen Cluster Beams with a Solid Surface." Proceedings of the Sixth International Rarefied Gas Dynamics Symposium, Vol. II, New York, Academic Press 1969, pp. 1349-1356.

18. Becker, E. W., Gspann, J., and Krieg, G. "Reflection of Condensed Molecular Beams of Helium at Solid Surfaces." Entropie No. 30, November-December 1969, pp. 59-61.

19. Milne, Thomas A., Vandegrift, A. Eugene, and Greene, Frank T. "Mass-Spectrometric Observations of Argon Clusters in Nozzle Beams II. The Kinetics of Dimer Growth." The Journal of Chemical Physics, Vol. 52, No. 3, February 1970, pp. 1552-1560.

20. Anderson, J. B., Andres, R. P., Fenn, J. B., and Maise, G. "Studies of Low Density Supersonic Jets." Proceedings of the Fifth International Rarefied Gas Dynamics Symposium, Vol. II, New York, Academic Press, 1966, pp. 106-127.

APPENDIX
ILLUSTRATIONS

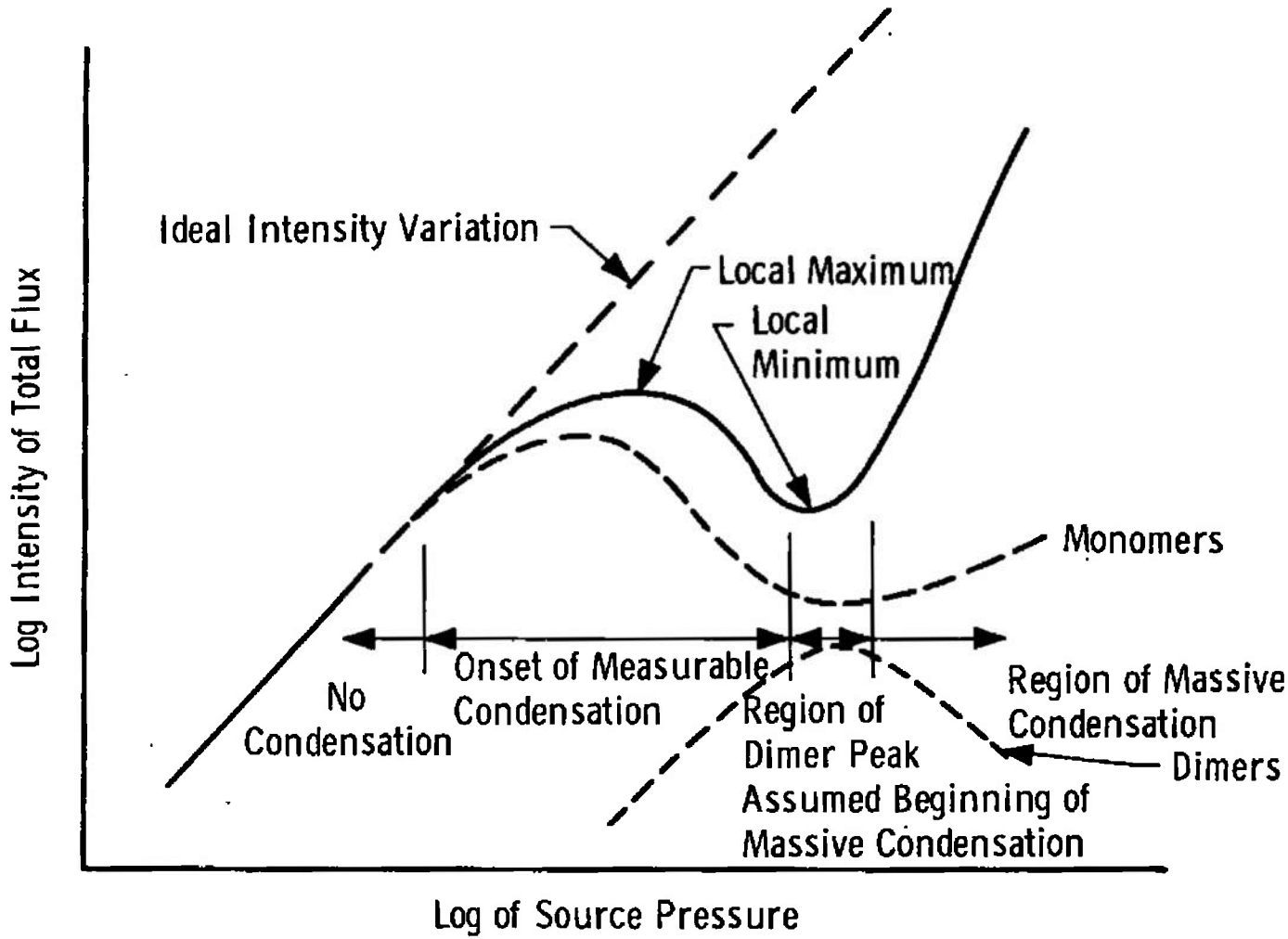

Fig. 1 Illustration of Regions of Condensation in Free-Jet Expansion

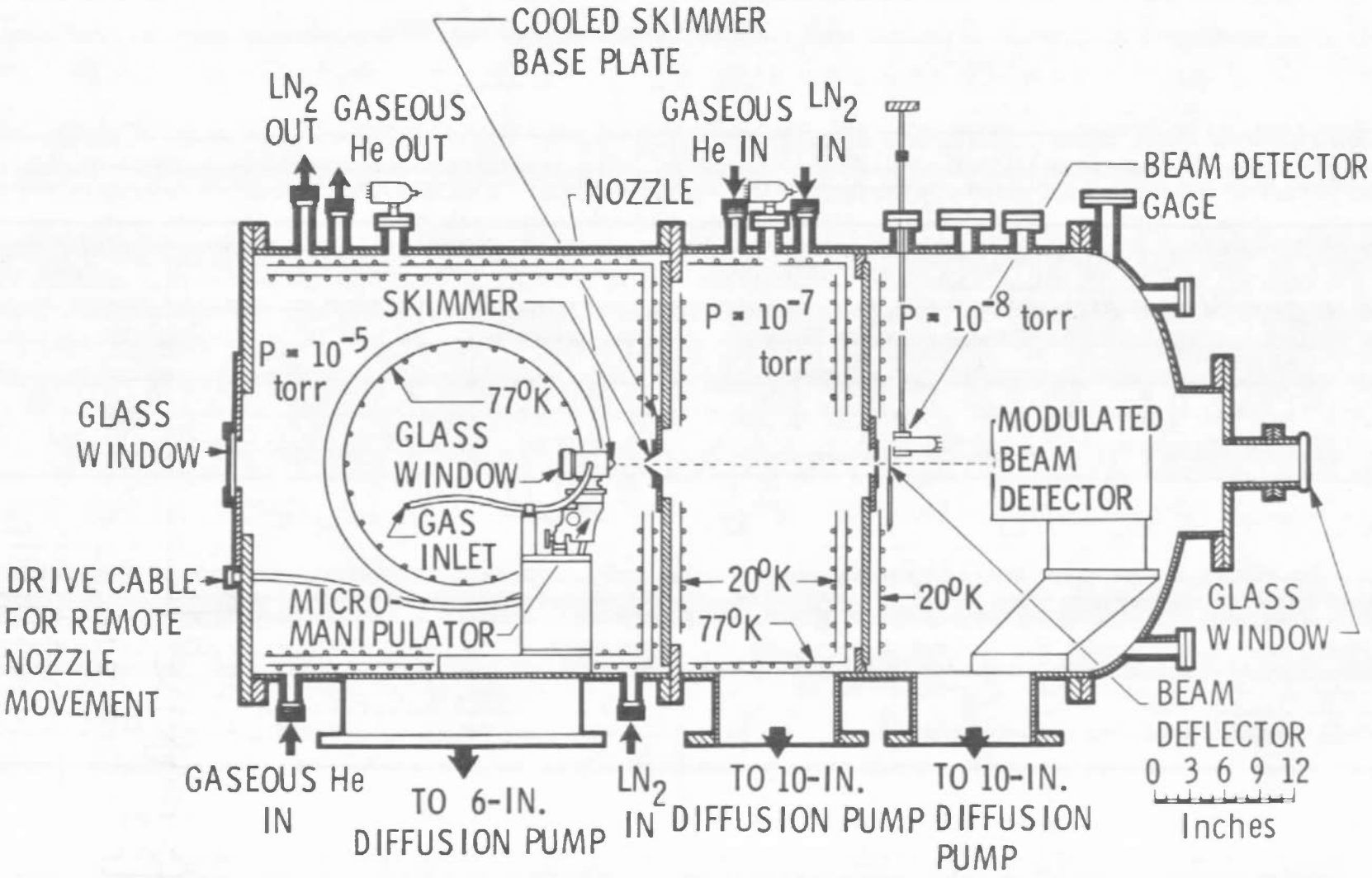

Fig. 2 Schematic of the AEDC Aerodynamic Molecular Beam Chamber

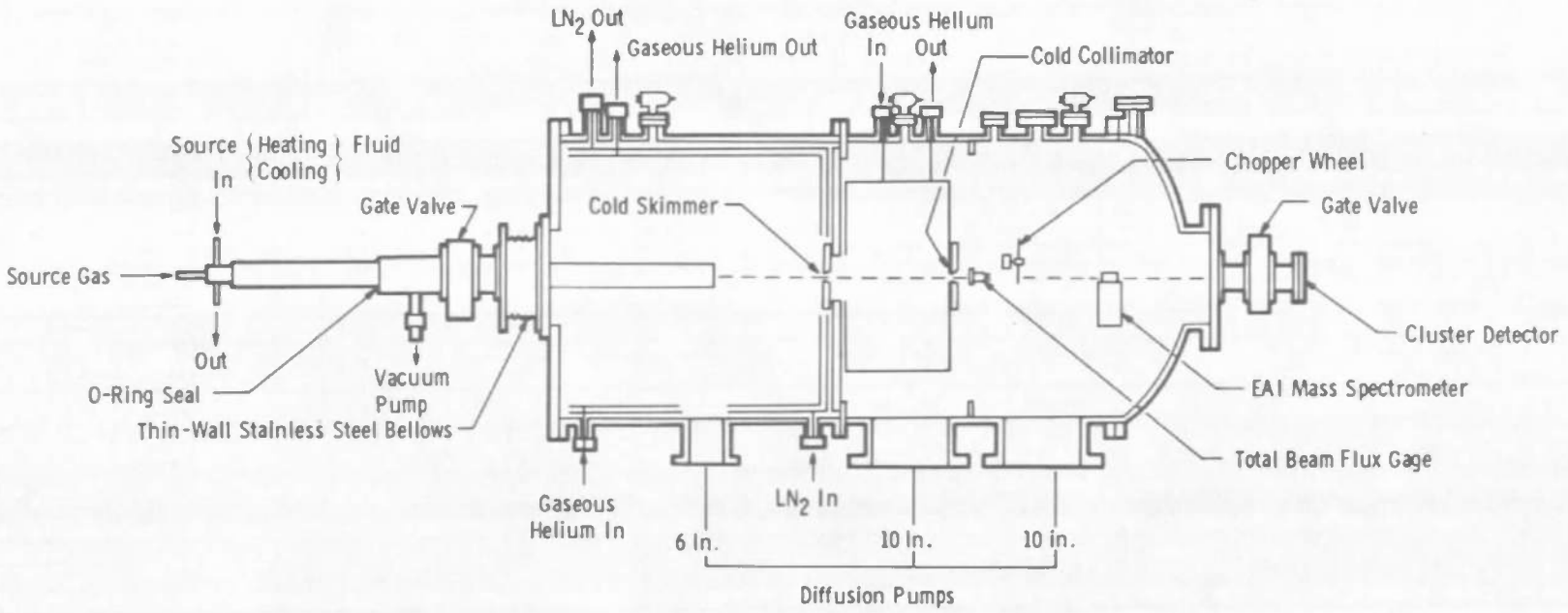

Fig. 3 Schematic of the Molecular Beam Chamber

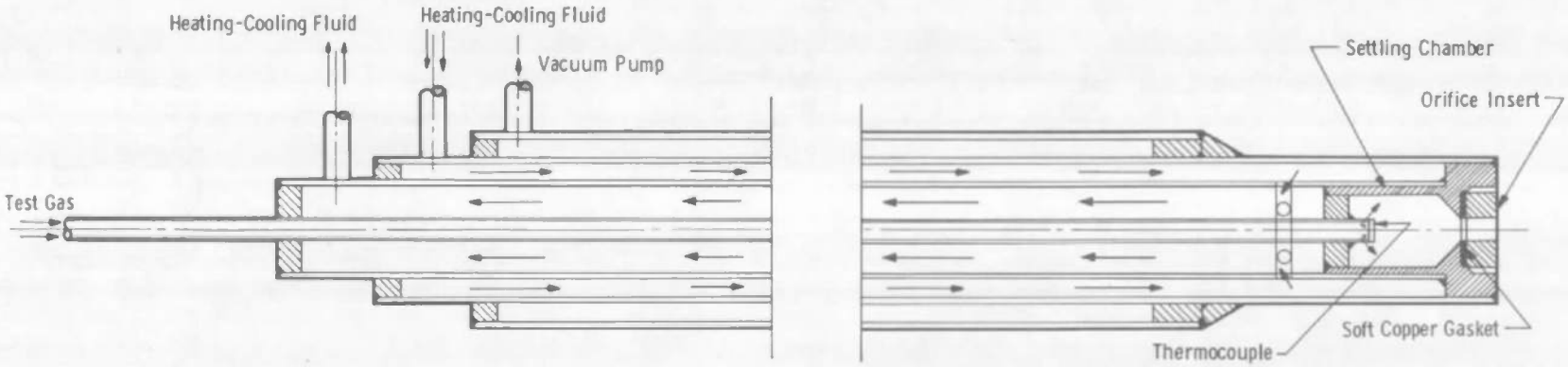

Fig. 4 Schematic of Temperature-Controlled Molecular Beam Source

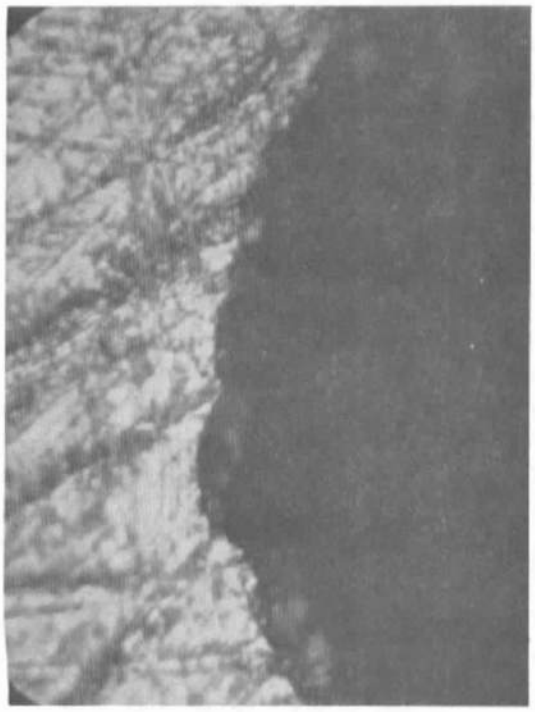

Before Polishing

After Polishing

Magnification 320

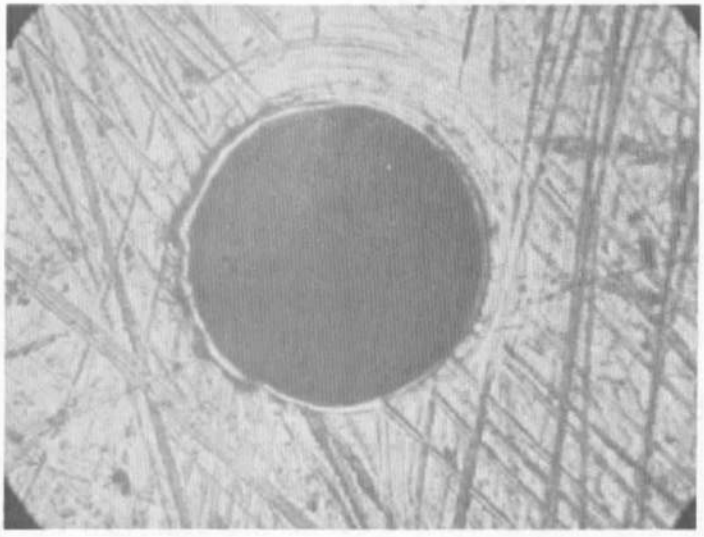

After Polishing, Magnification 80

a. Nominal Diam 0.0356 cm, Measured Diam 0.0364 cm

Fig. 5 Orifices Used in the Present Investigation

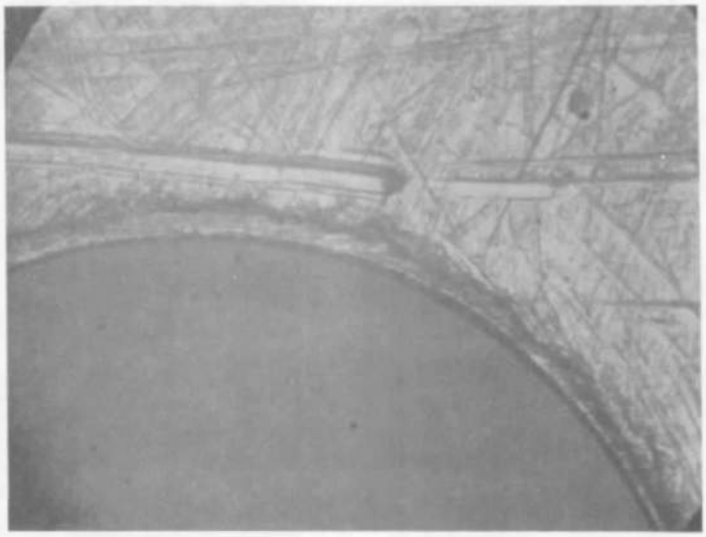

Magnification 80

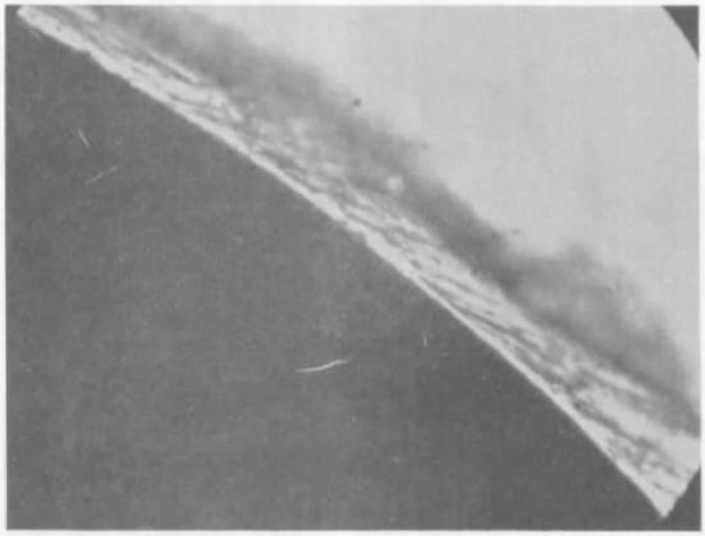

Magnification 320

b. Measured Diam 0.125 cm
Fig. 5 Continued

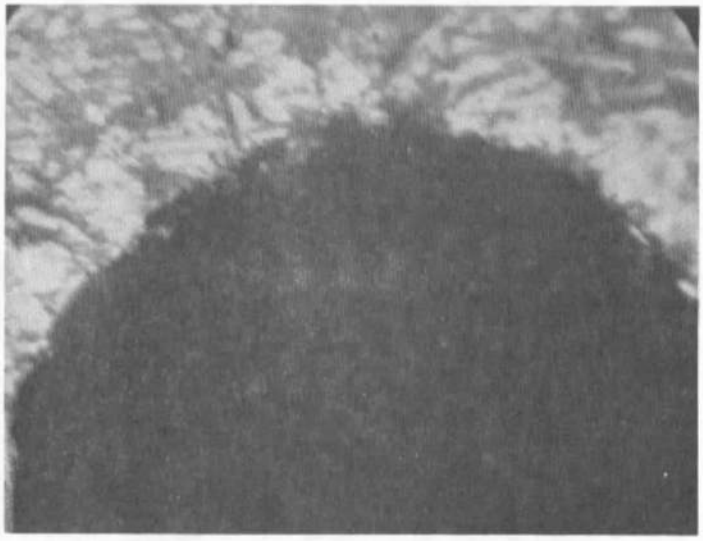

Before Polishing, Magnification 320

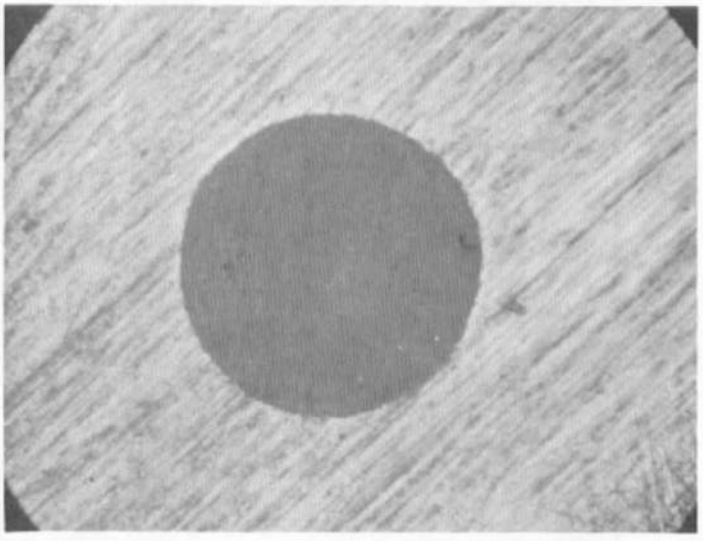

After Polishing, Magnification 80

c. Nominal Diam 0.0204 cm, Measured Diam 0.0386 cm
Fig. 5 Continued

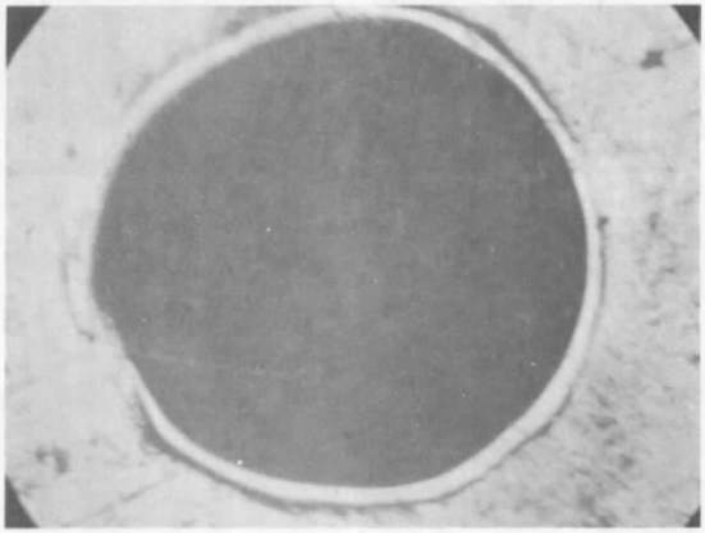

Sonic Orifice After Polishing,
Magnification 320

d. Nominal Diam 0.0102 cm, Measured Diam 0.0147 cm
Fig. 5 Concluded

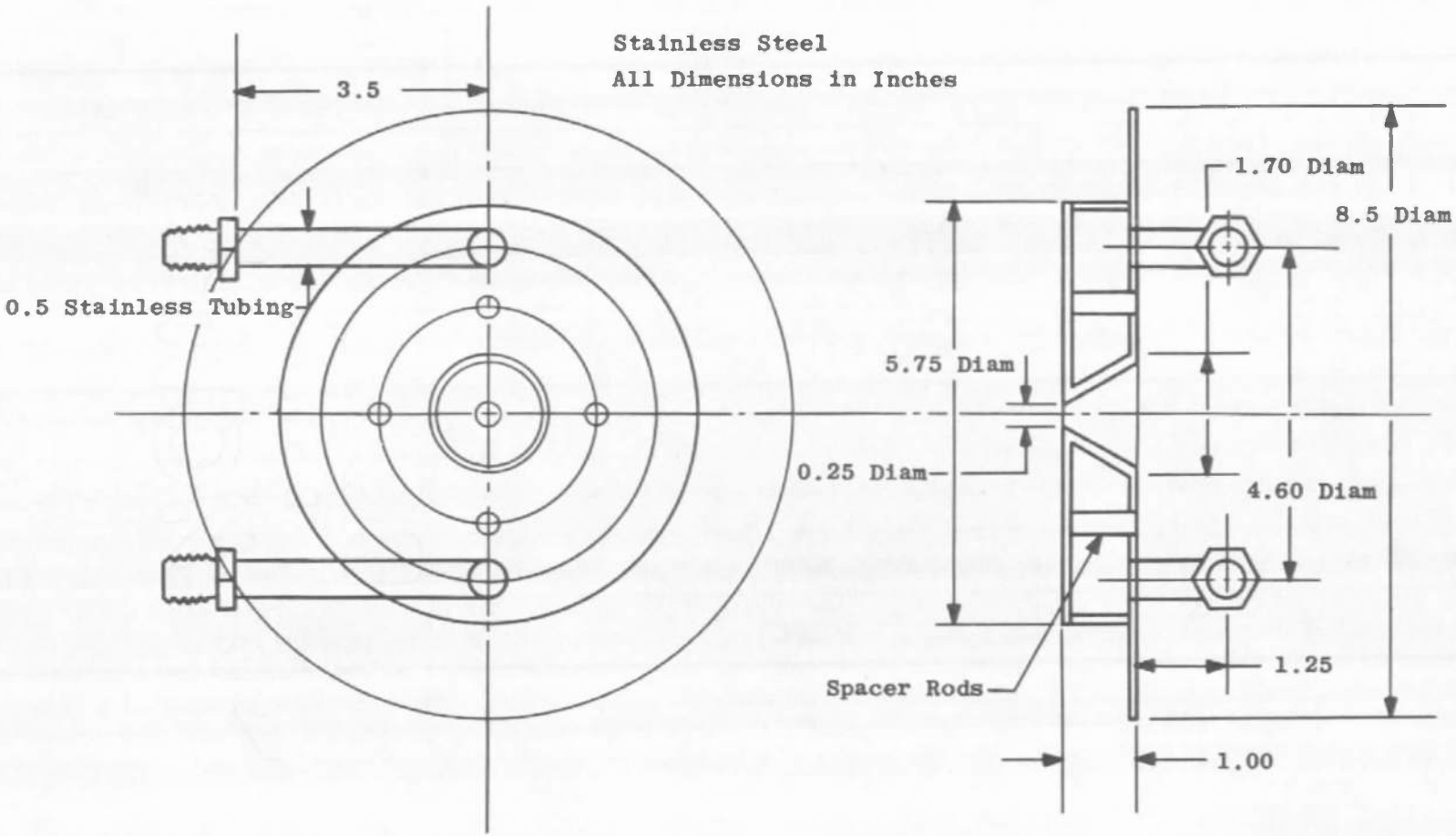

Fig. 6 Gaseous-Helium-Cooled Collimator

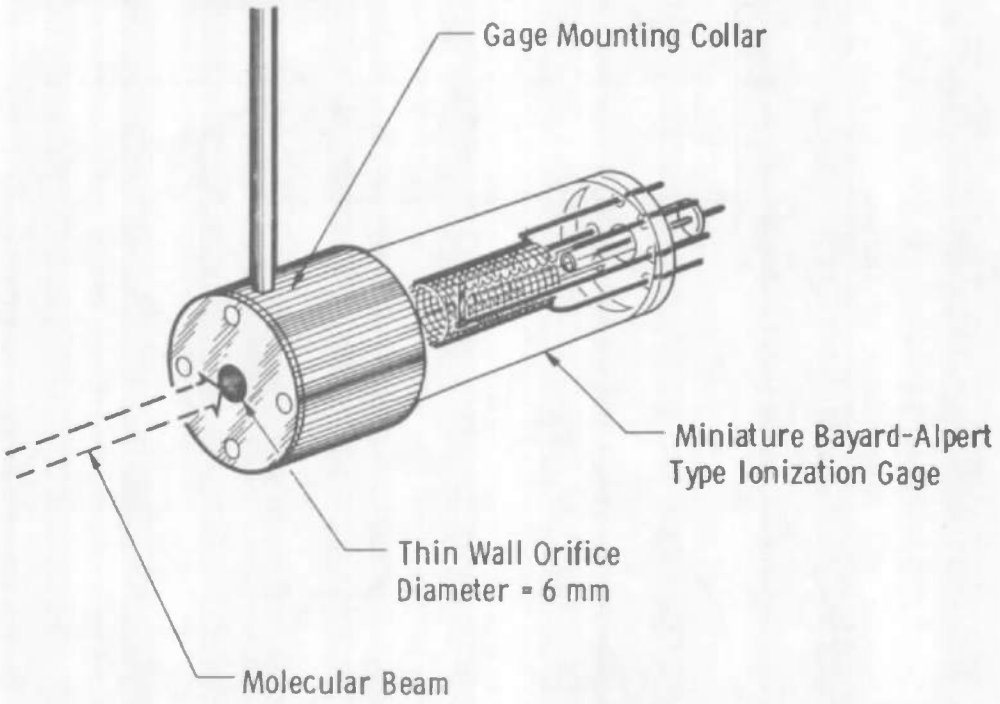

Fig. 7 Total Incident Beam Intensity Gage

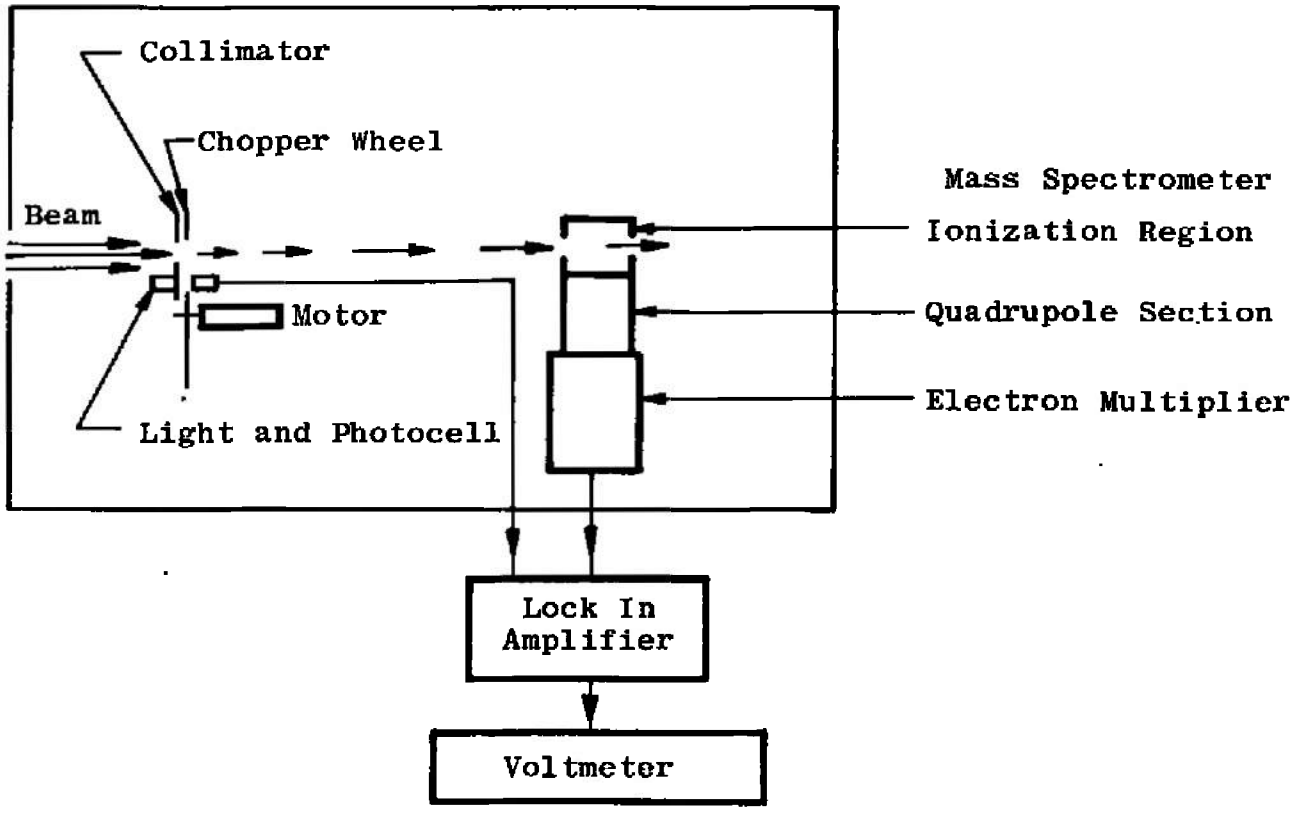

Fig. 8 Schematic Diagram of the Modulated Beam Detection System Used in Relative Cluster Abundance Measurements

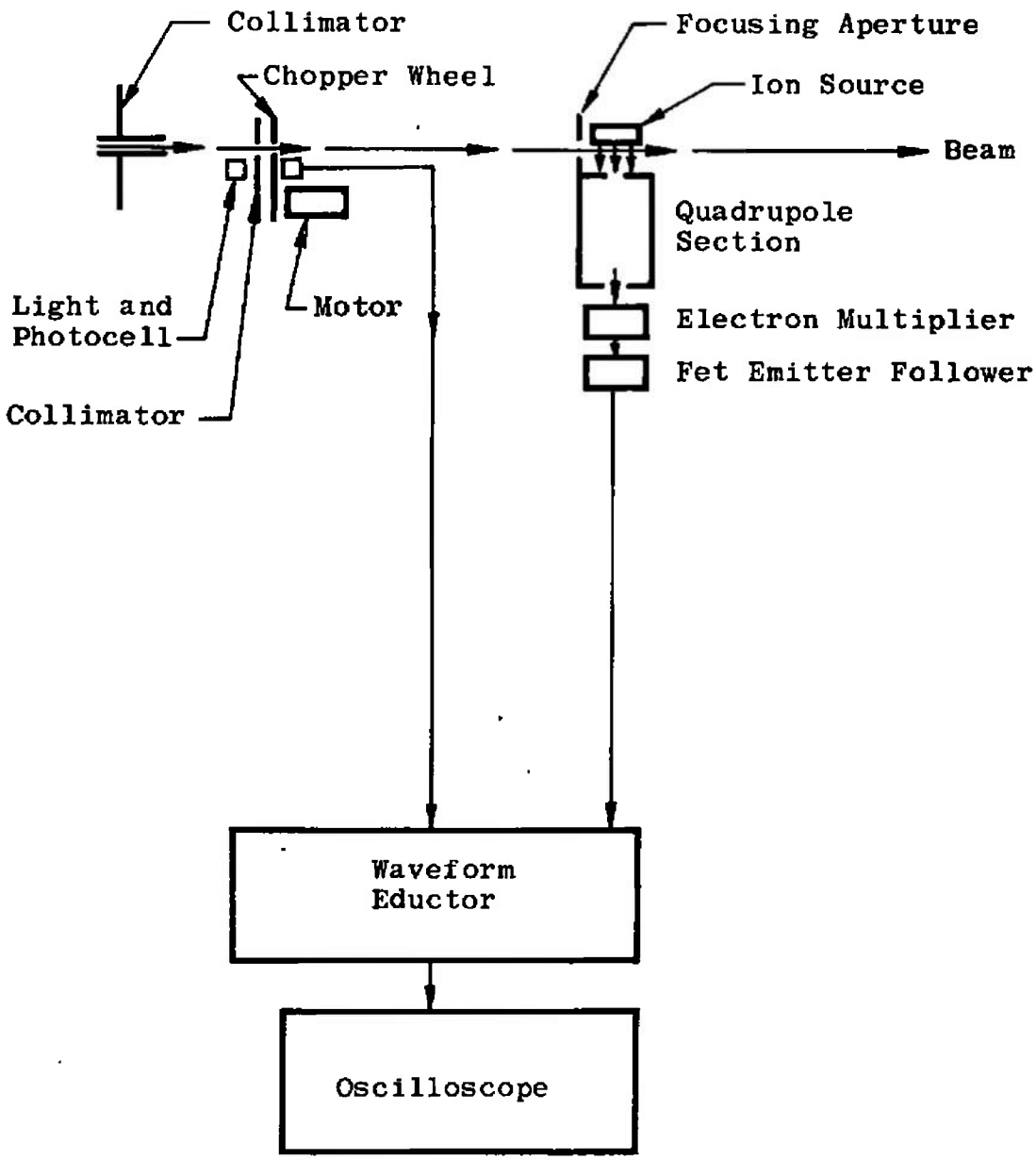

Fig. 9 Schematic Diagram of the Modulated Beam Detection System Used in the Time-of-Flight Measurements

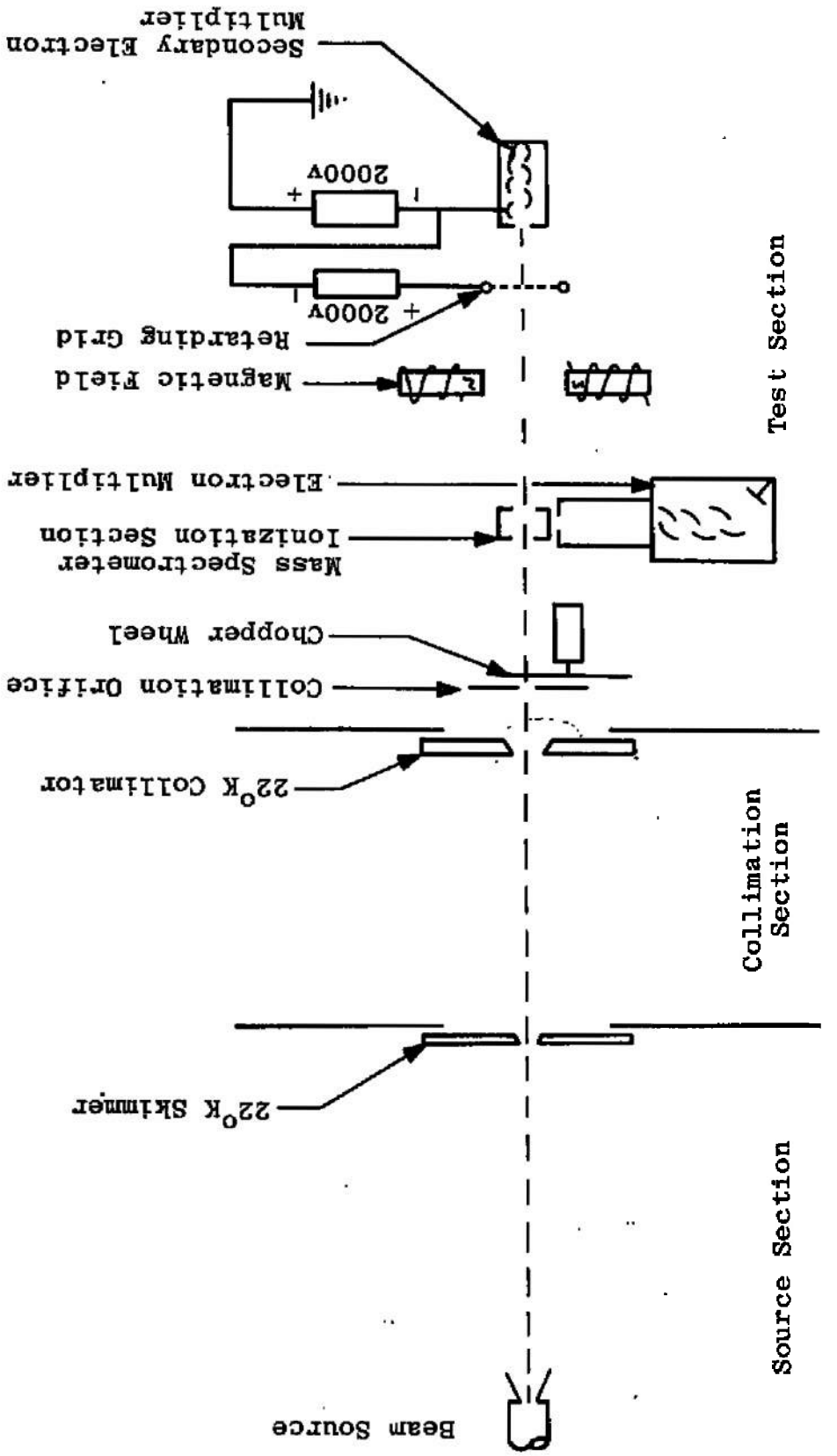

Fig. 10 Schematic of the Electrostatic and Magnetic Deflection Technique for Measurement of Cluster Size

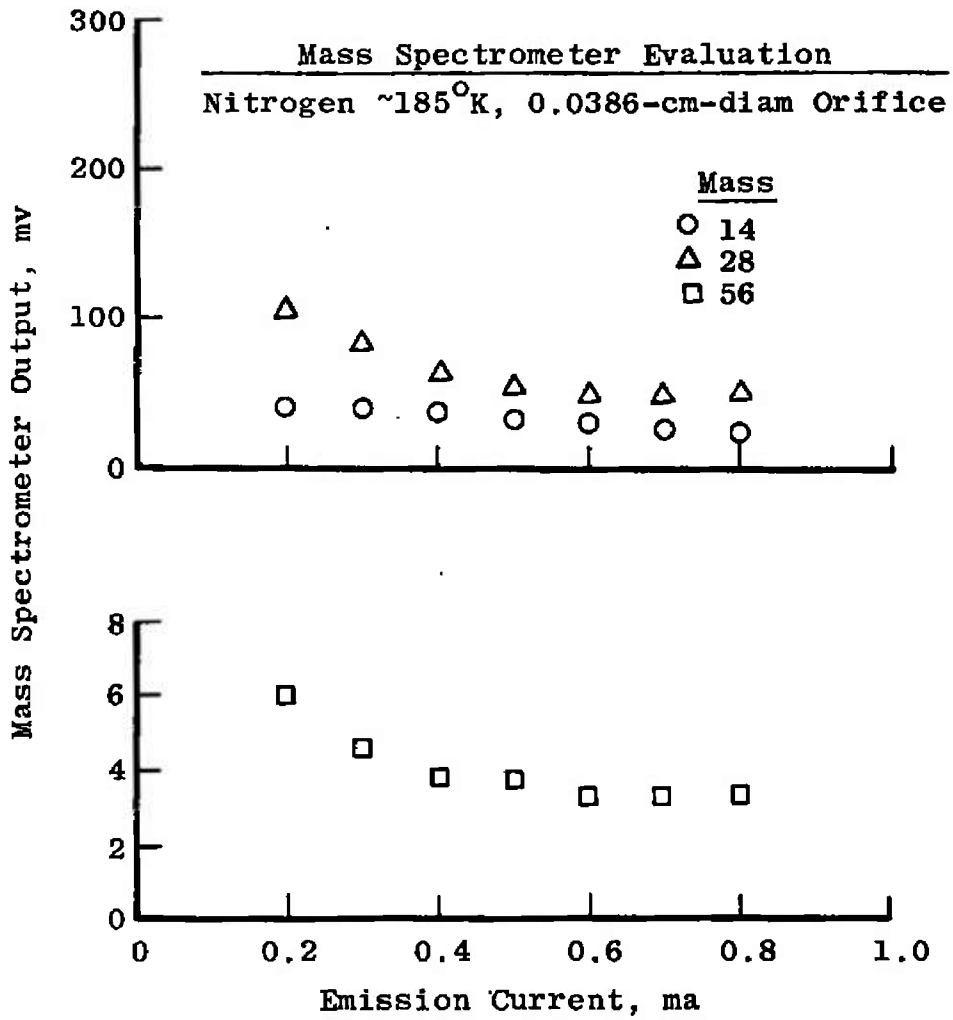

a. Extractor 10v, Focus 135v, Ion Energy 22v, Electron Energy 90v, Electron Multiplier Voltage ~ 2900, p = 1250 torr

Fig. 11 Effect of Variation of Mass Spectrometer Operating Conditions on Output Signal

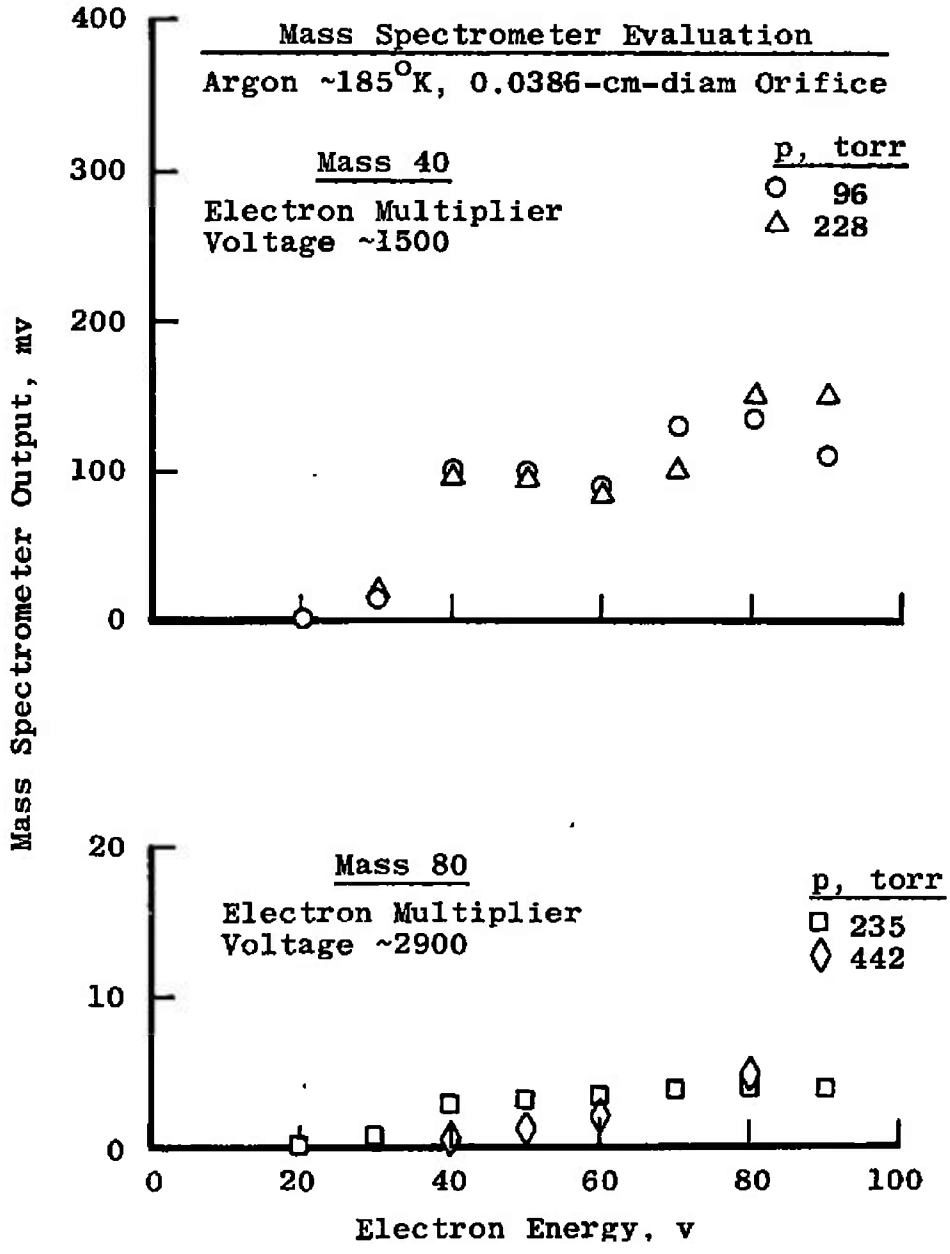

b. Extractor 10v, Focus 135v, Ion Energy 22v (These Values Held Constant), Emission Current 0.2 ma

Fig. 11 Continued

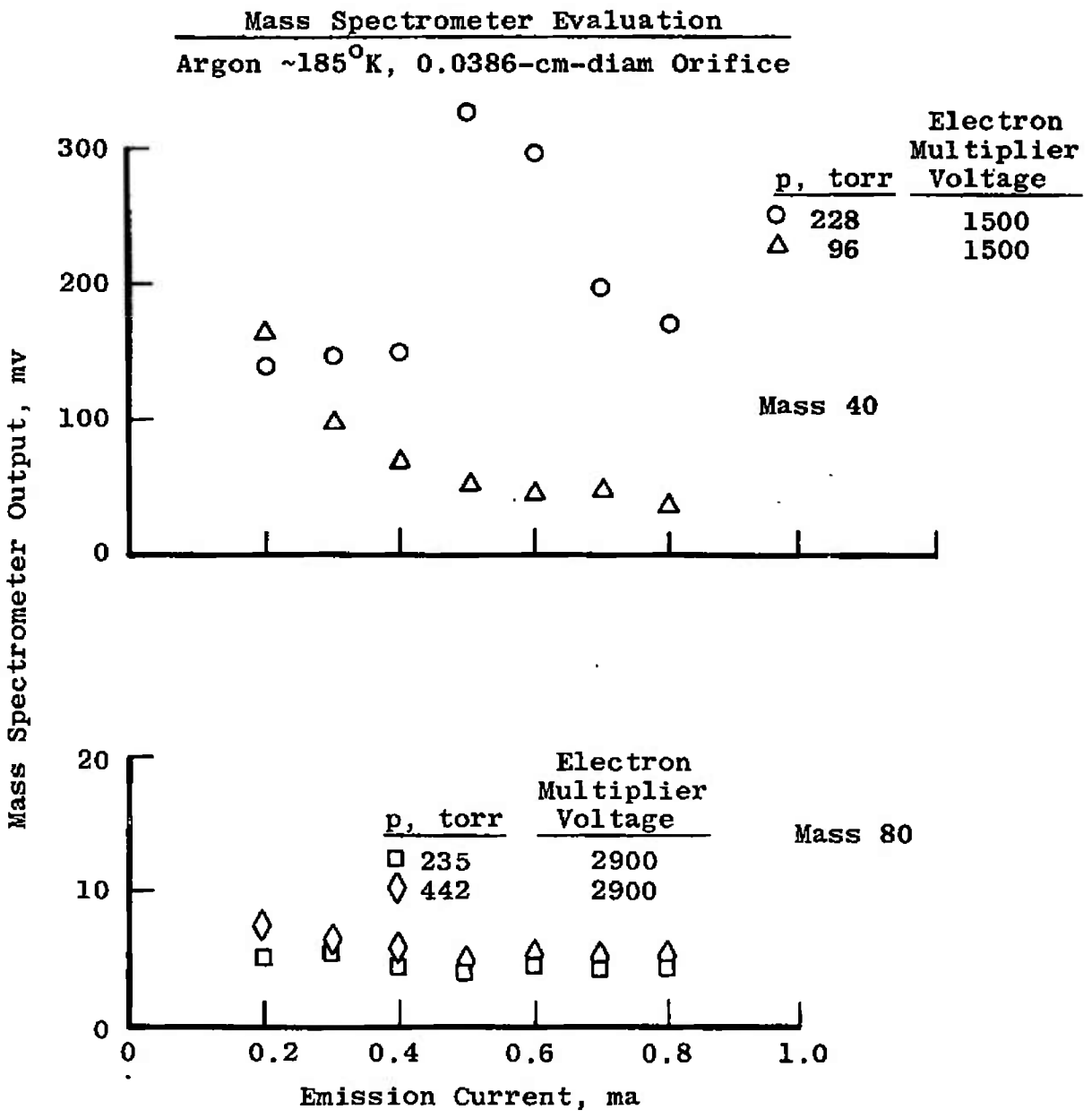

c. Extractor 10v, Focus 135v, Ion Energy 22v (These Values Held Constant), Electron Energy 90v

Fig. 11 Continued

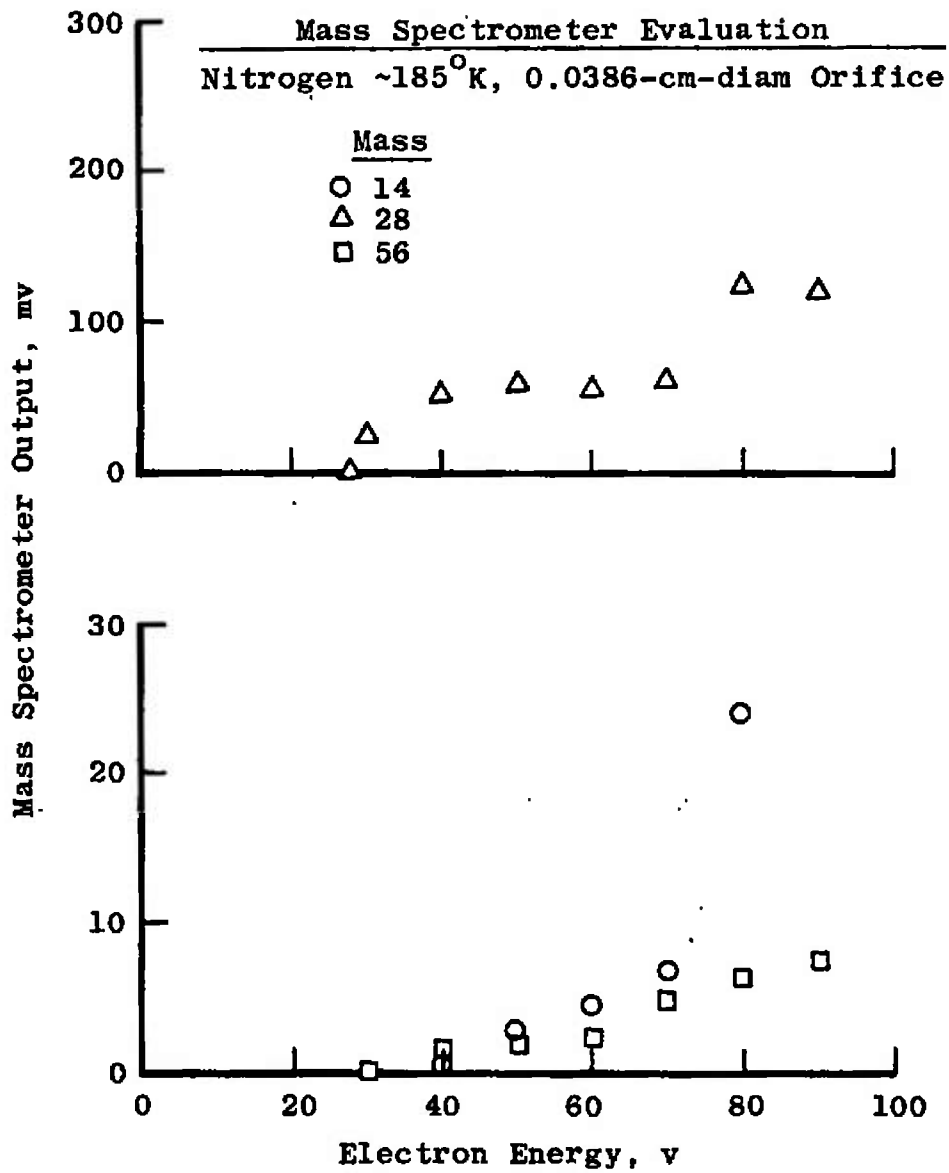

d. Extractor 10v, Focus 135v, Ion Energy 22v, Emission Current ~ 0.2 ma, Electron Multiplier Voltage = 2900

Fig. 11 Concluded

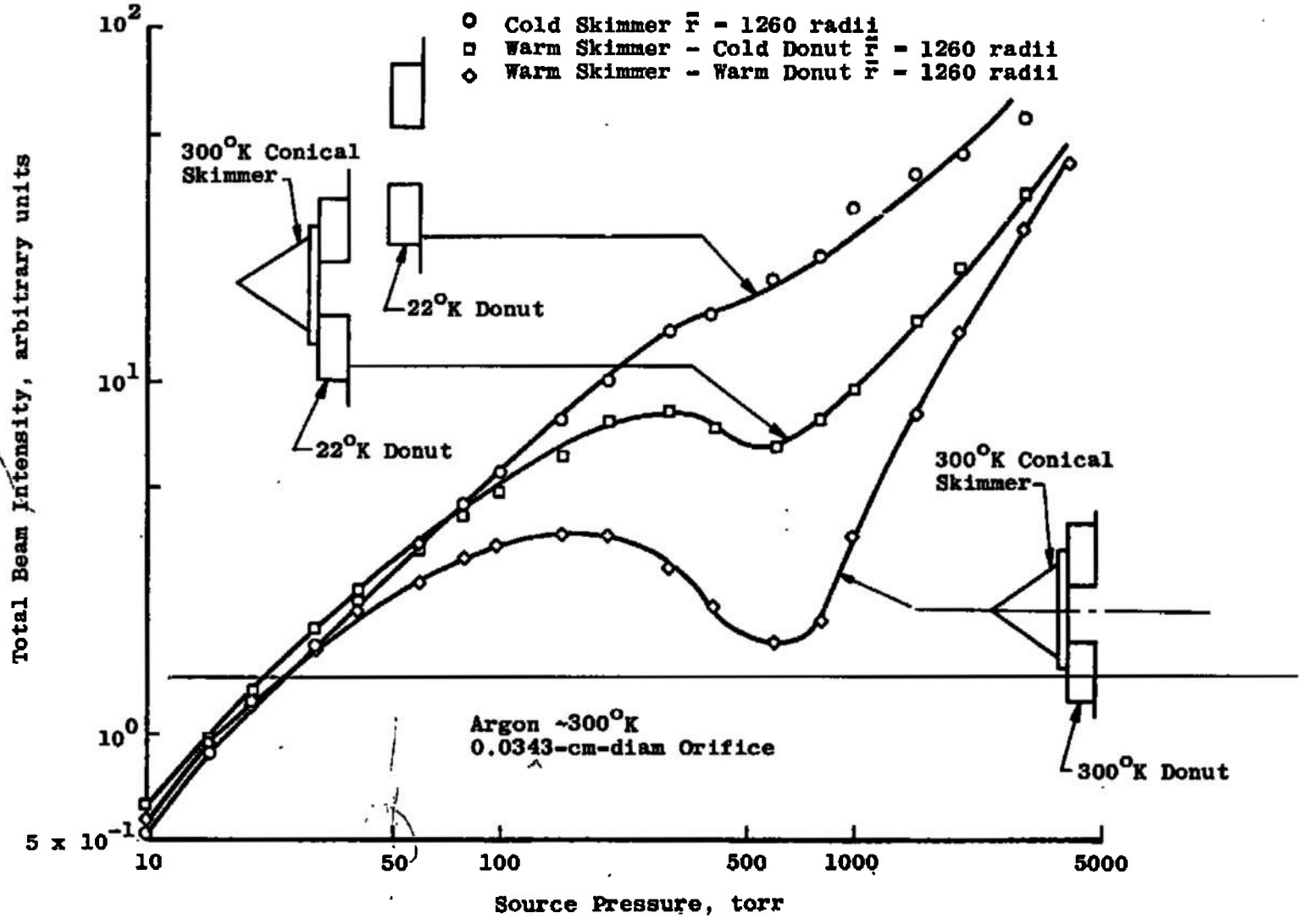

Fig. 12 Effect of Skimmer Interaction on Total Beam Intensity

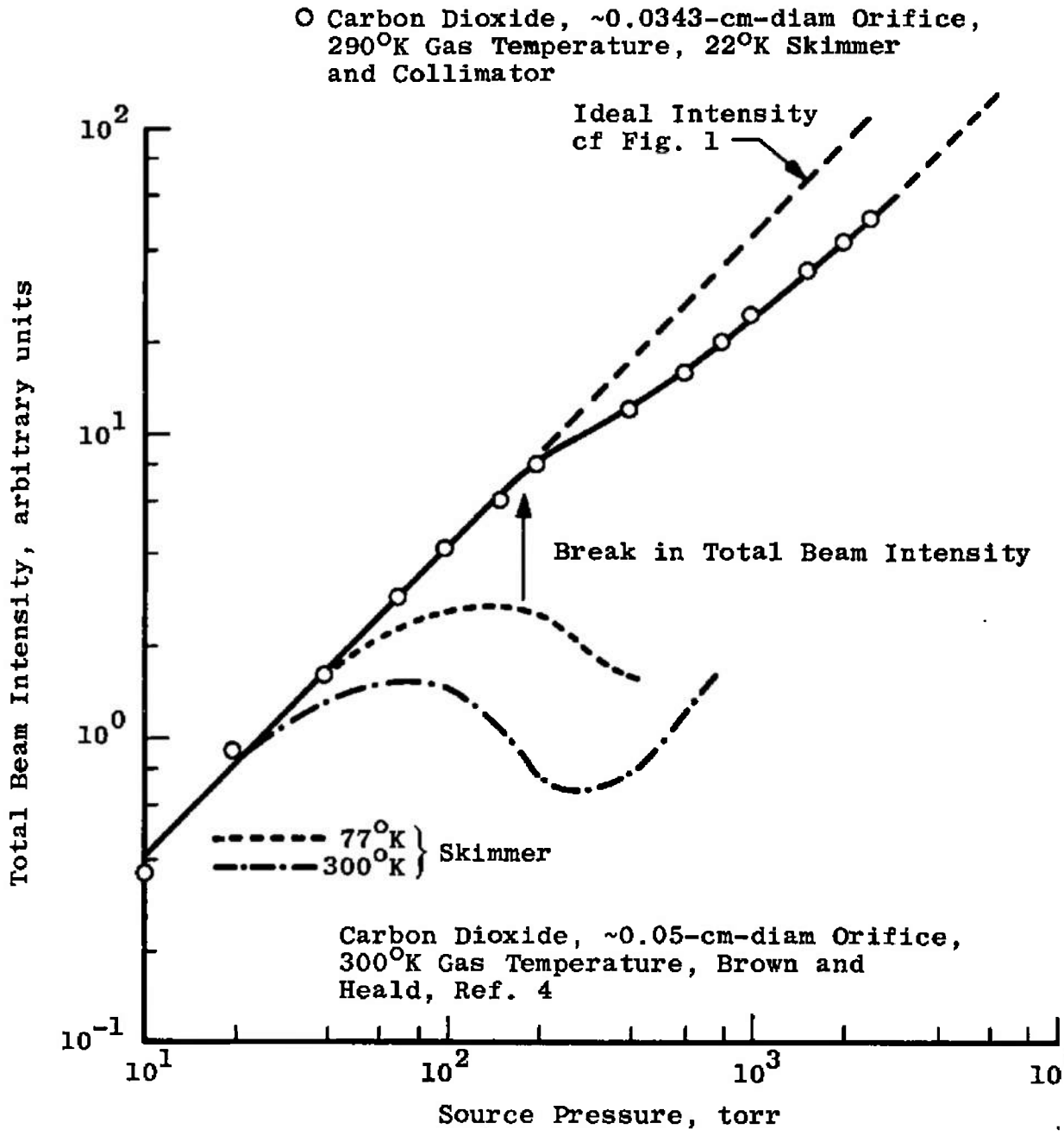

Fig. 13 Effect of Skimmer Interaction on Carbon Dioxide Beam Intensity

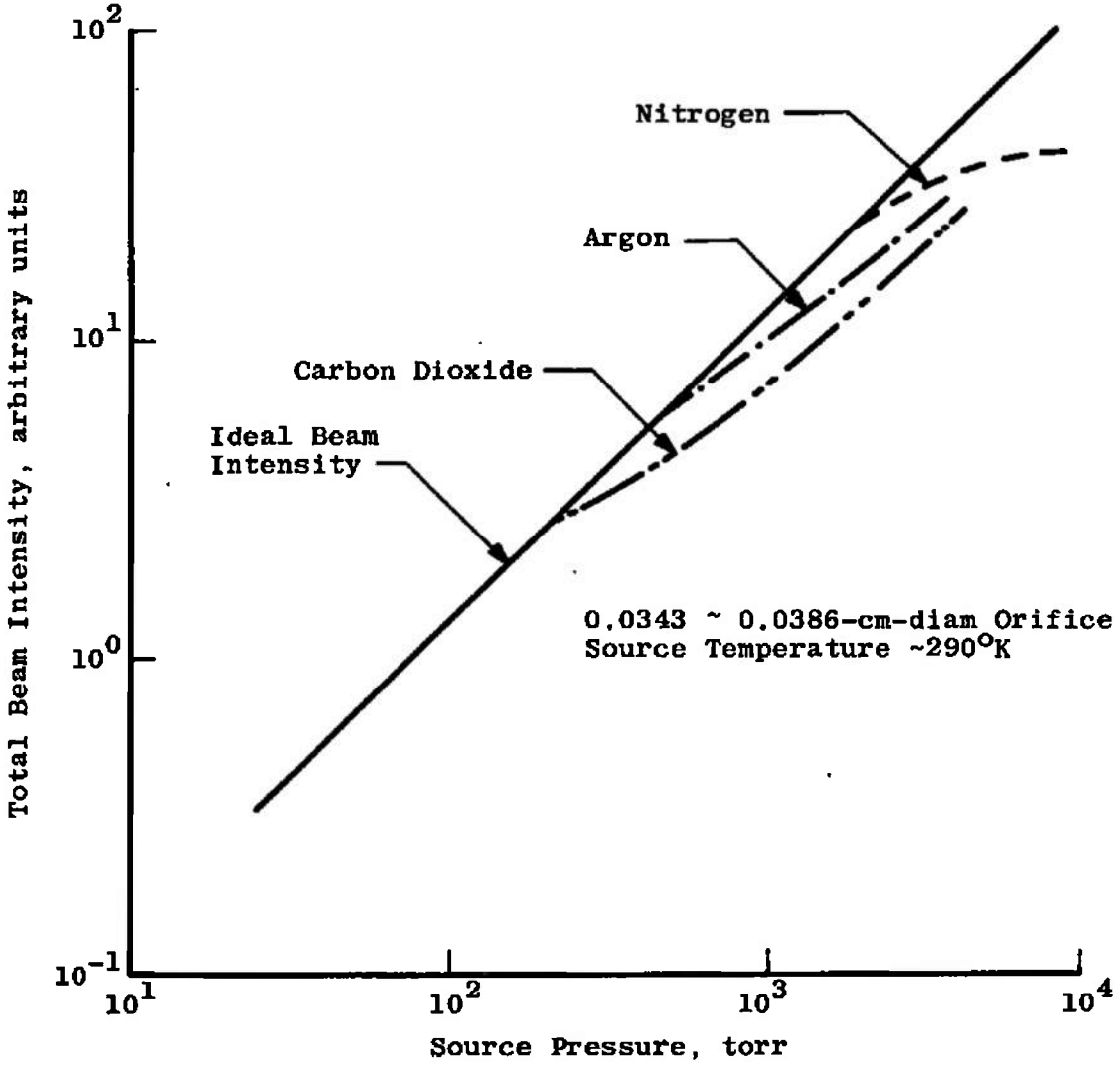

Fig. 14 Variation of Total Beam Intensity with Source Pressure for Various Gases

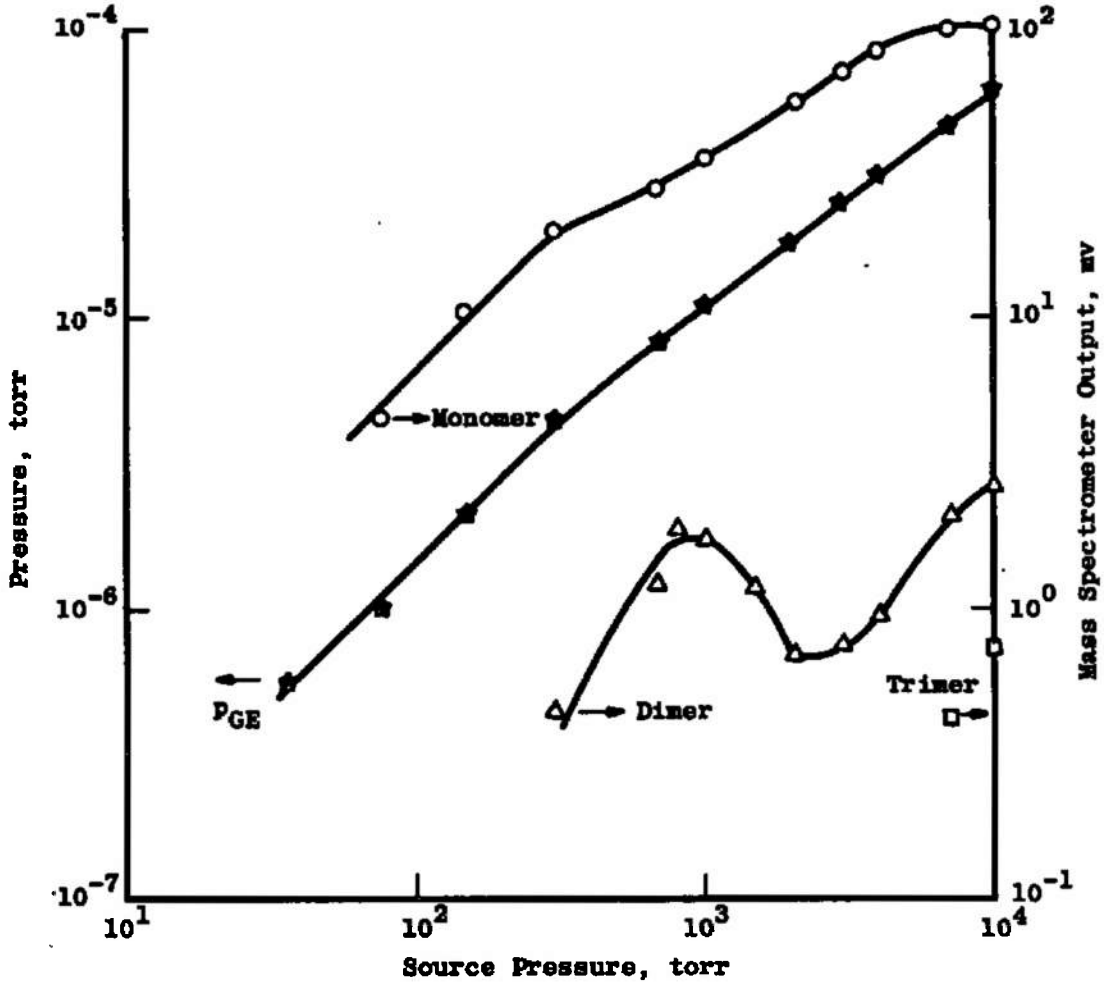

a. Argon ~ 185°K, 0.0147-cm-Diam Orifice

Fig. 15 Total and Individual Mass Beam Intensity as a Function of Source Pressure

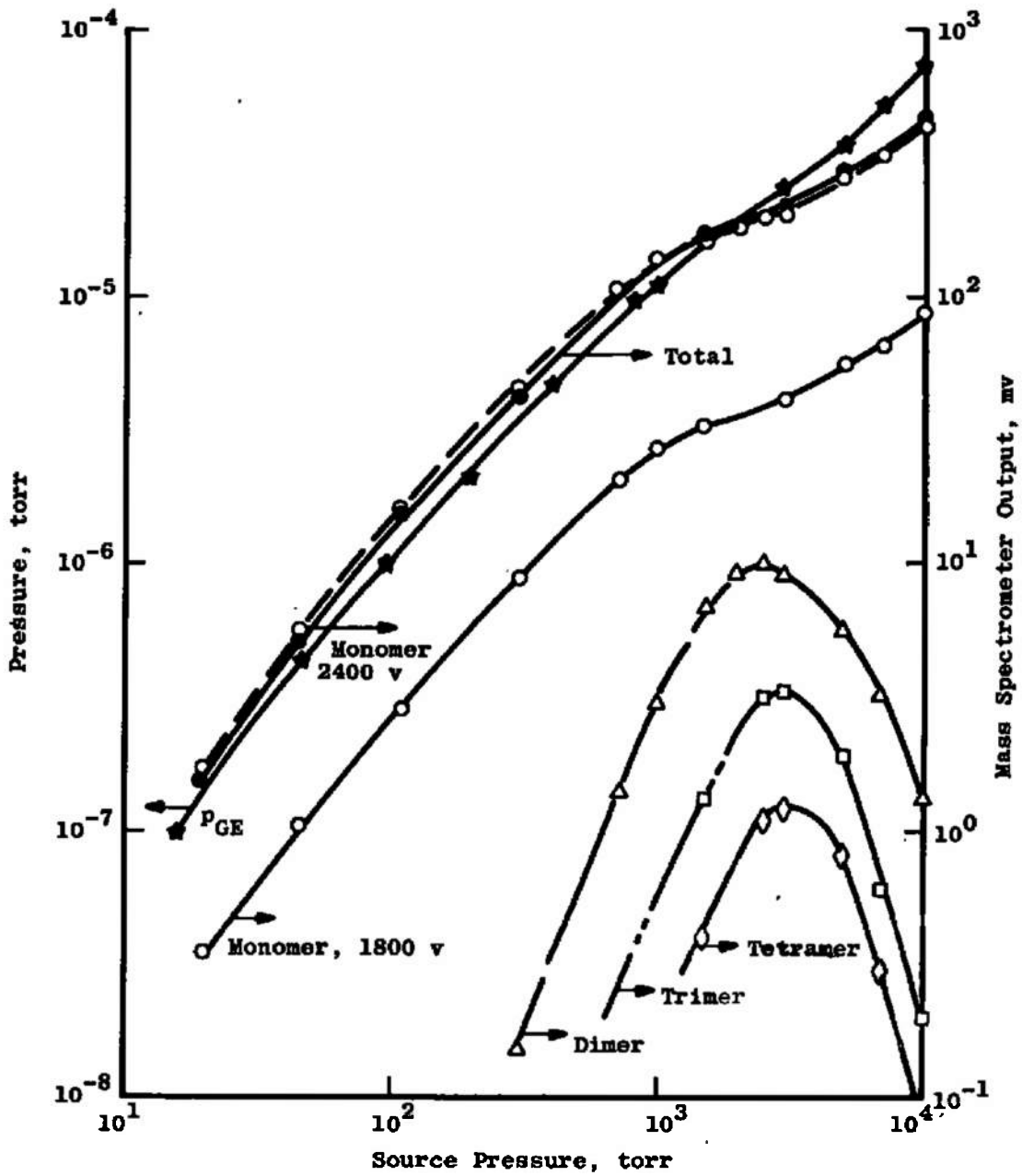

b. Argon ~ 287°K, 0.0147-cm-Diam Orifice
Fig. 15 Continued

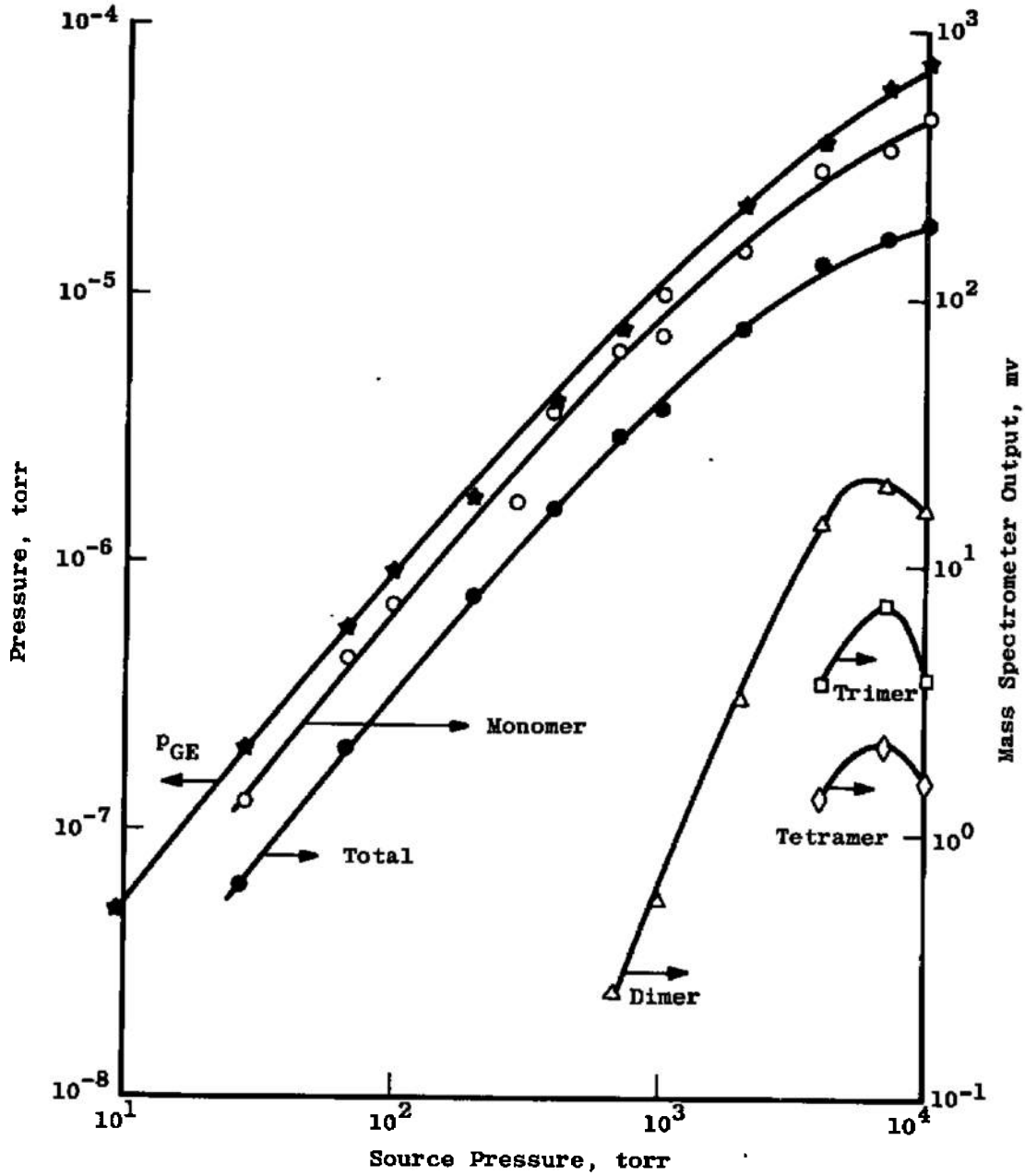

c. Argon ~ 415°K, 0.0147-cm-Diam Orifice
Fig. 15 Continued

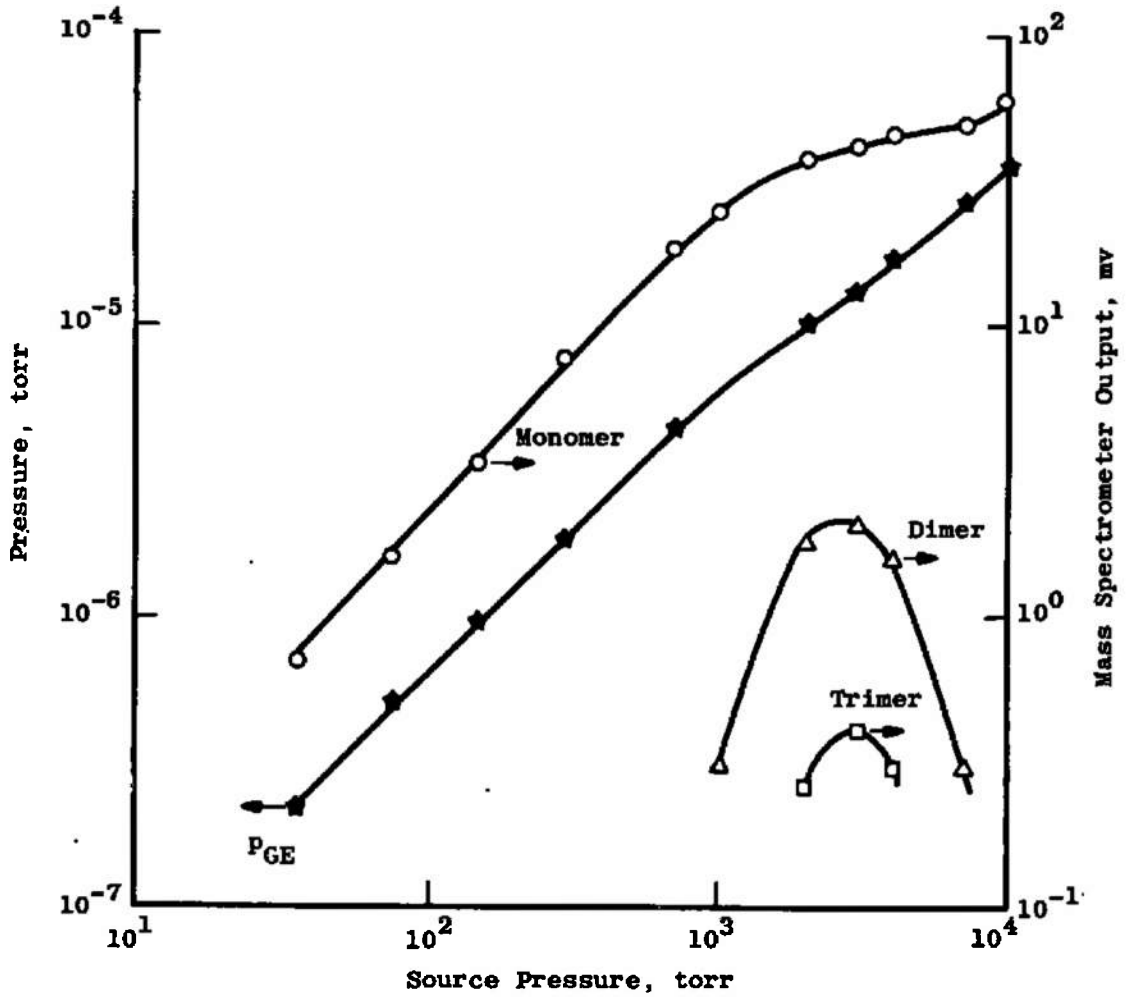

d. Nitrogen ~ 185°K, 0.0147-cm-Diam Orifice
Fig. 15 Continued

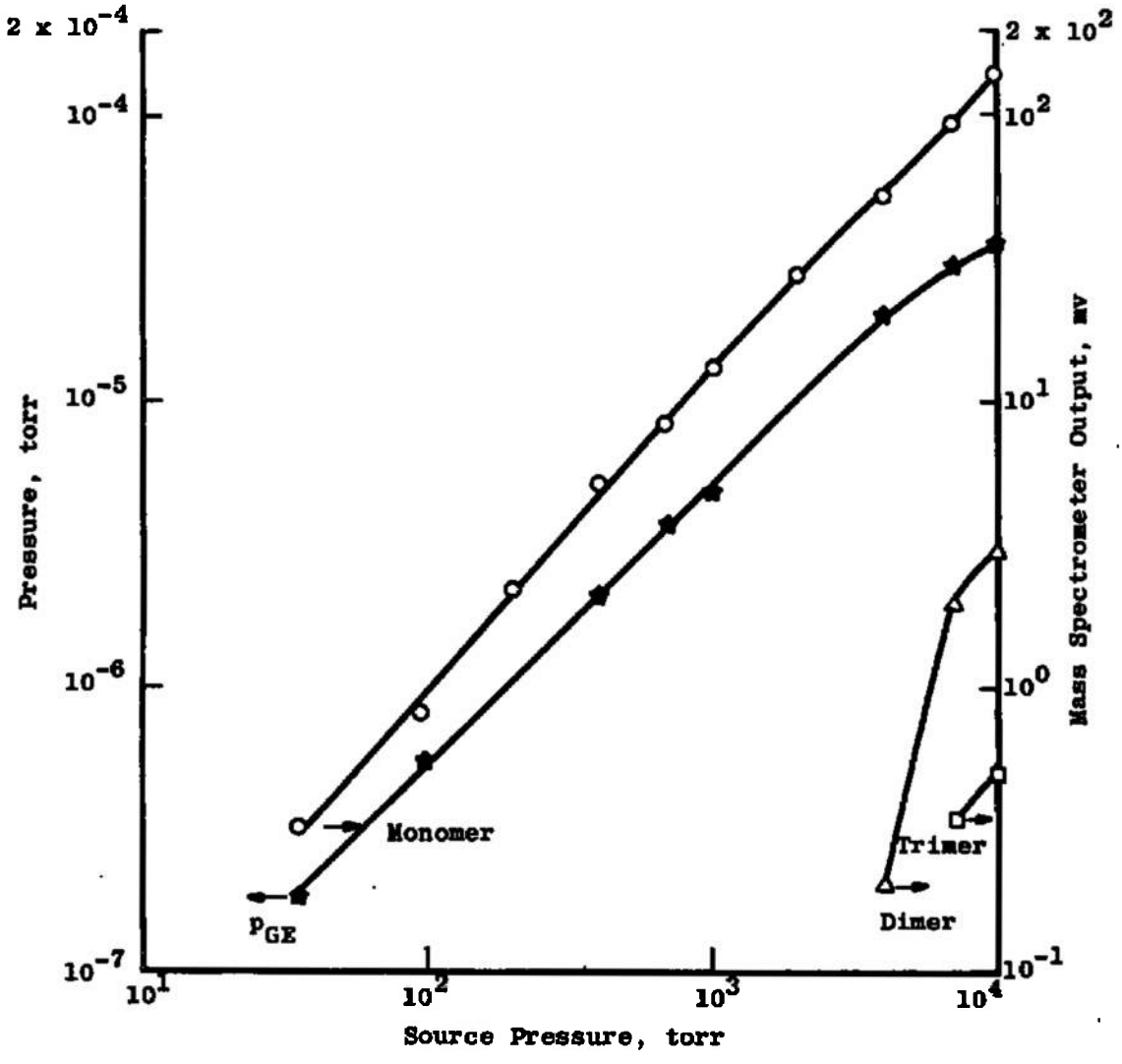

e. Nitrogen ~ 2 85°K, 0.0147-cm-Diam Orifice
Fig. 15 Continued

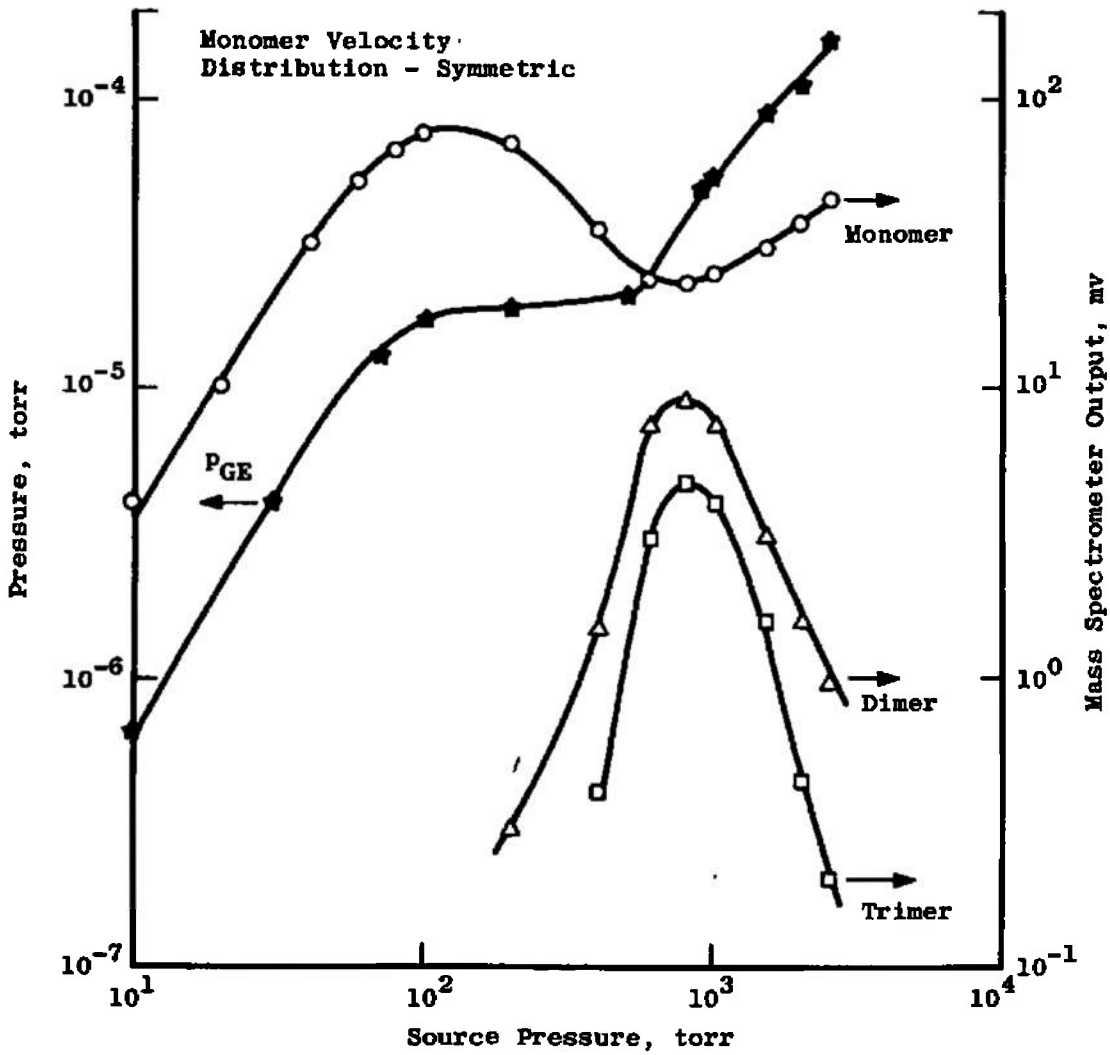

f. Argon ~ 285°K, 0.1245-cm-Diam Orifice
Fig. 15 Continued

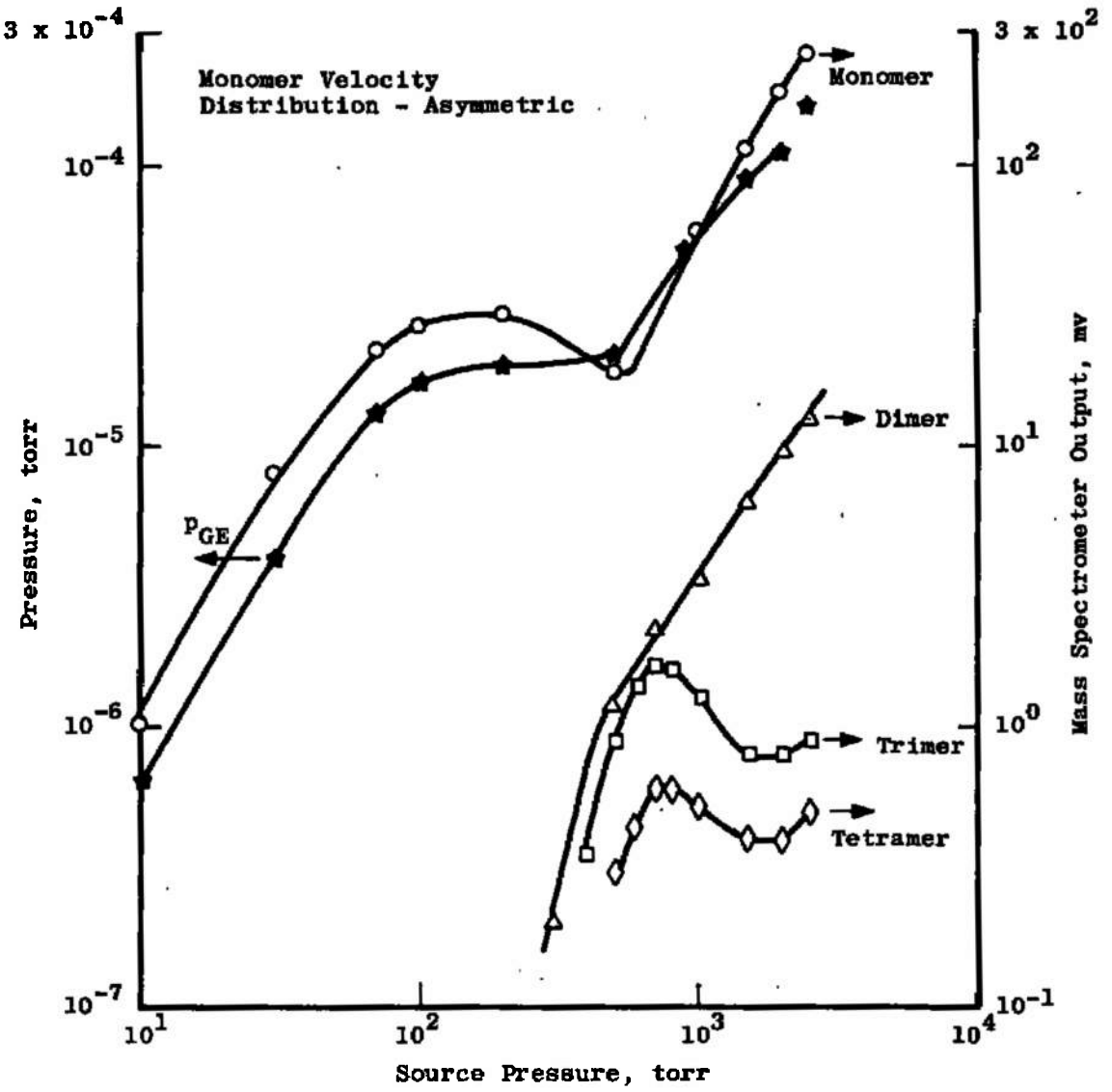

g. Argon ~ 285° K, 0.1245-cm-Diam Orifice

Fig. 15 Continued

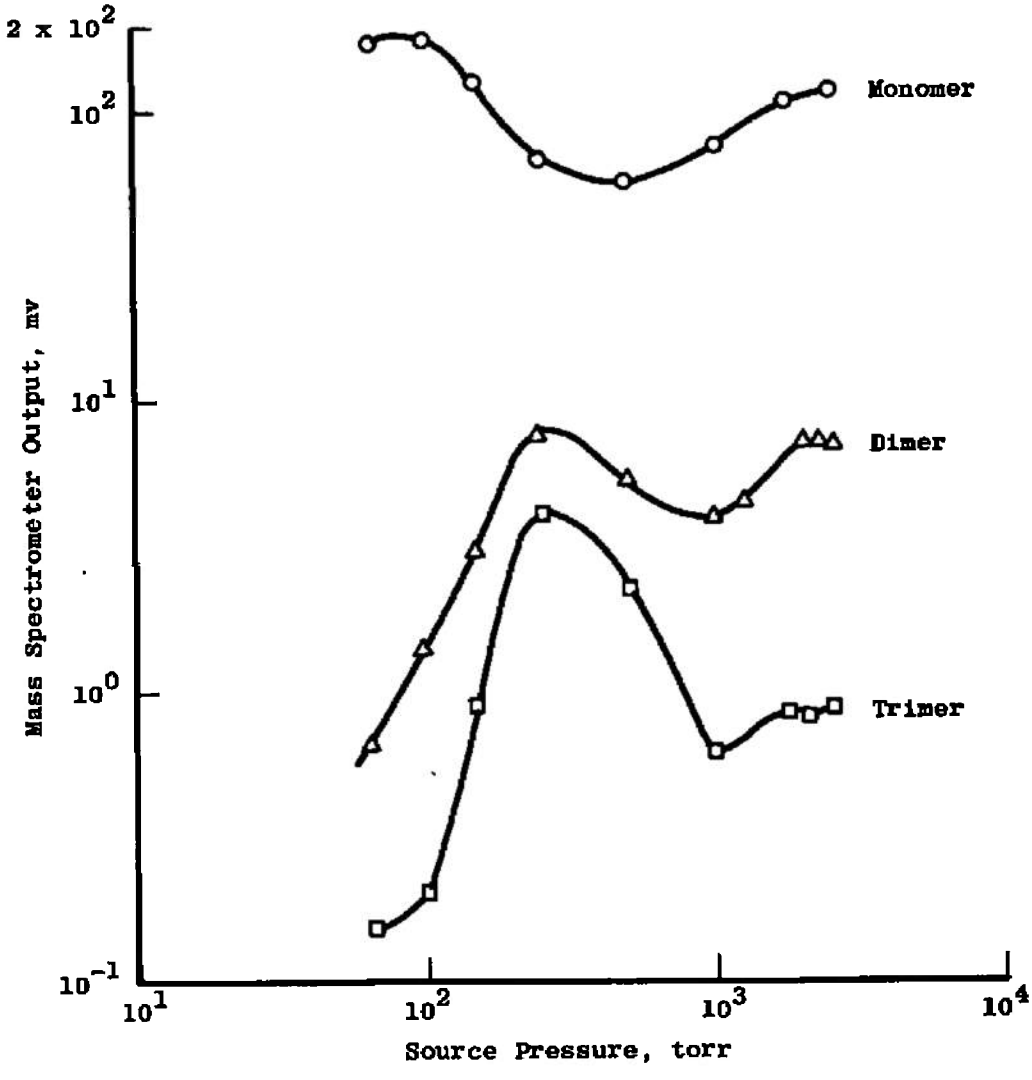

h. Argon ~ 287°K, 0.111-cm-Diam Orifice
Fig. 15 Continued

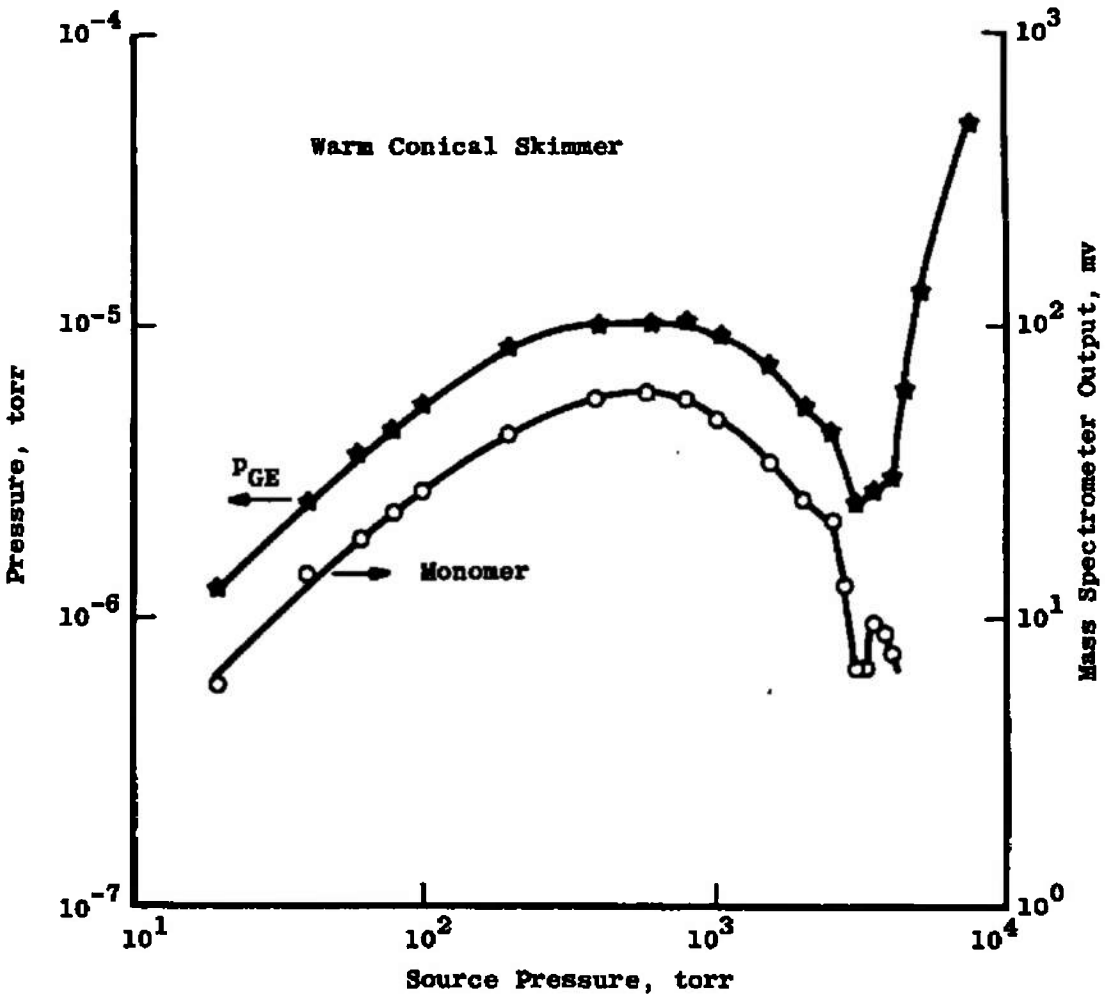

i. Argon ~ 600°K, 0.0343-cm-Diam Orifice
Fig. 15 Continued

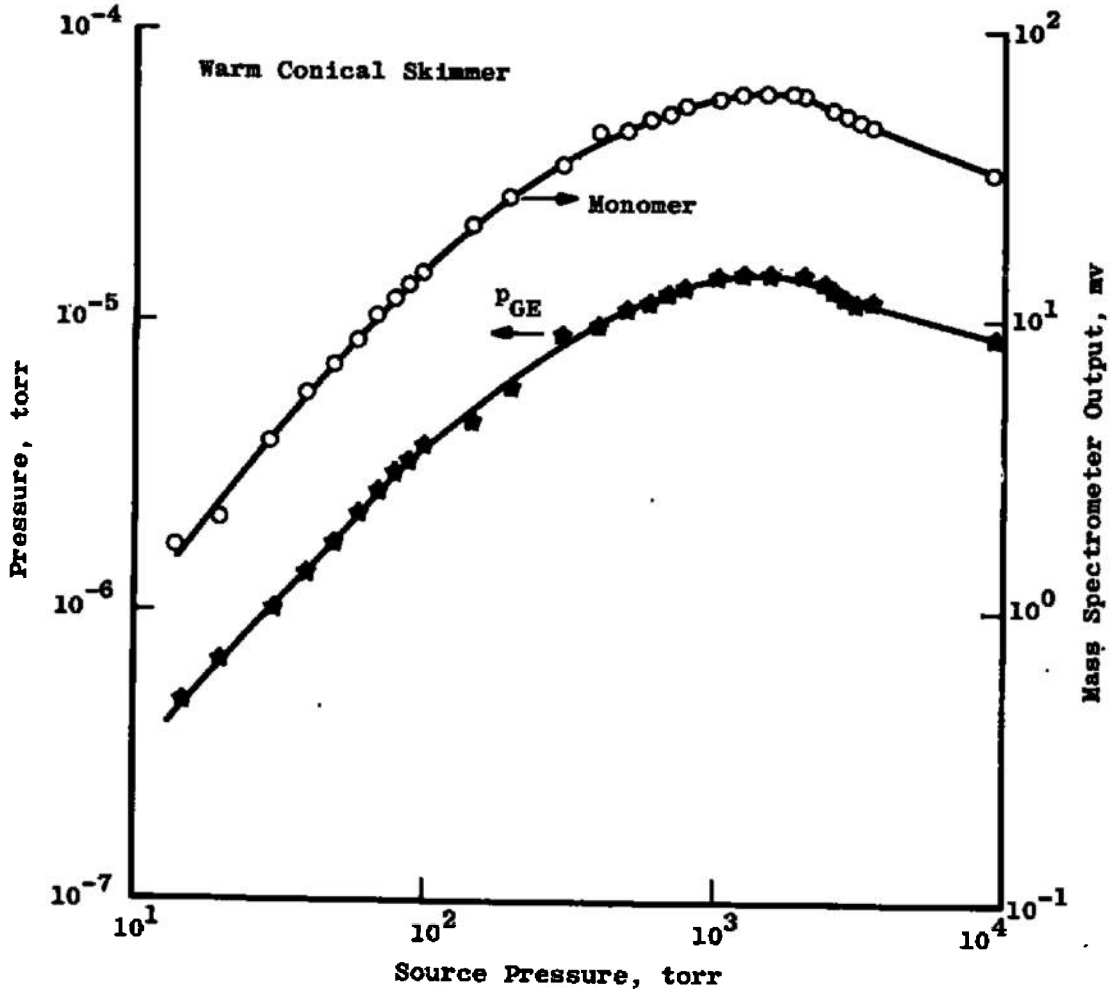

j. Argon ~ 1300°K, 0.0343-cm-Diam Orifice
Fig. 15 Concluded

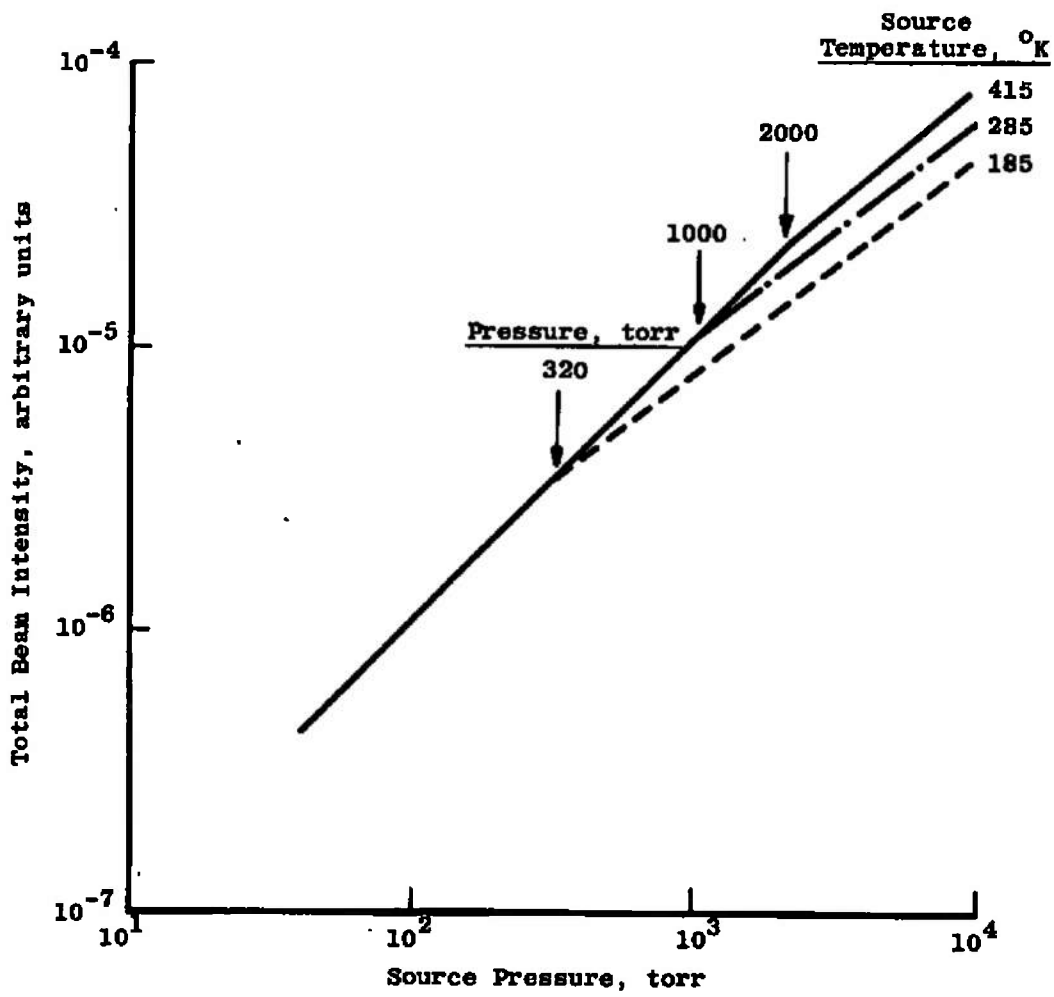

a. Argon, 0.0147-cm Orifice

Fig. 16 Total Beam Intensity Variation with Source Pressure

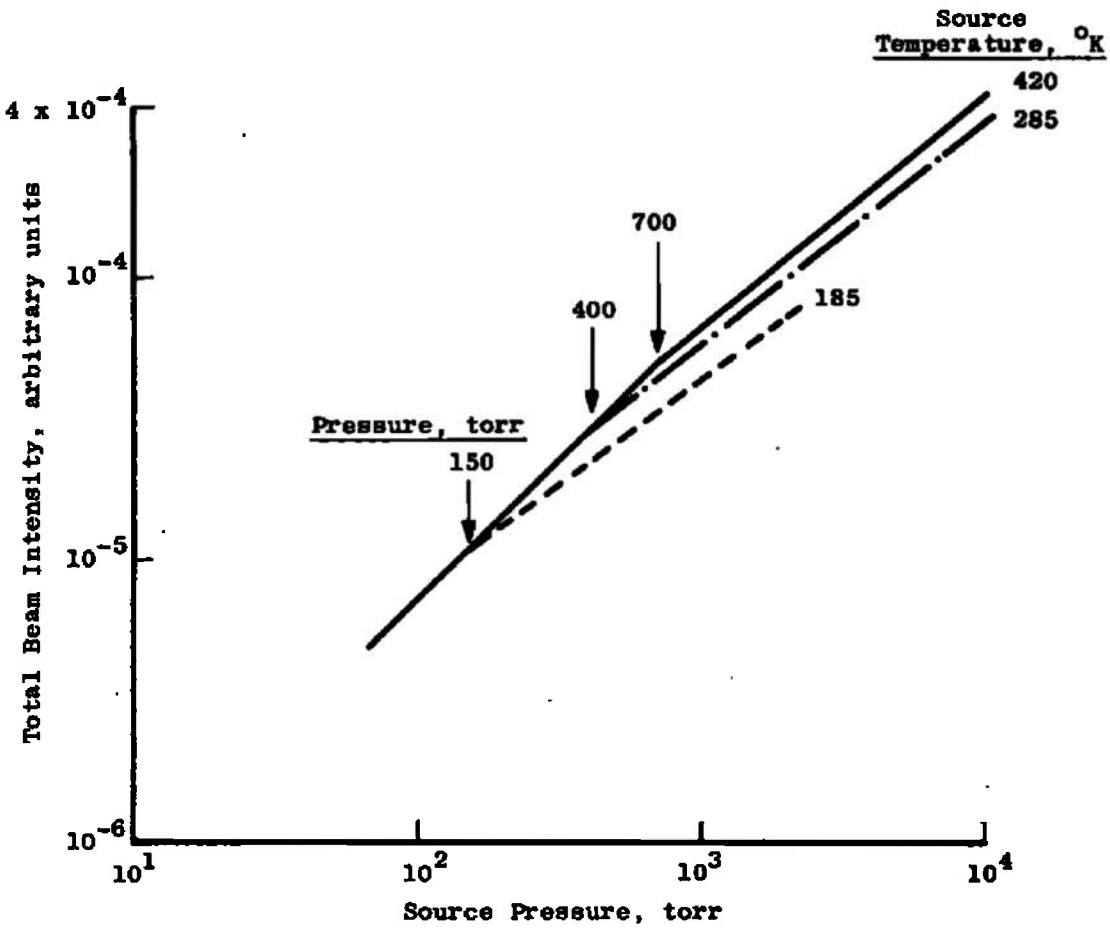

b. Argon, 0.0386-cm Orifice
Fig. 16 Continued

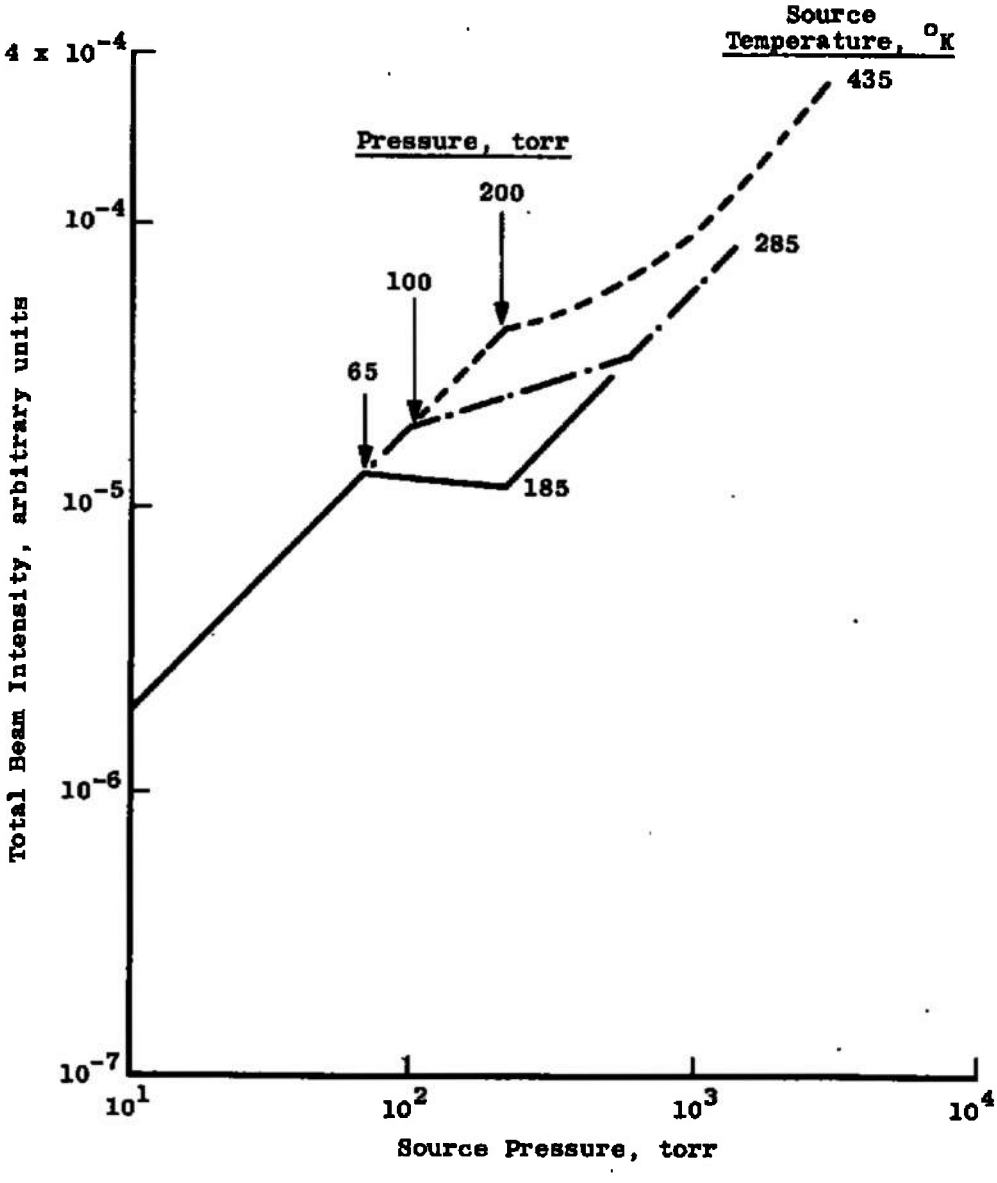

c. Argon, 0.1245-cm Orifice
Fig. 16 Concluded

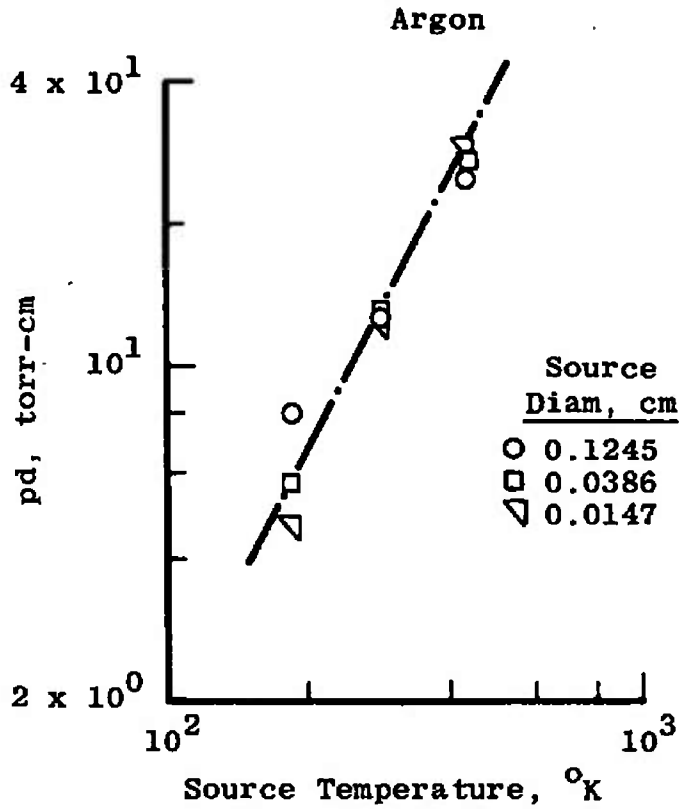

Fig. 17 Temperature Dependence of the Pressure-Diameter Product at Which the Break in Total Beam Intensity Occurs

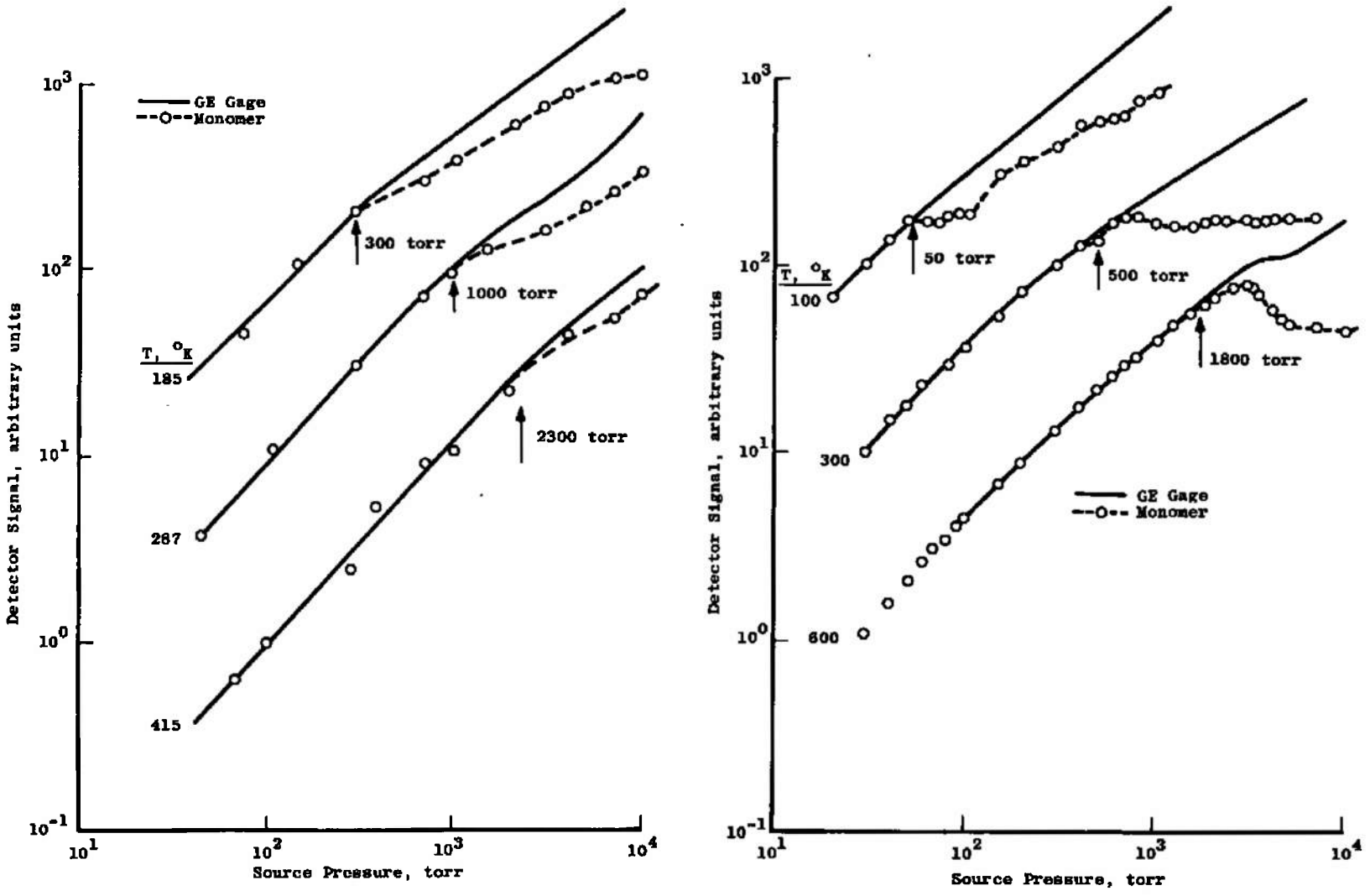

a. Argon-Present Test, 0.0147-cm Orifice, Cold Skimmer

b. Argon-Ref. 2, 0.0343-cm Orifice, Cold Skimmer

Fig. 18 Comparison of Total and Monomer Beam Intensity Measurements

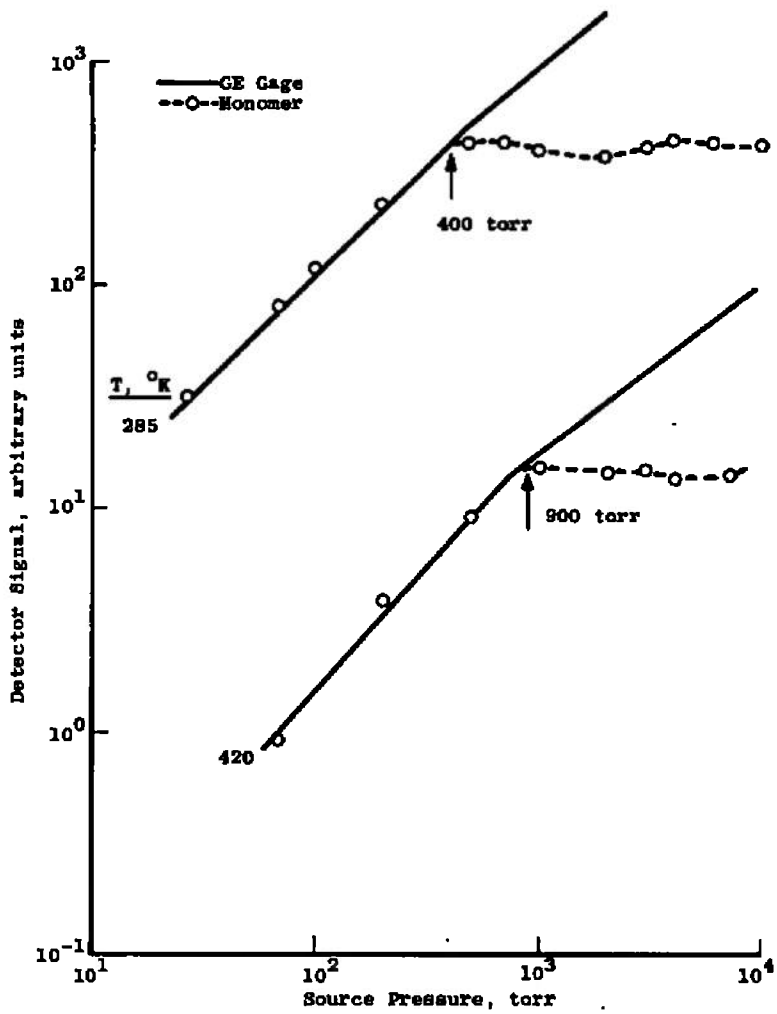

c. Argon-Present Test, 0.0386-cm Orifice, Cold Skimmer
Fig. 18 Continued

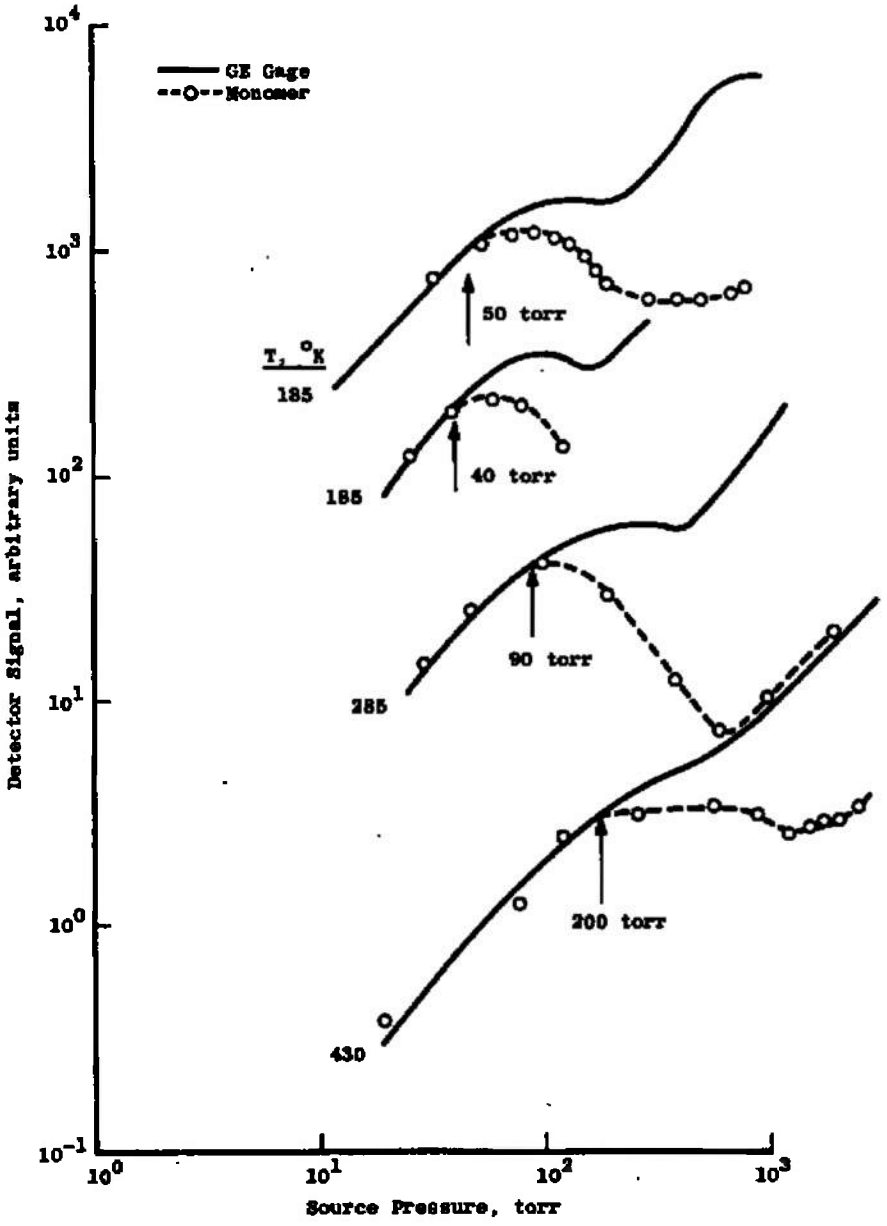

d. Argon-Present Test, 0.1245-cm Orifice, Cold Skimmer
Fig. 18 Continued

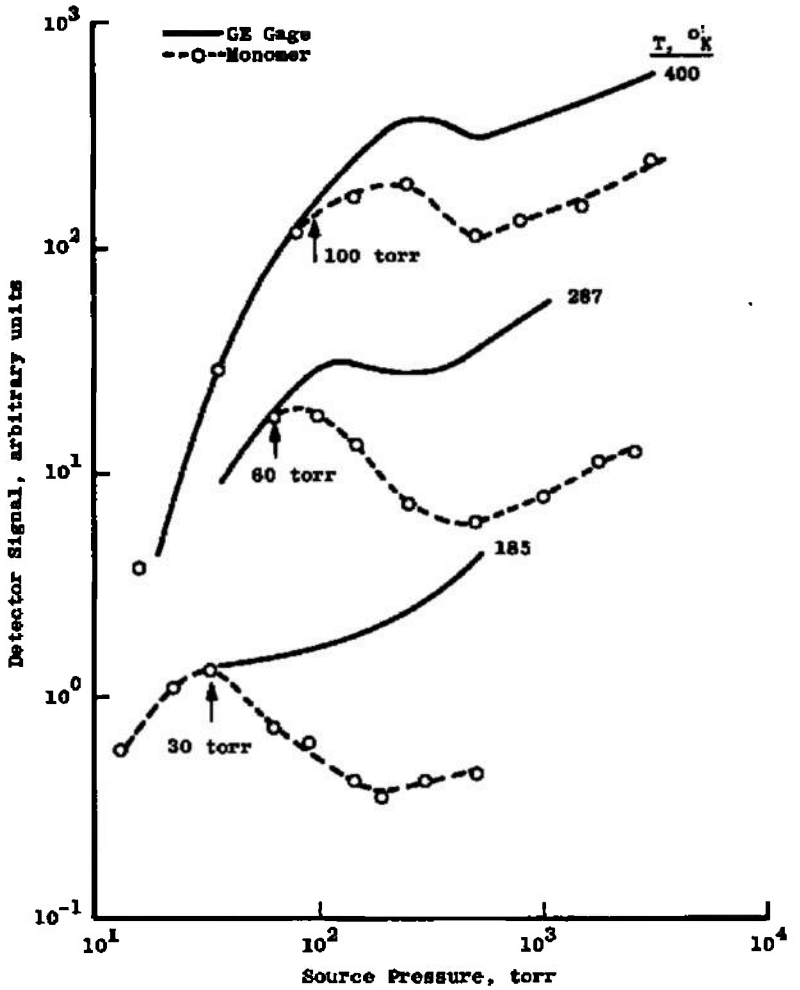

e. Argon-Present Test, 0.111-cm Conical Nozzle, Cold Skimmer
Fig. 18 Continued

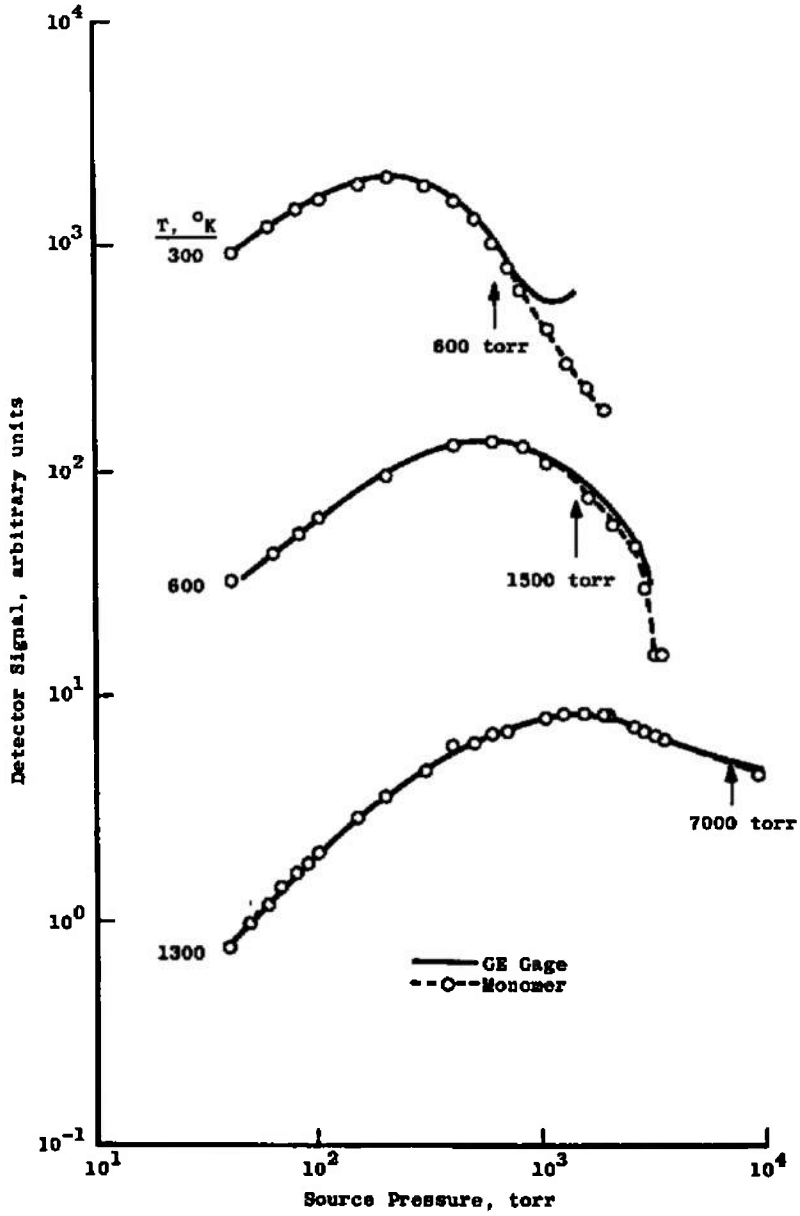

f. Argon-Present Test, 0.0343-cm Orifice, Warm Conical Skimmer
Fig. 18 Continued

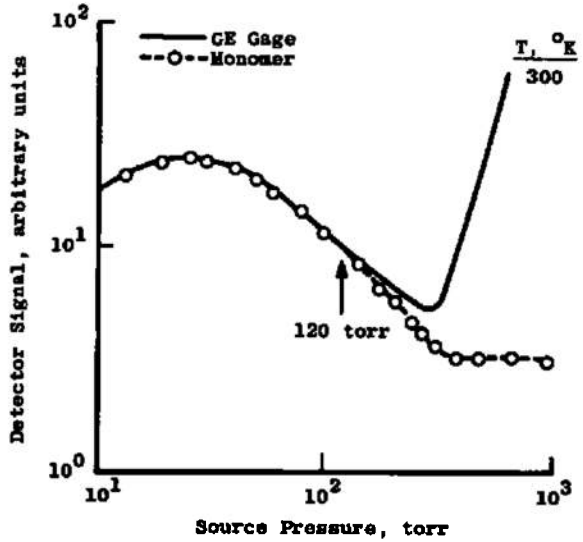

g. Argon-Ref. 7, 0.117-cm Orifice, Warm Conical Skimmer

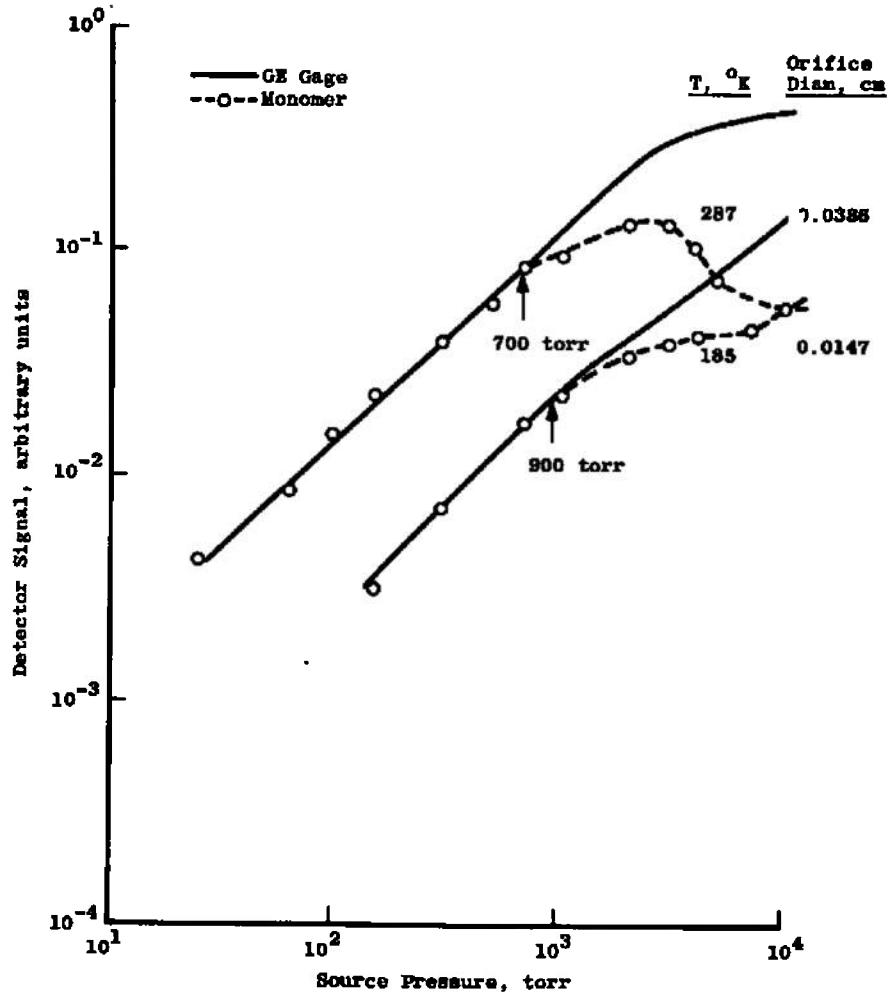

h. Nitrogen-Present Test, Cold Skimmer

Fig. 18 Continued

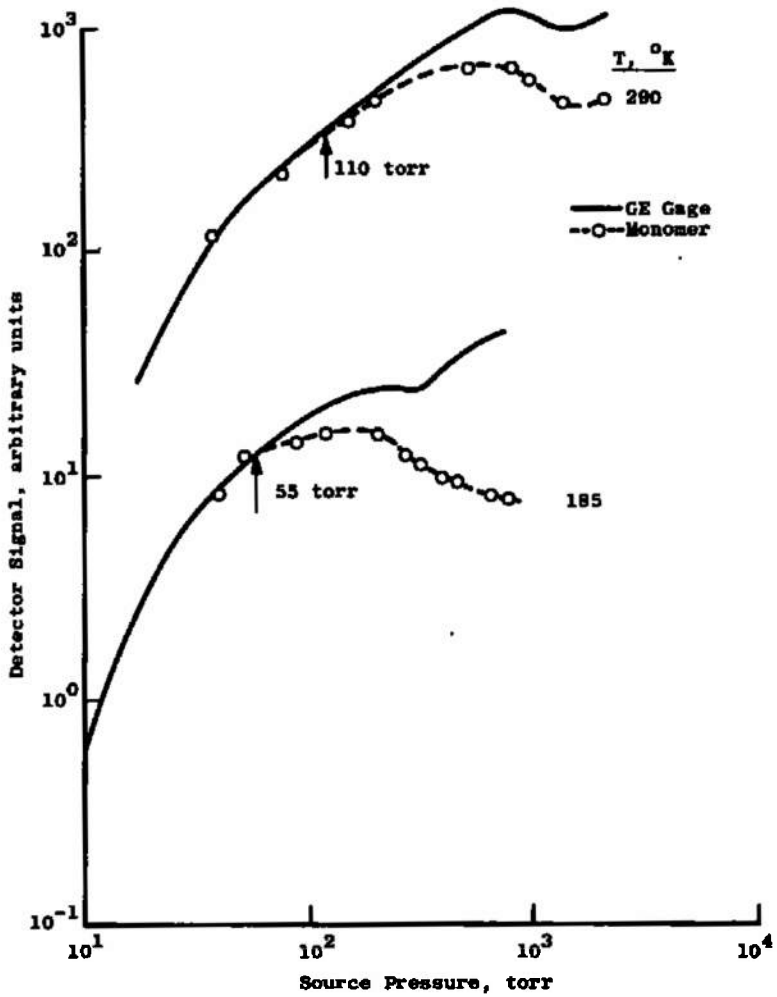

i. Nitrogen-Present Test, 0.111-cm Conical Nozzle, Cold Skimmer

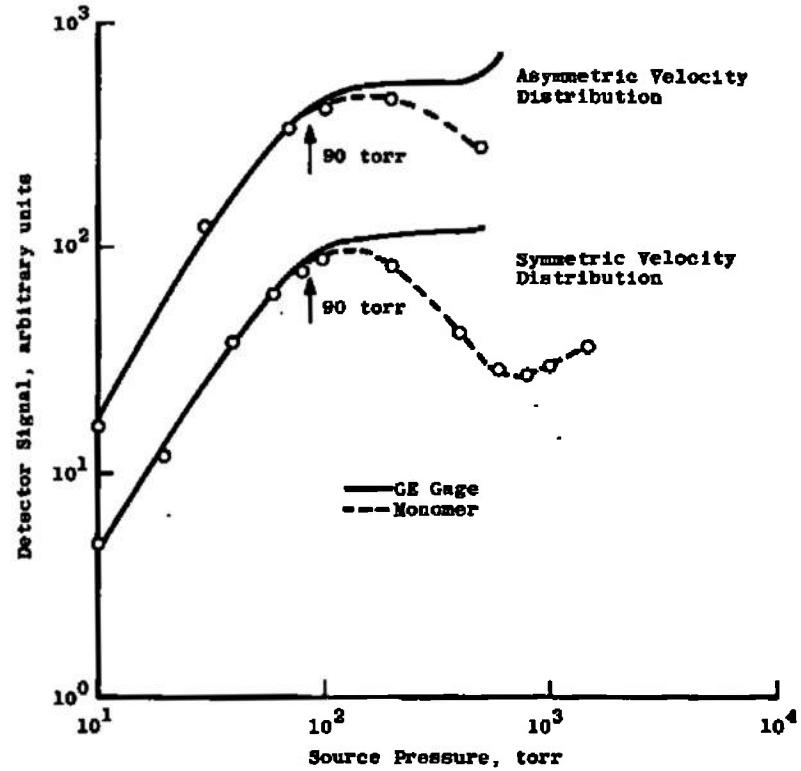

j. Argon ~ 285°K-Present Test, 0.1245-cm Orifice, Cold Skimmer

Fig. 18 Concluded

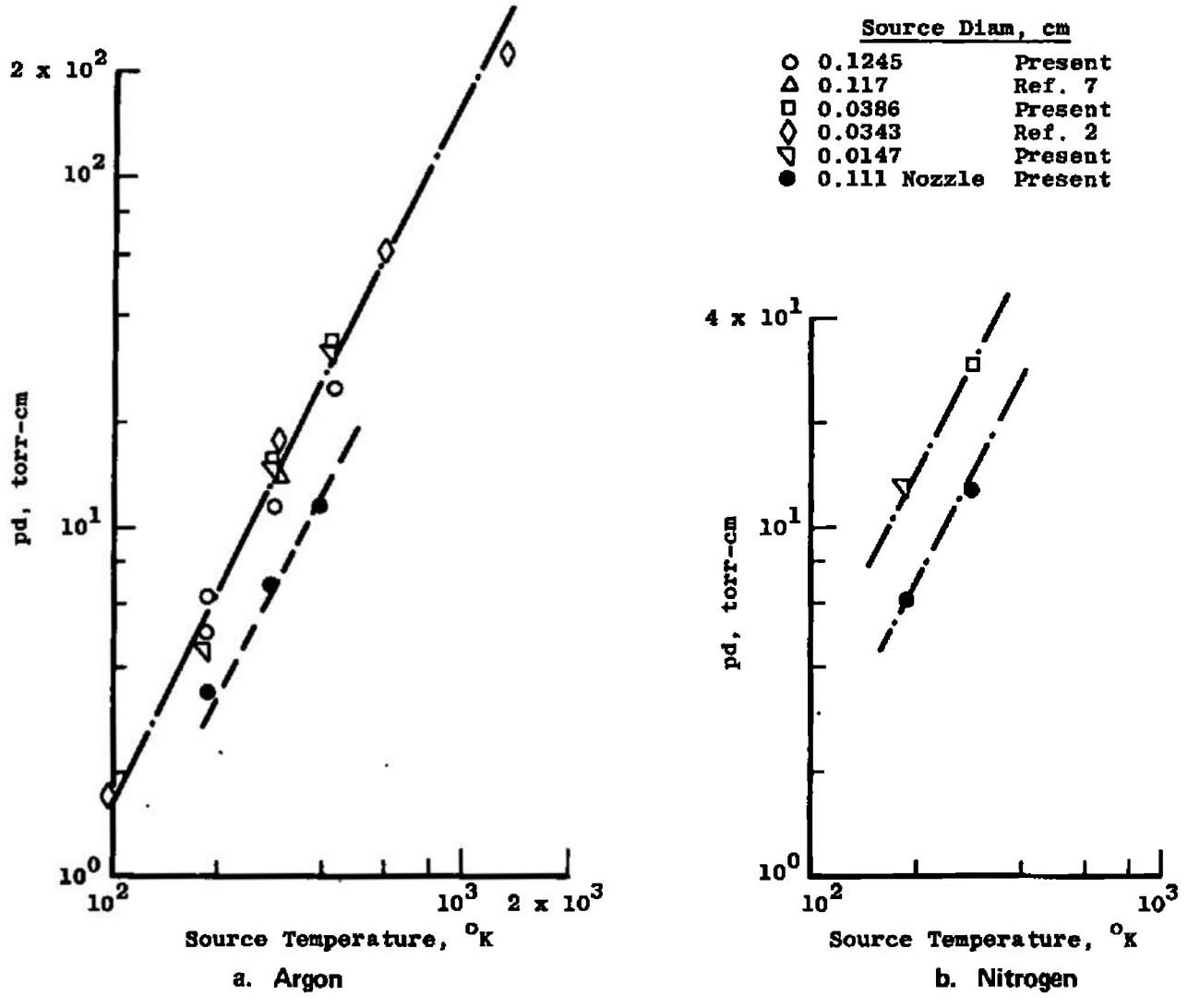

Fig. 19 Pressure at Which Total and Monomer Beam Intensities First Deviate

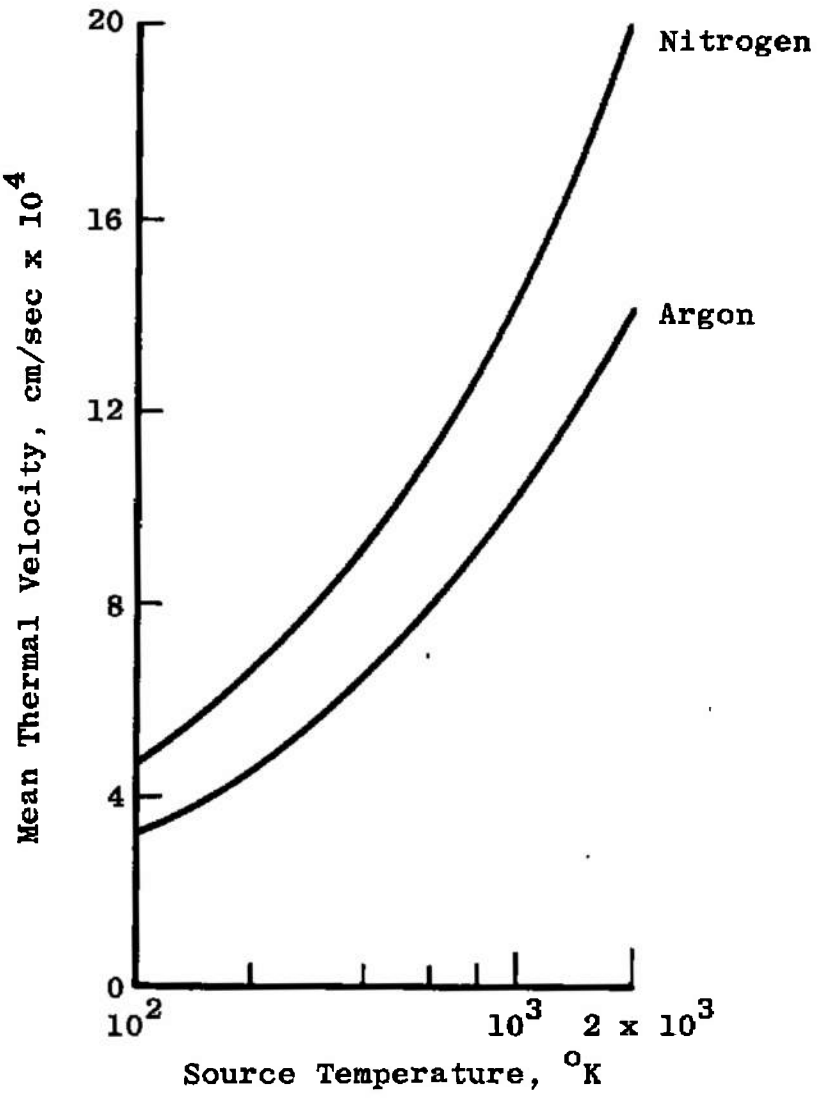

Fig. 20 Thermal Speed of a Gas as a Function of Temperature

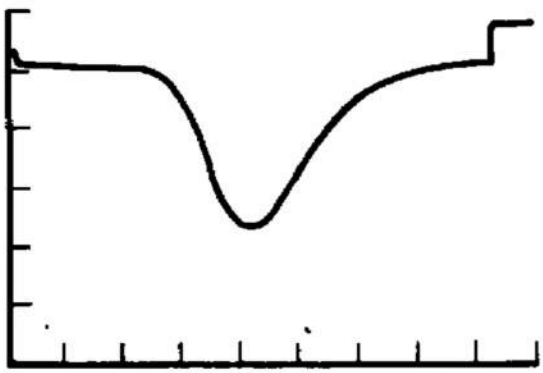

10,000 torr

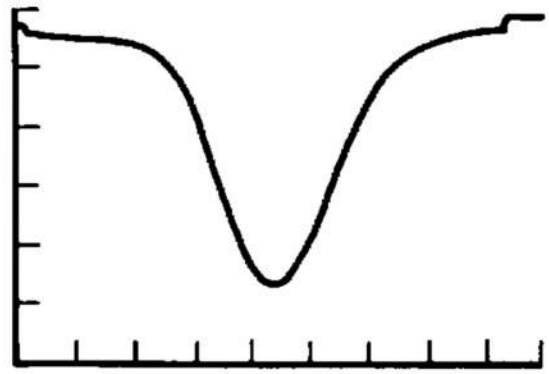

40 torr

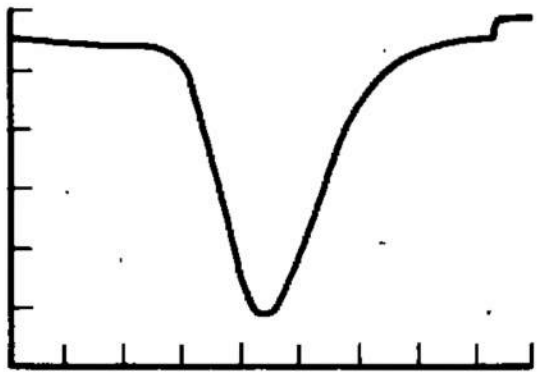

3000 torr

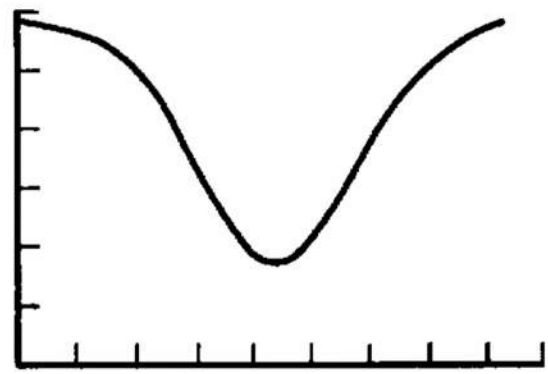

10 torr

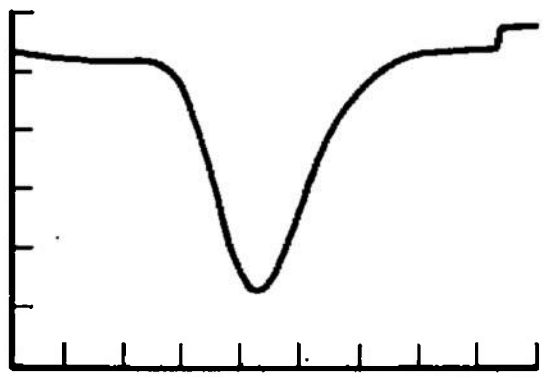

550 torr, Source Pressure

a. Argon-Monomer, Temperature ~ 300°K, Diameter ~ 0.0386 cm

Fig. 21 Velocity Distribution for an Argon Beam

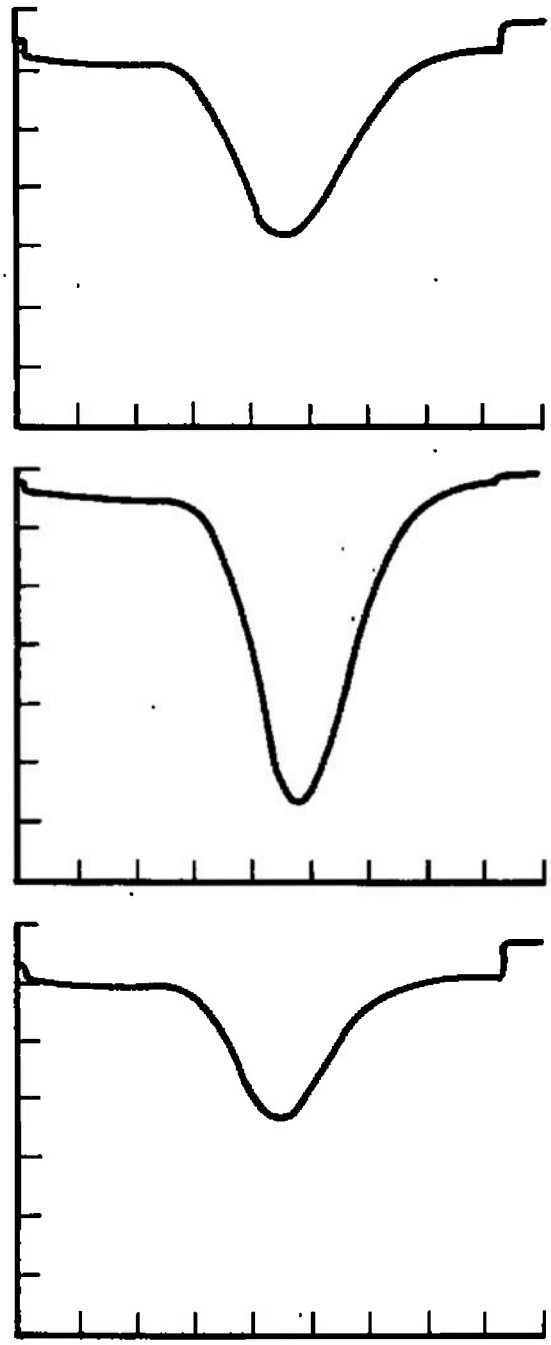

b. Argon-Dimer, Temperature ~ 300°K, Diameter ~ 0.0386 cm
Fig. 21 Concluded

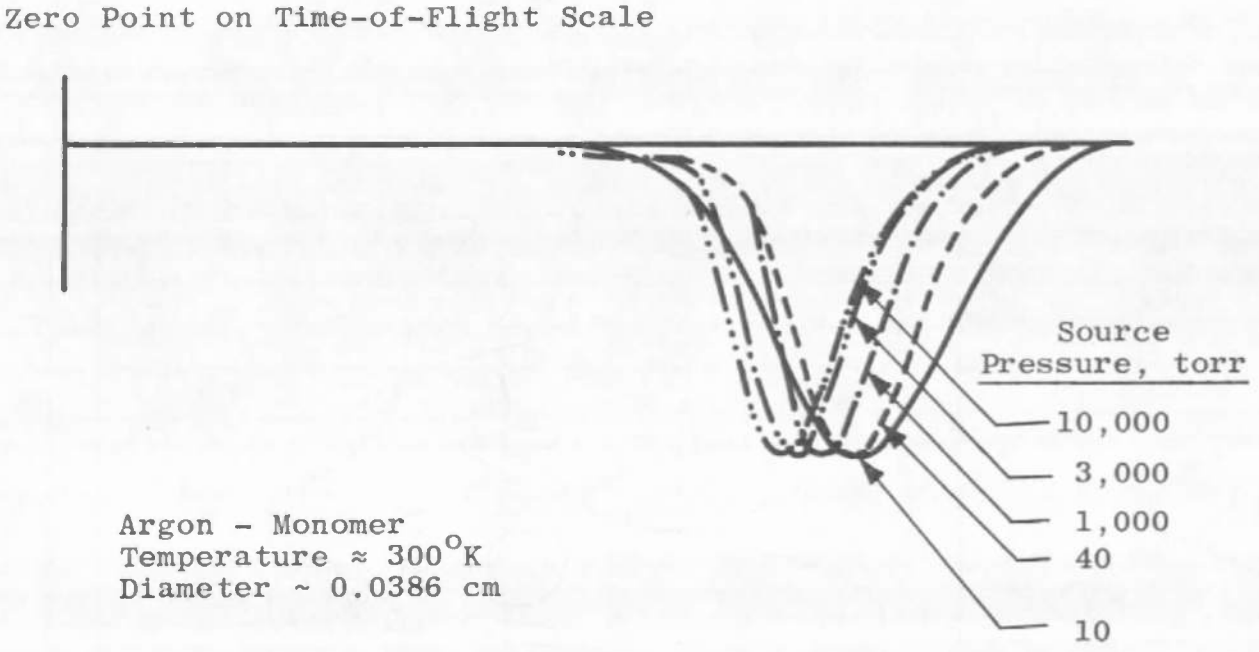

Fig. 22 Effect of Source Pressure on Velocity Distribution

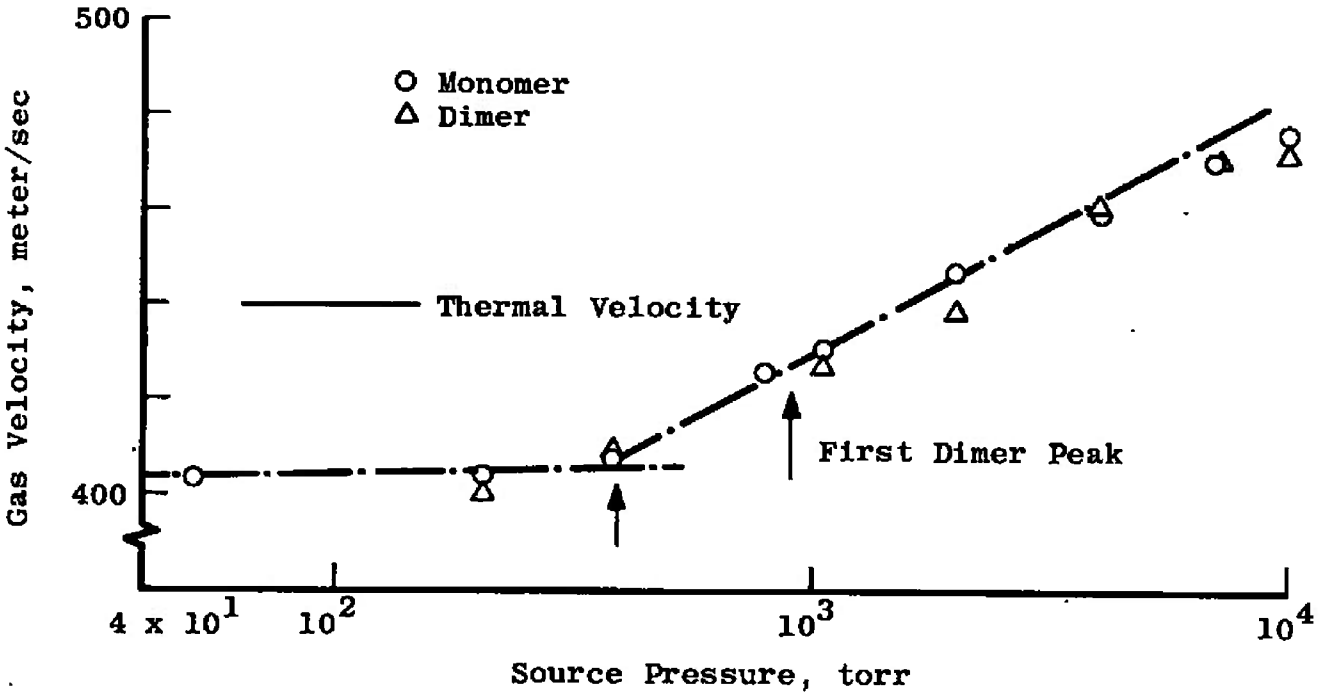

a. Argon ~ 185°K, 0.0147-cm Orifice

Fig. 23 Gas Velocity as a Function of Source Pressure

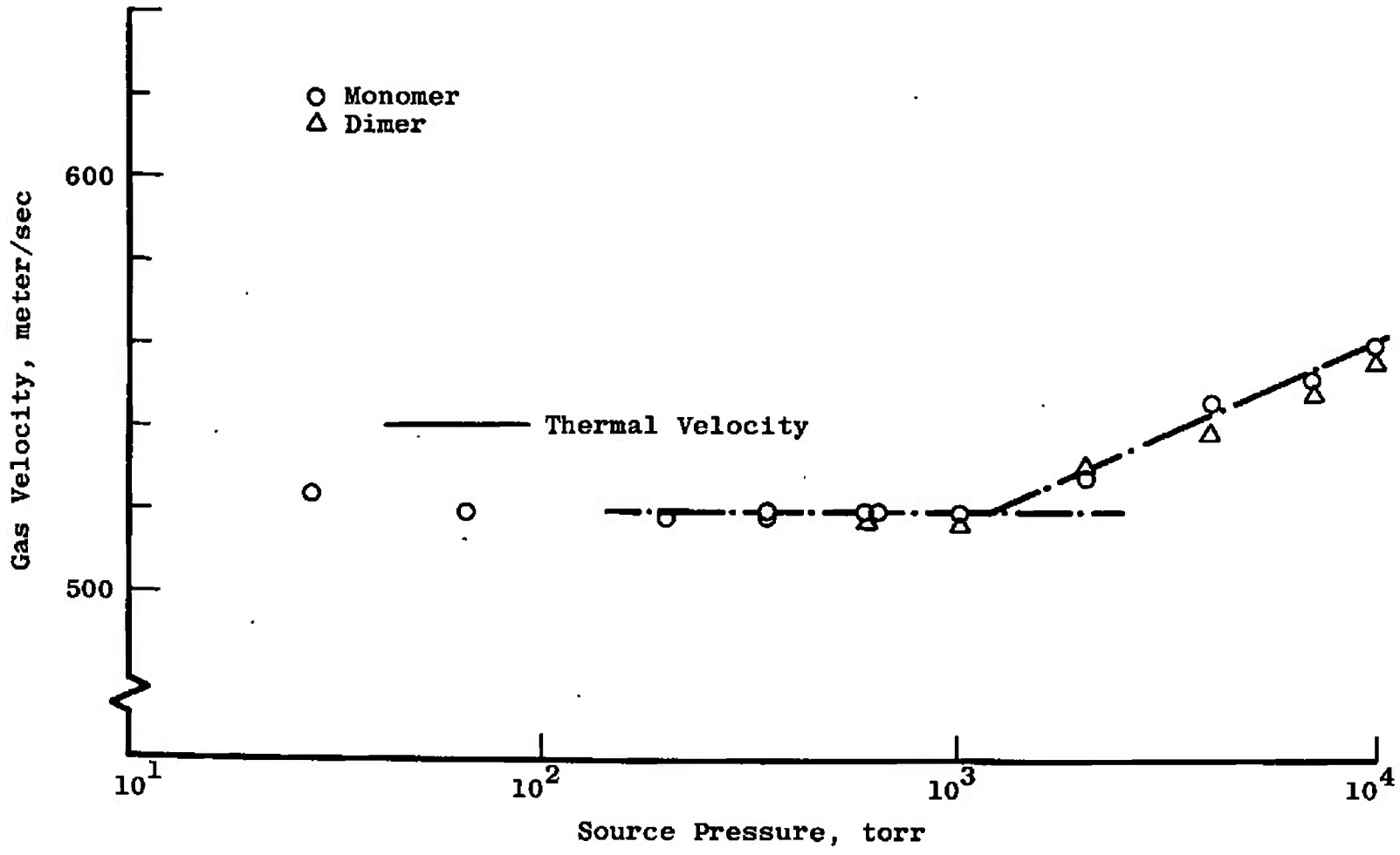

b. Argon ~ 285 ± 3°K, 0.0147-cm Orifice
Fig. 23 Continued

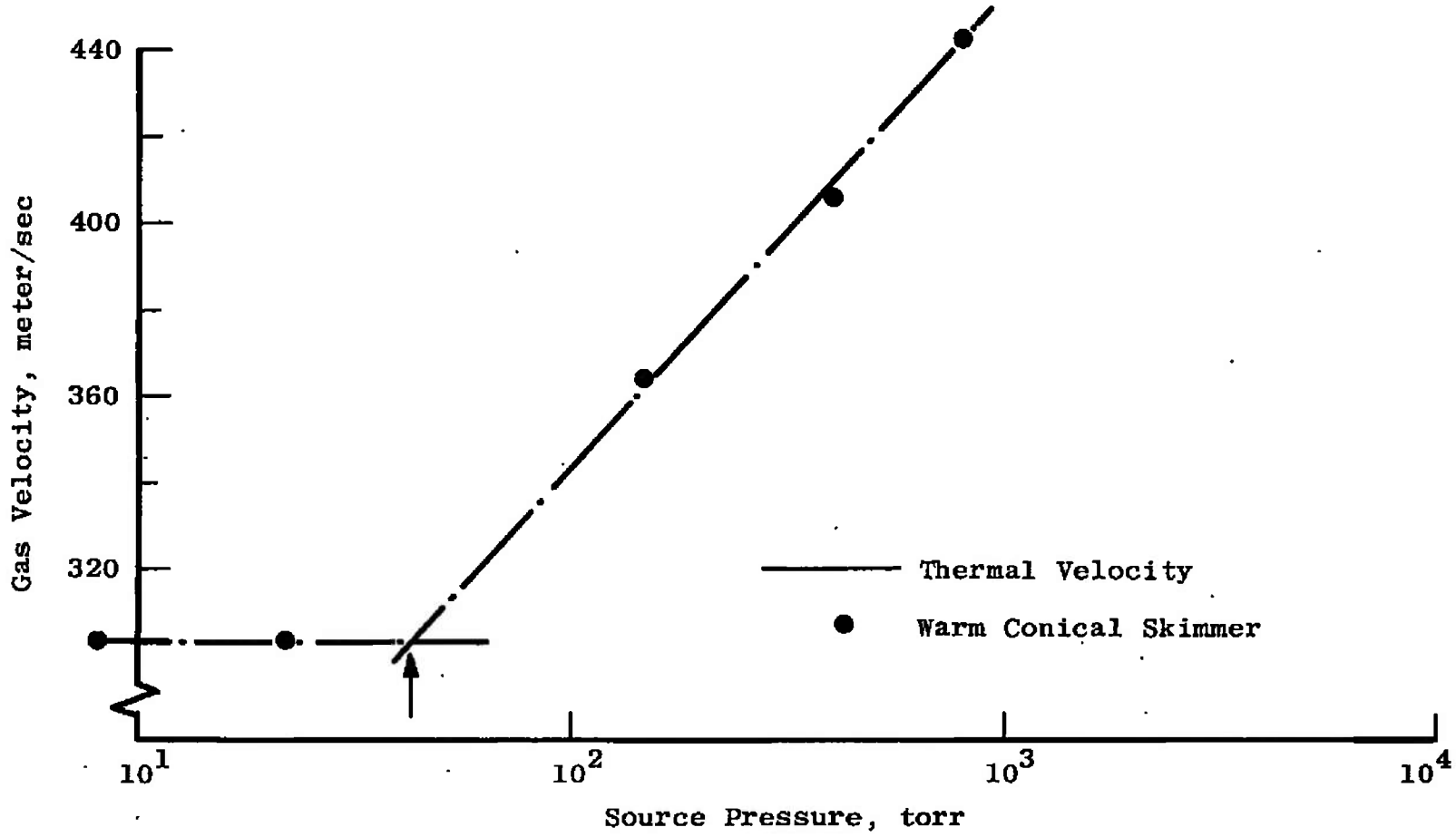

c. Argon ~ 100°K, Ref. 2, 0.0343-cm Orifice, Monomer Velocity
Fig. 23 Continued

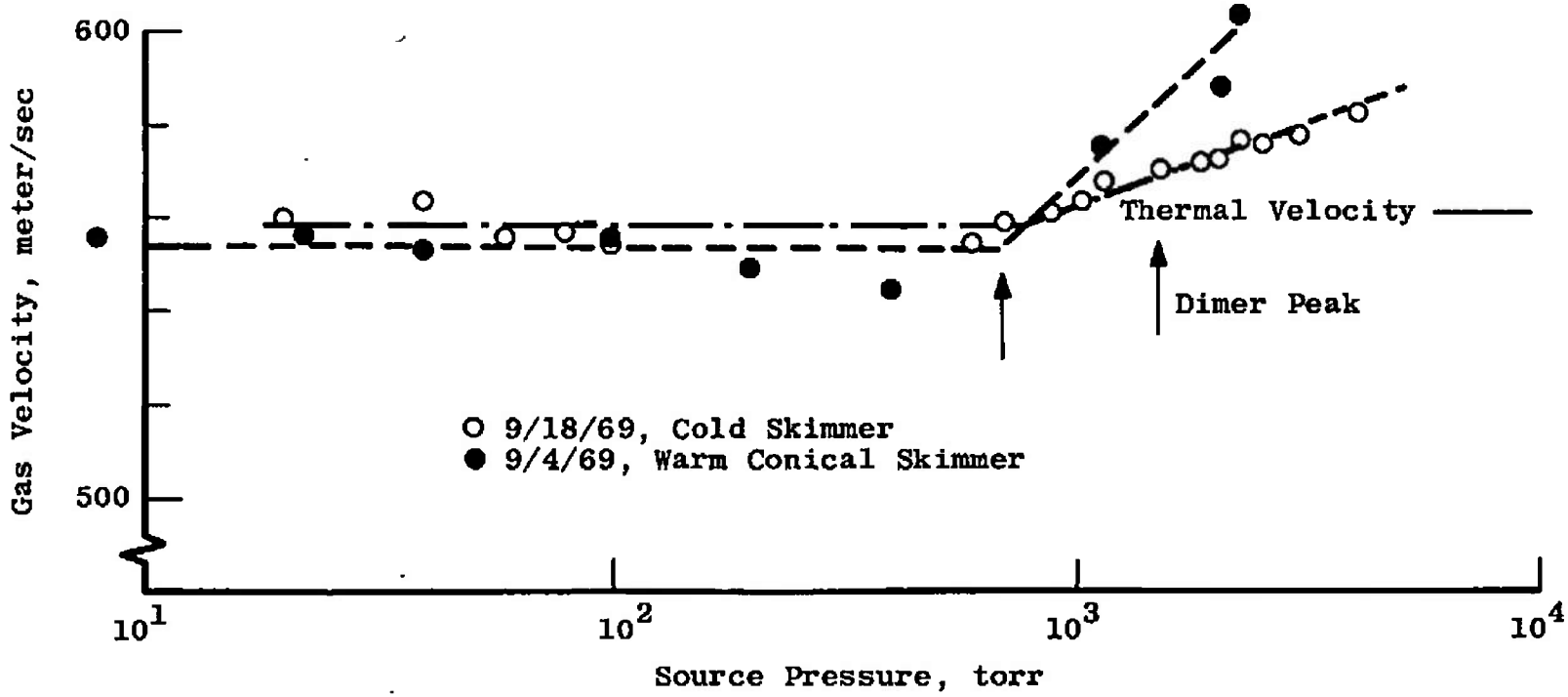

d. Argon ~ 300°K, Ref. 2, 0.0343-cm Orifice, Monomer Velocity
Fig. 23 Continued

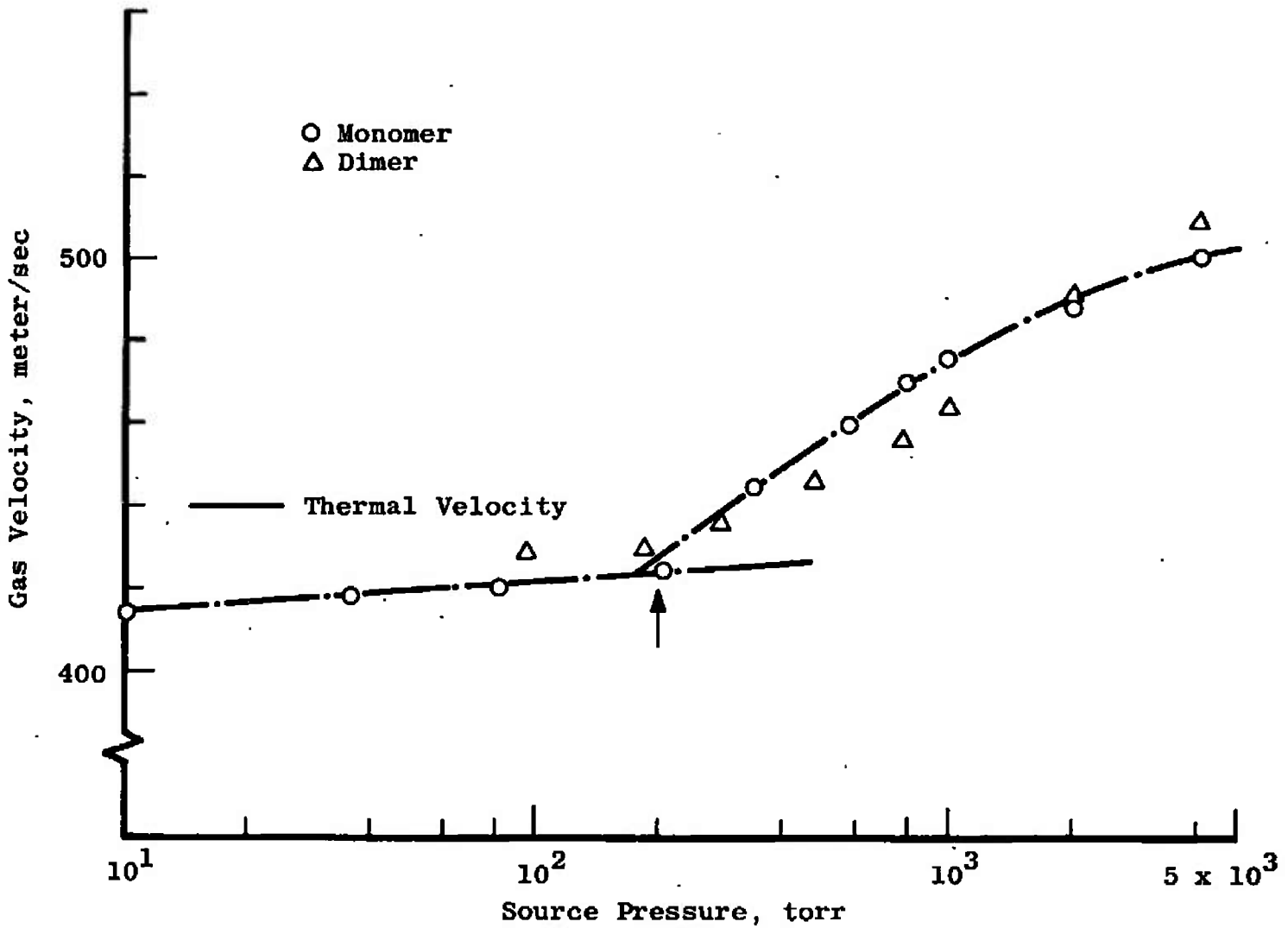

e. Argon ~ 185°K, 0.0386-cm Orifice
Fig. 23 Continued

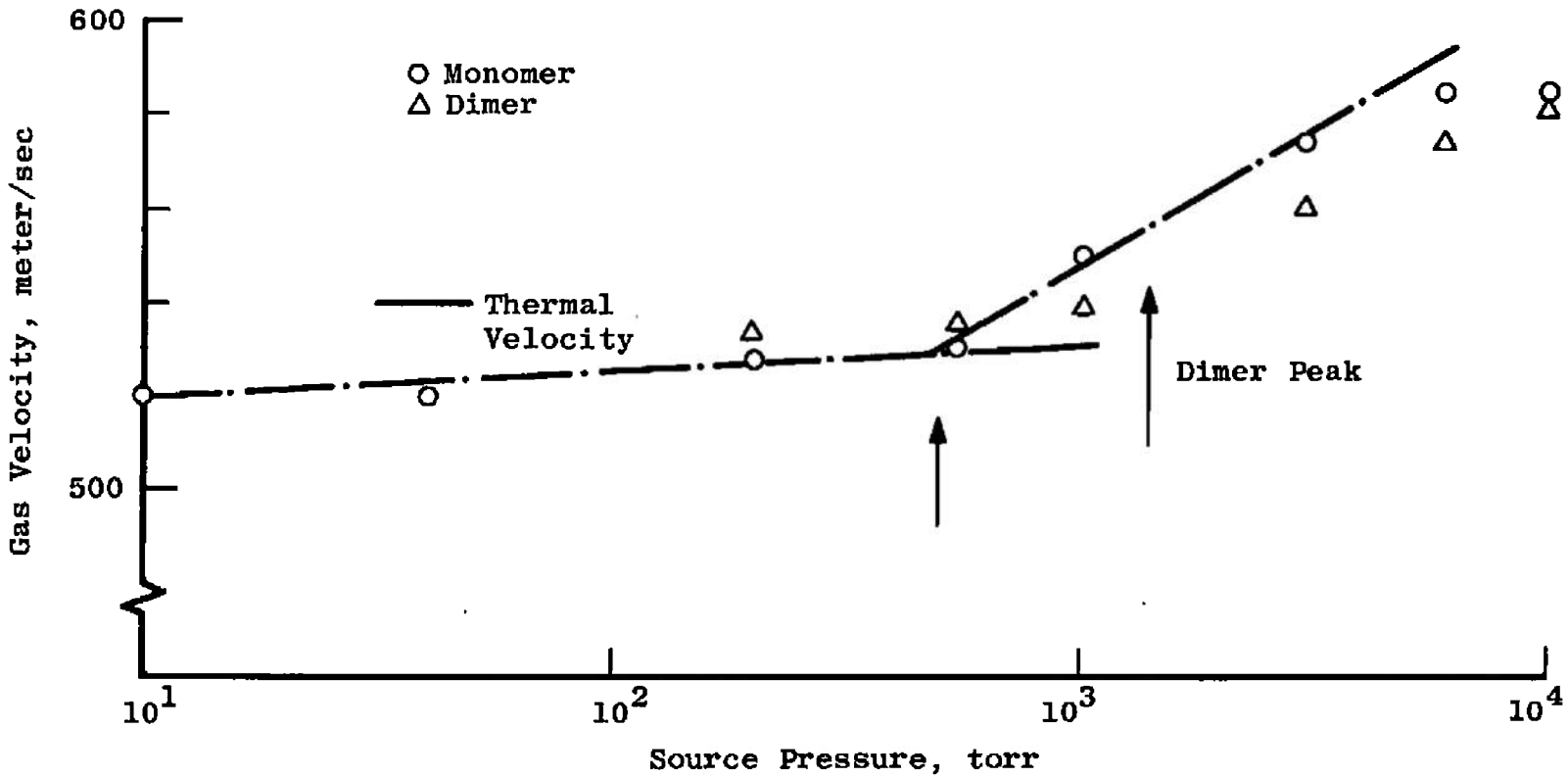

f. Argon ~ 290°K, 0.0386 cm Orifice
Fig. 23 Continued

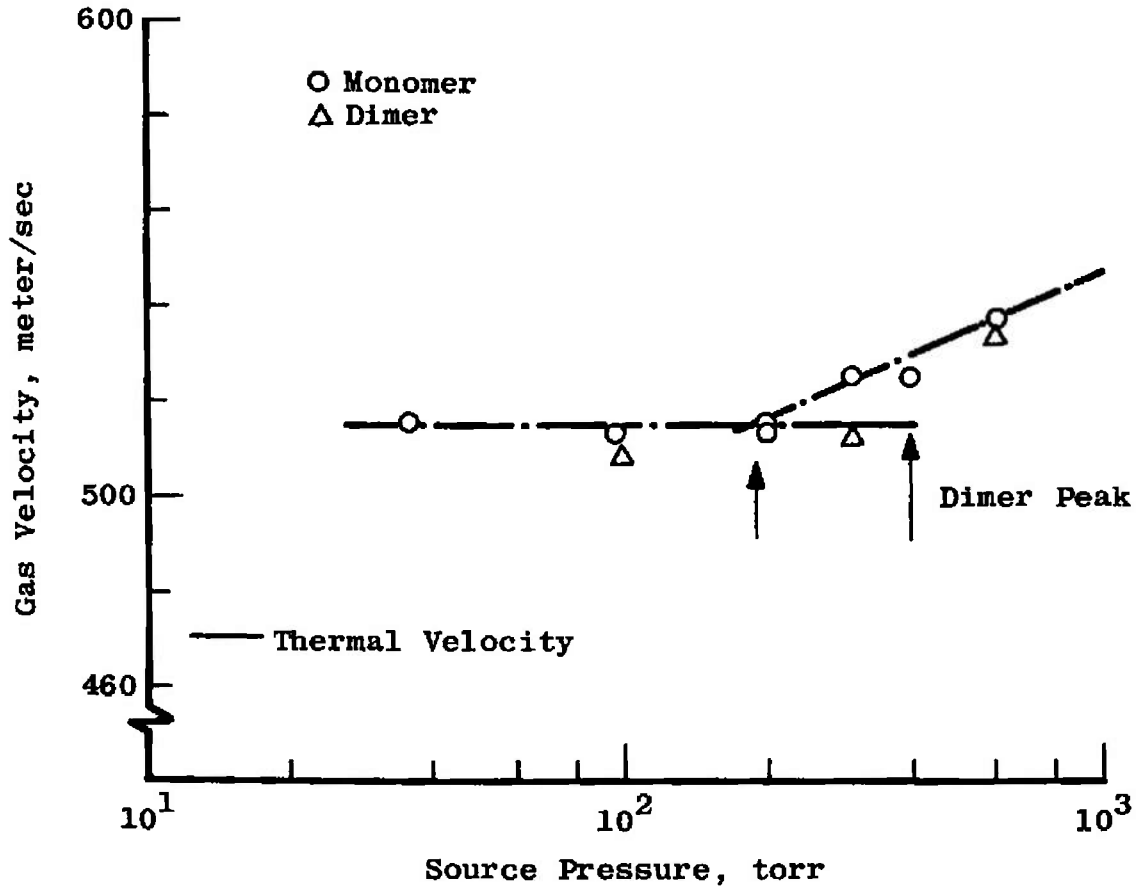

g. Argon ~ 217 ± 7°K, 0.1245-cm Orifice
Fig. 23 Continued

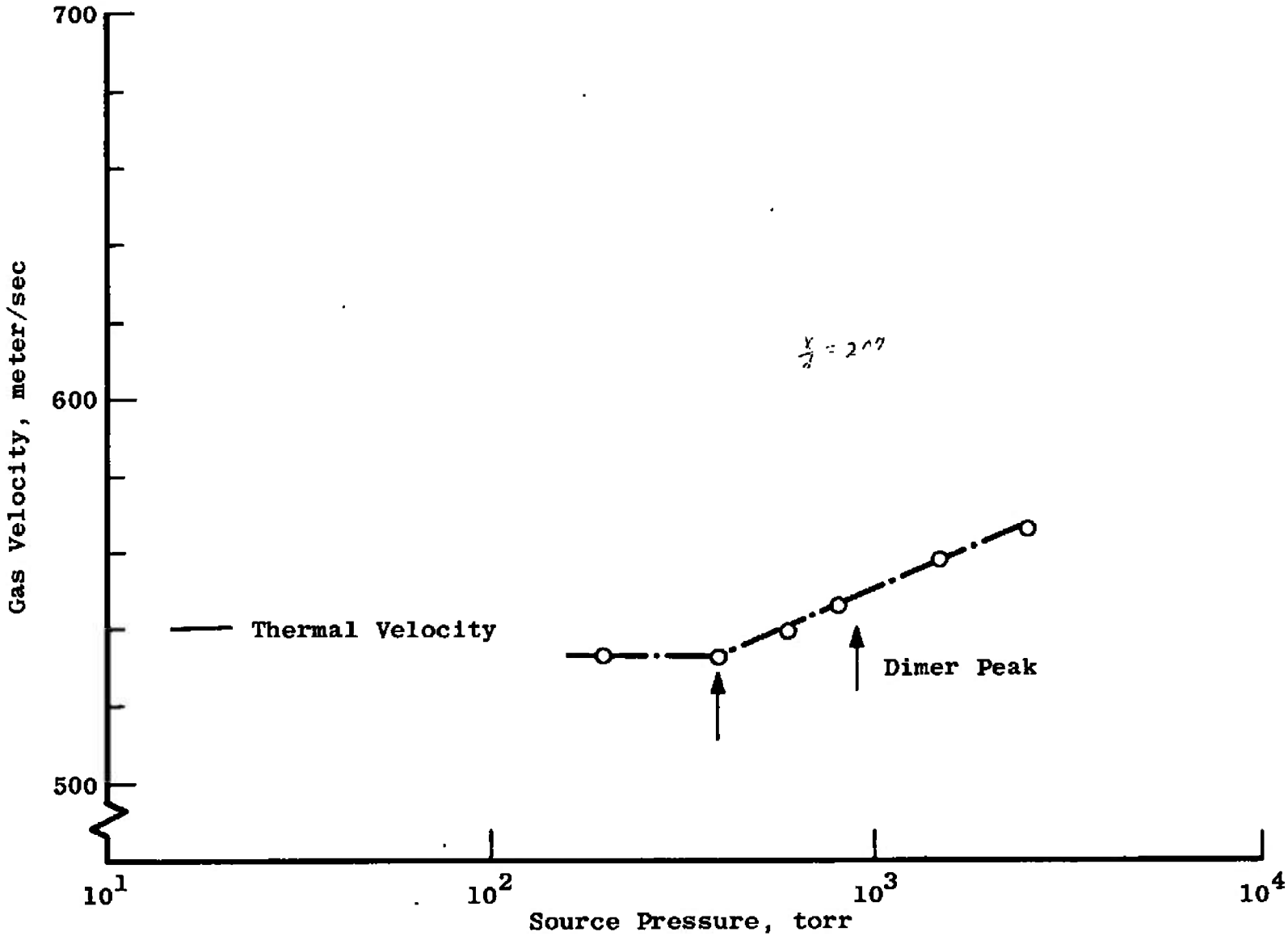

h. Argon ~ 285°K, 0.1245-cm Orifice, Monomer Velocity
Fig. 23 Continued

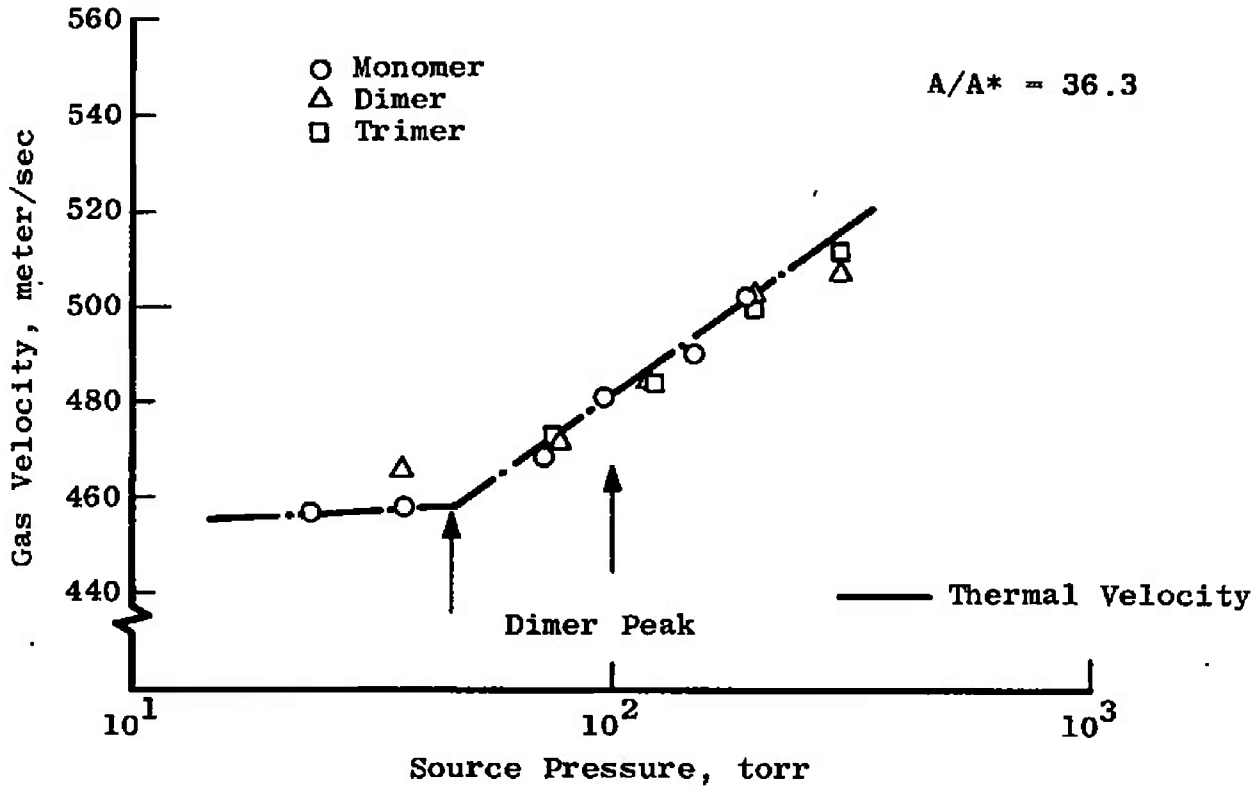

i. Argon ~ 185°K, 0.111-cm Nozzle
Fig. 23 Continued

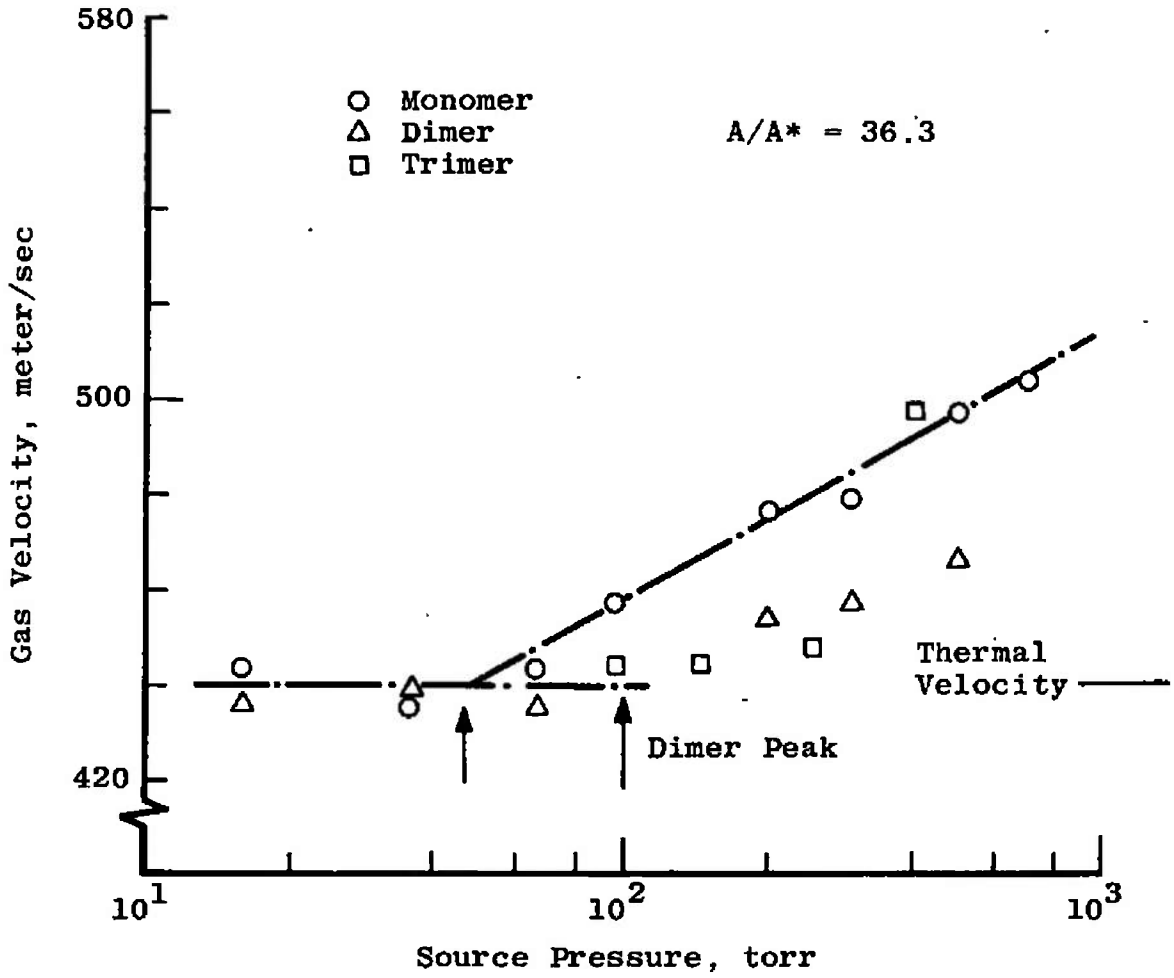

j. Argon ~ 185°K, 0.111-cm Nozzle
Fig. 23 Continued

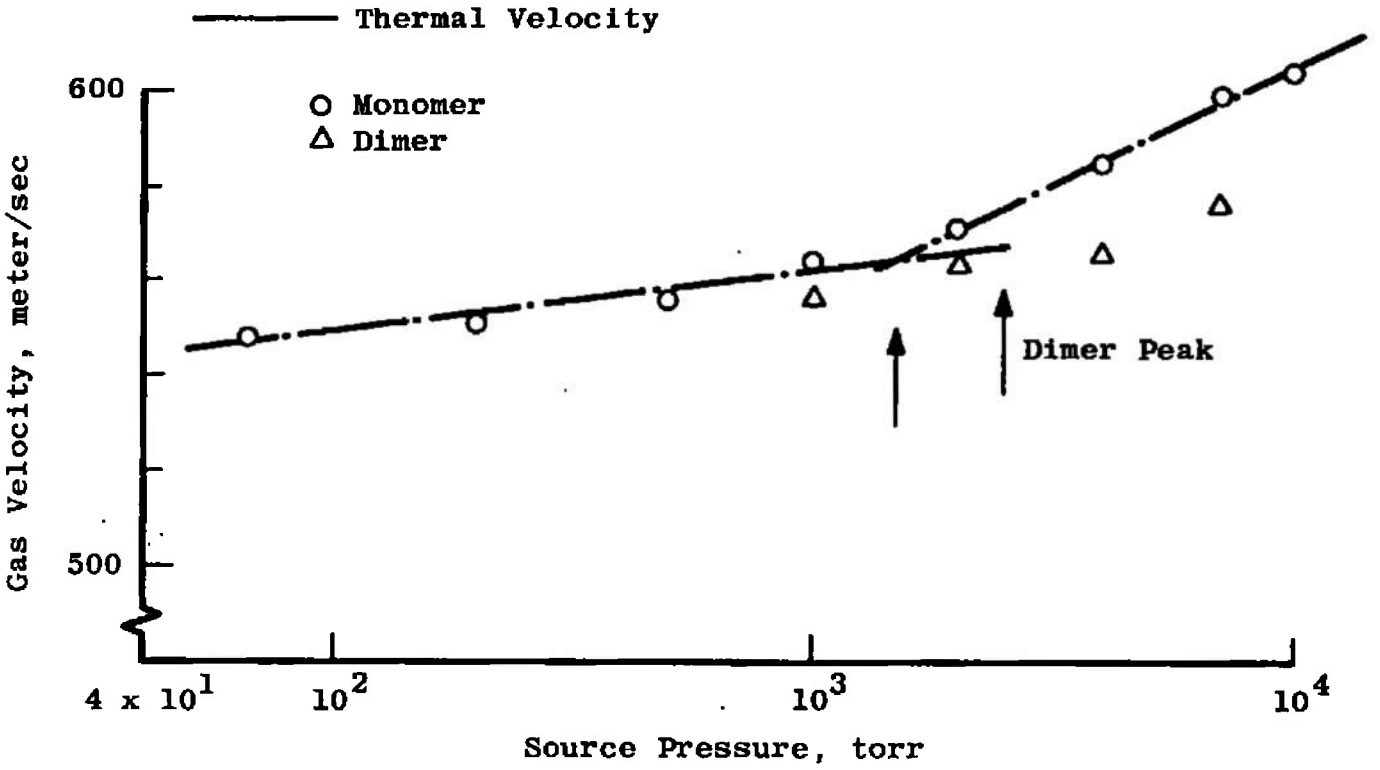

k. Nitrogen ~ 185°K, 0.0147-cm Orifice
Fig. 23 Continued

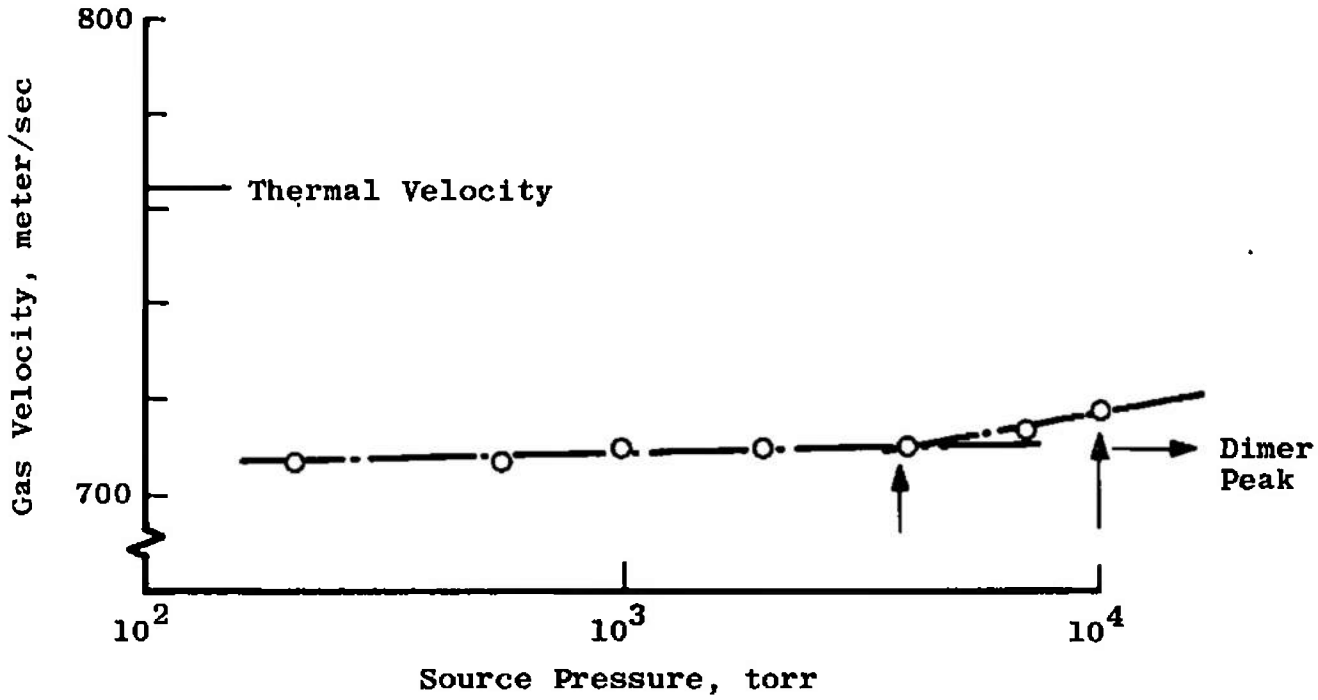

l. Nitrogen ~ 285 ± 3°K, 0.0147-cm Orifice, Monomer Velocity -
Fig. 23 Continued

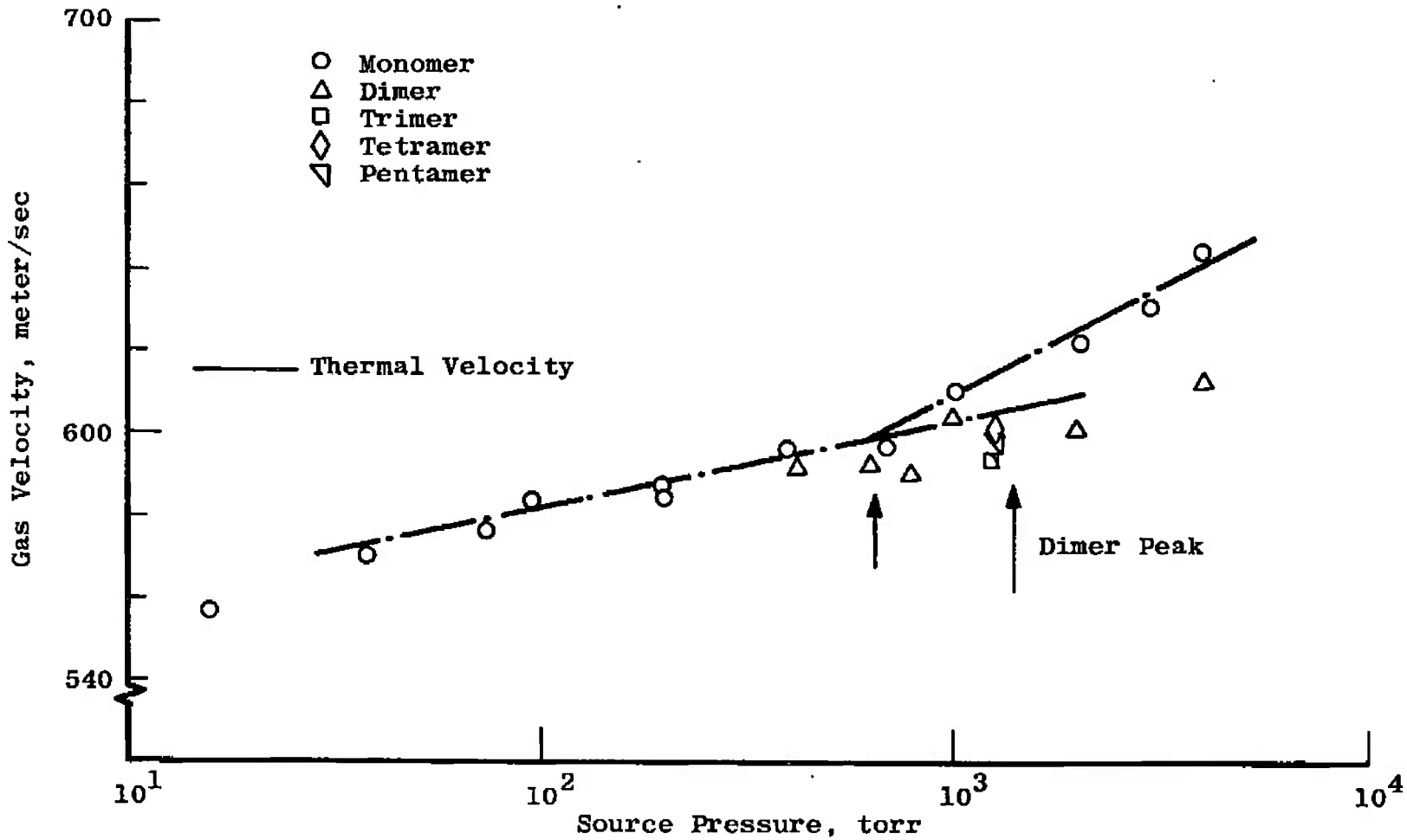

m. Nitrogen ~ 185°K, 0.0386-cm Orifice
Fig. 23 Continued

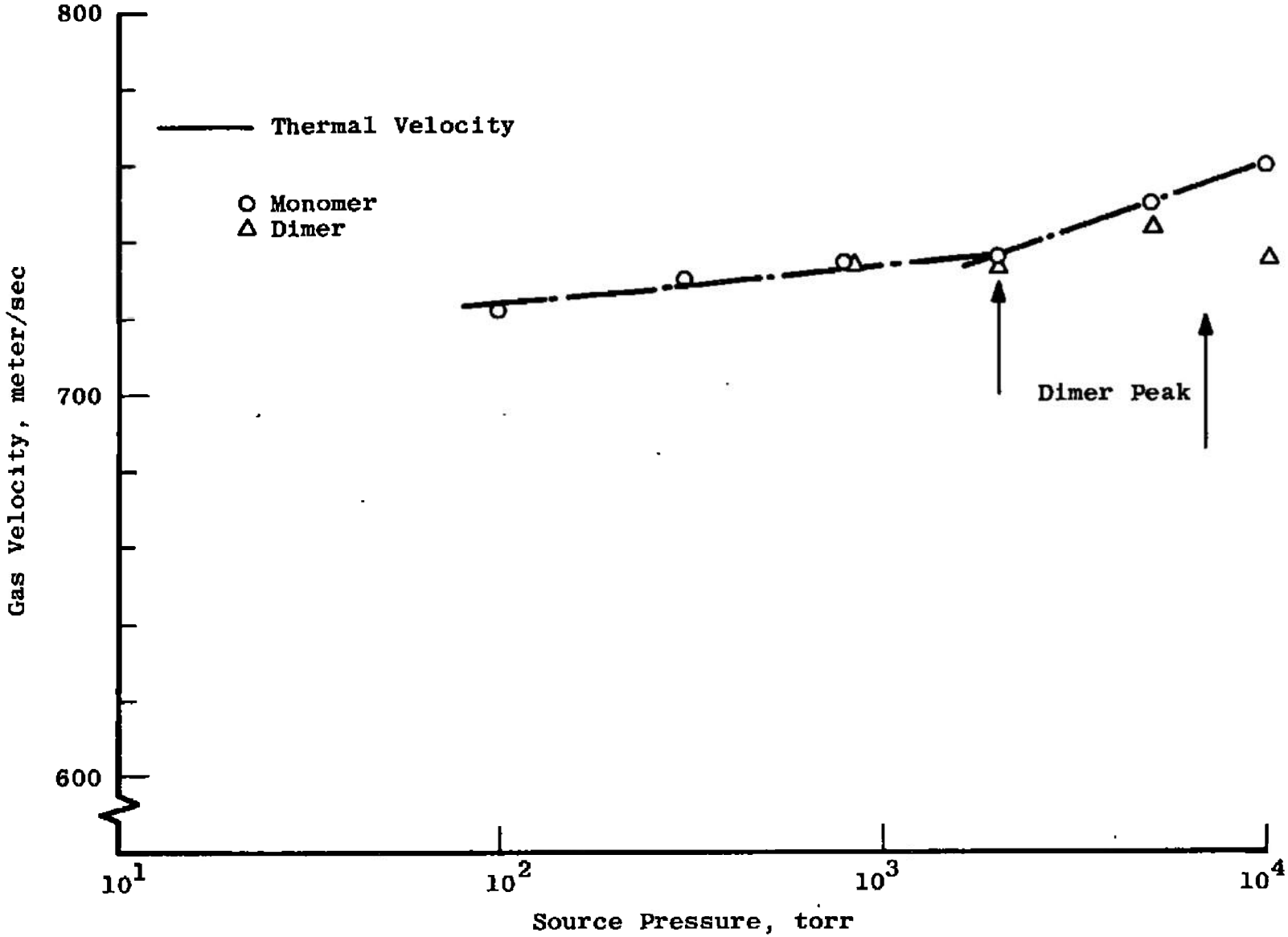

n. Nitrogen ~ 290°K, 0.0386-cm Orifice

Fig. 23 Continued

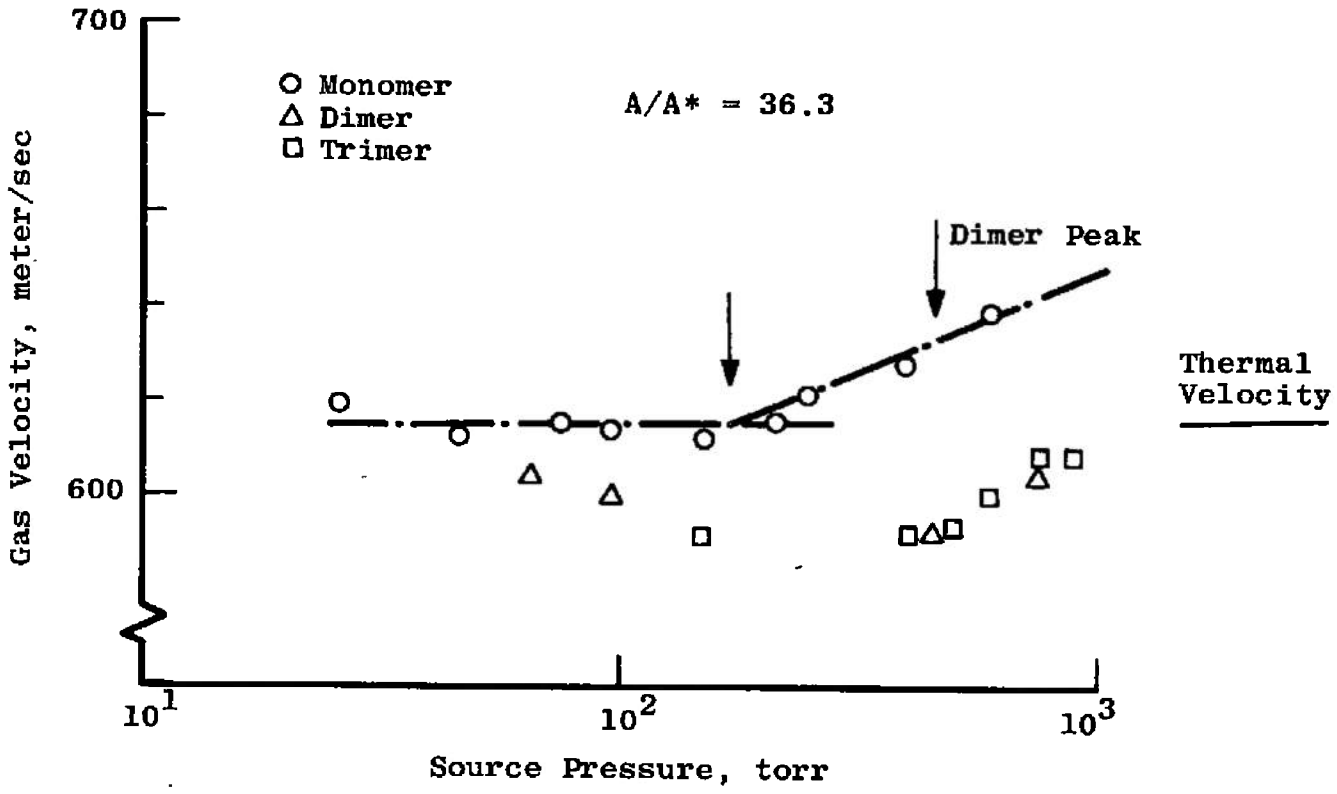

o. Nitrogen ~ 185°K, 0.111-cm Nozzle

Fig. 23 Continued

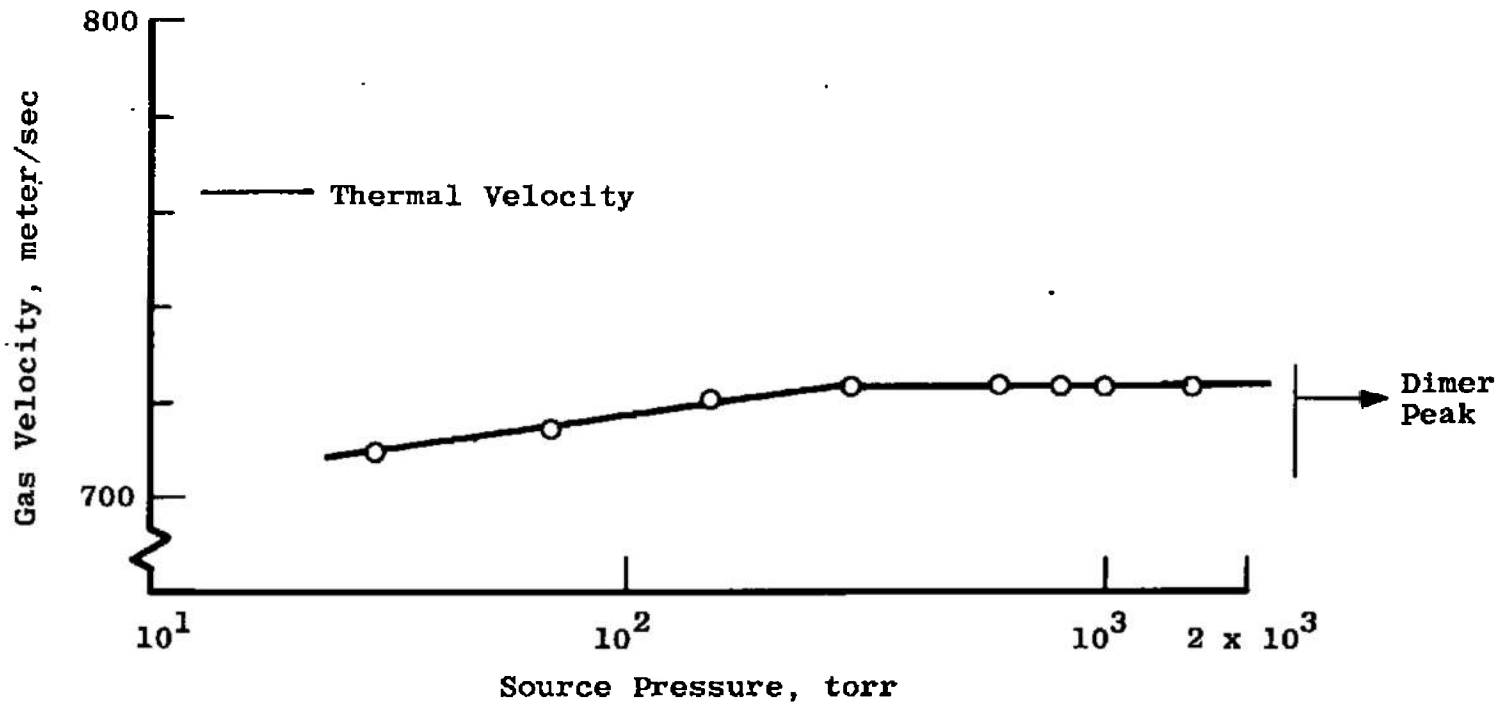

p. Nitrogen ~ 285°K, 0.1245-cm Orifice, Monomer Velocity
Fig. 23 Continued

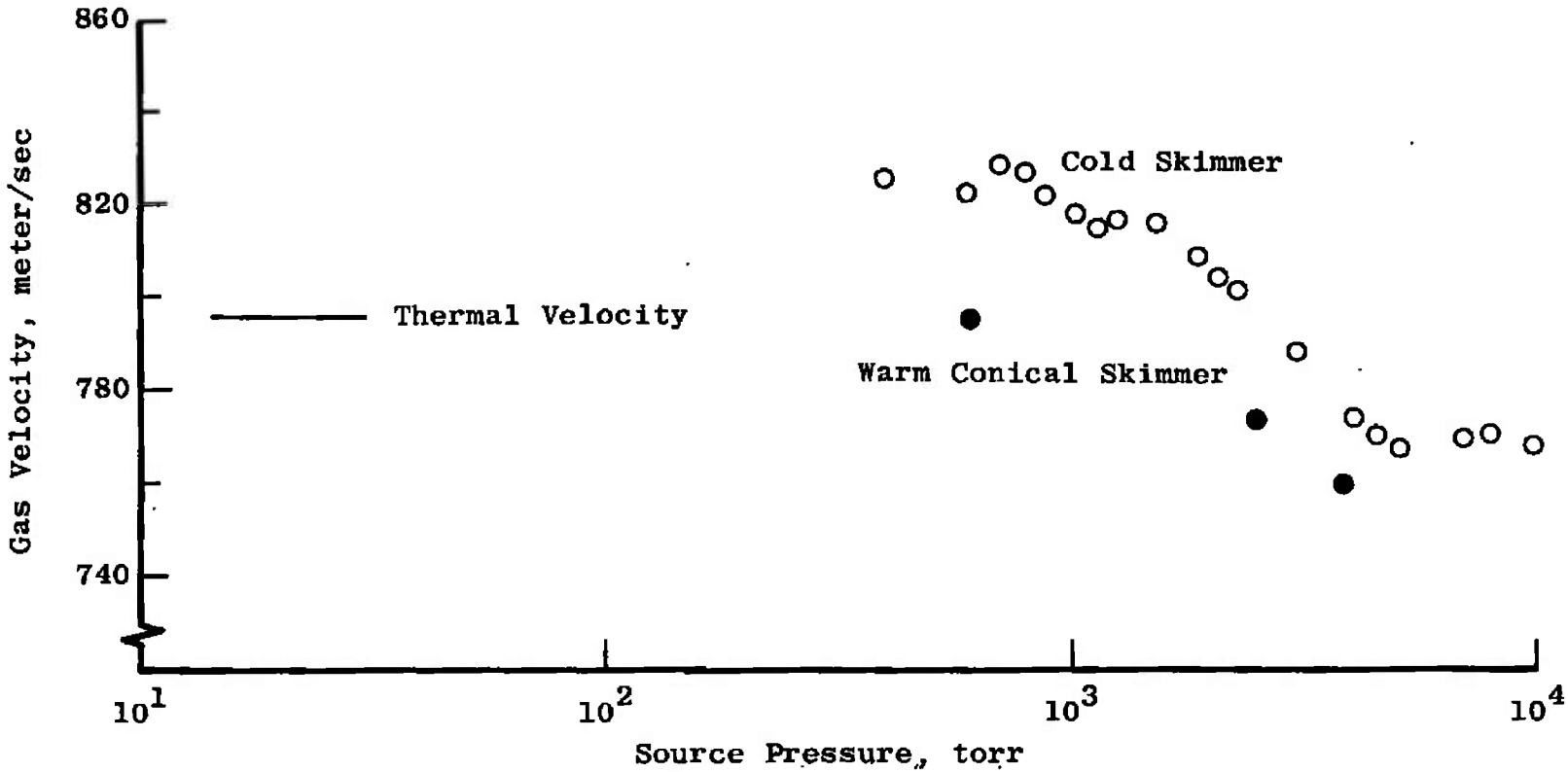

q. Argon ~ 600°K, Ref. 2, 0.0343-cm Orifice, Monomer Velocity
Fig. 23 Concluded

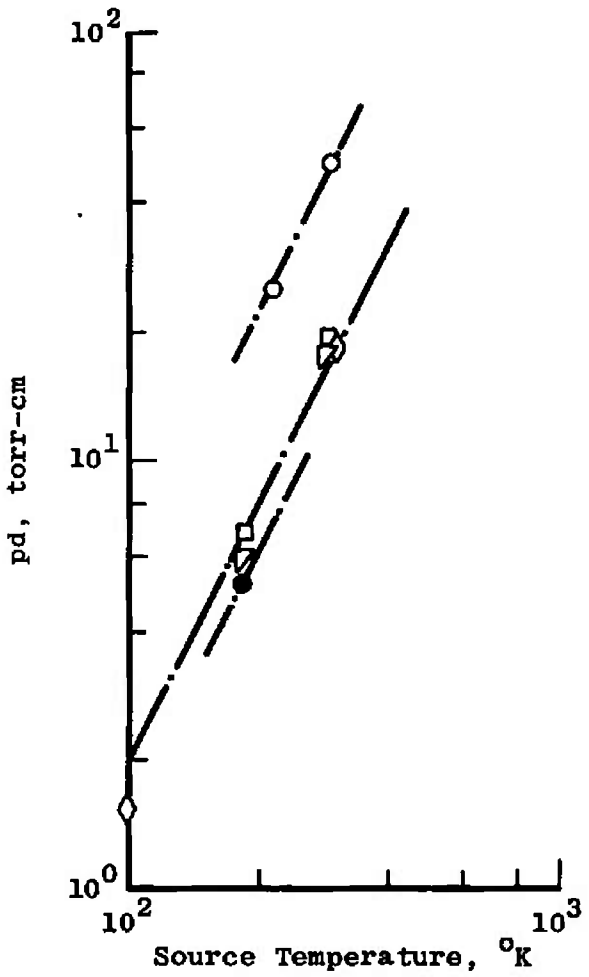

a. Argon

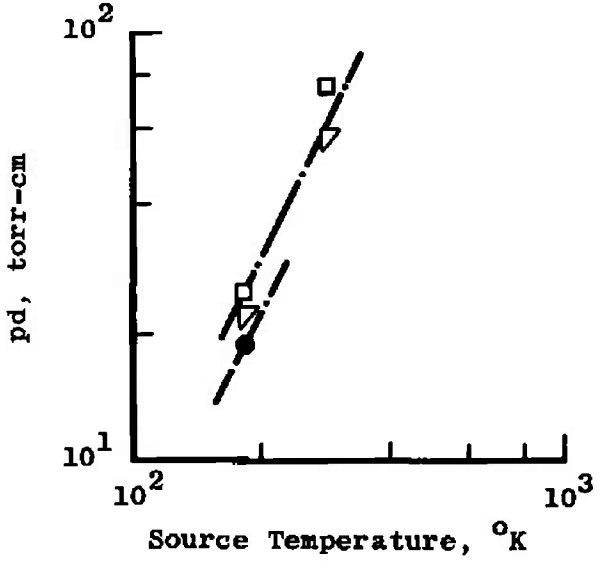

b. Nitrogen

Source Diam, cm
- 0.1245
- 0.0386
- 0.0343
- 0.0147
- 0.111 Nozzle

Fig. 24 Pressure at Which Gas Velocity Increases

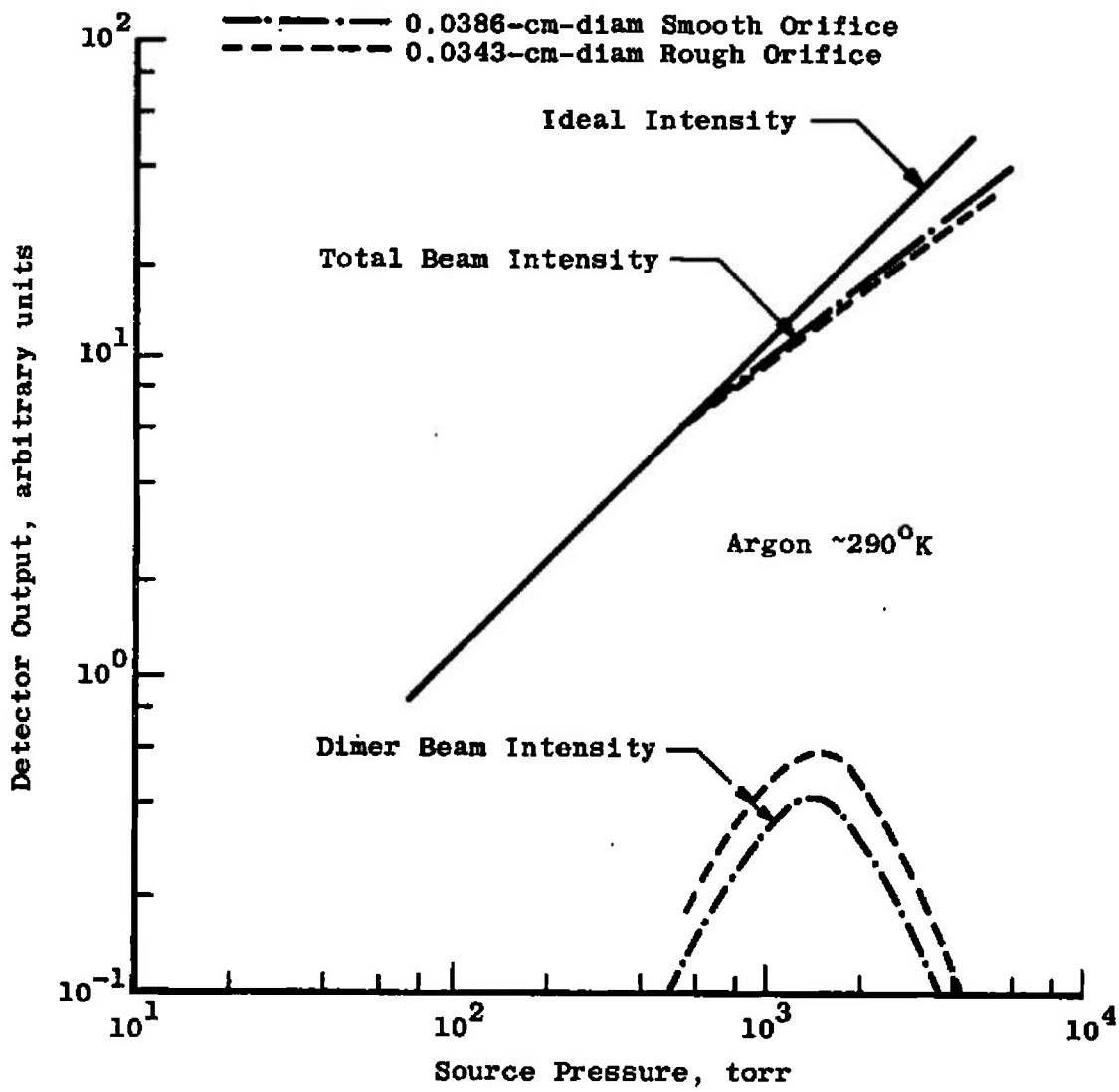

Fig. 25 Effect of Orifice Roughness on Cluster Beam Intensity

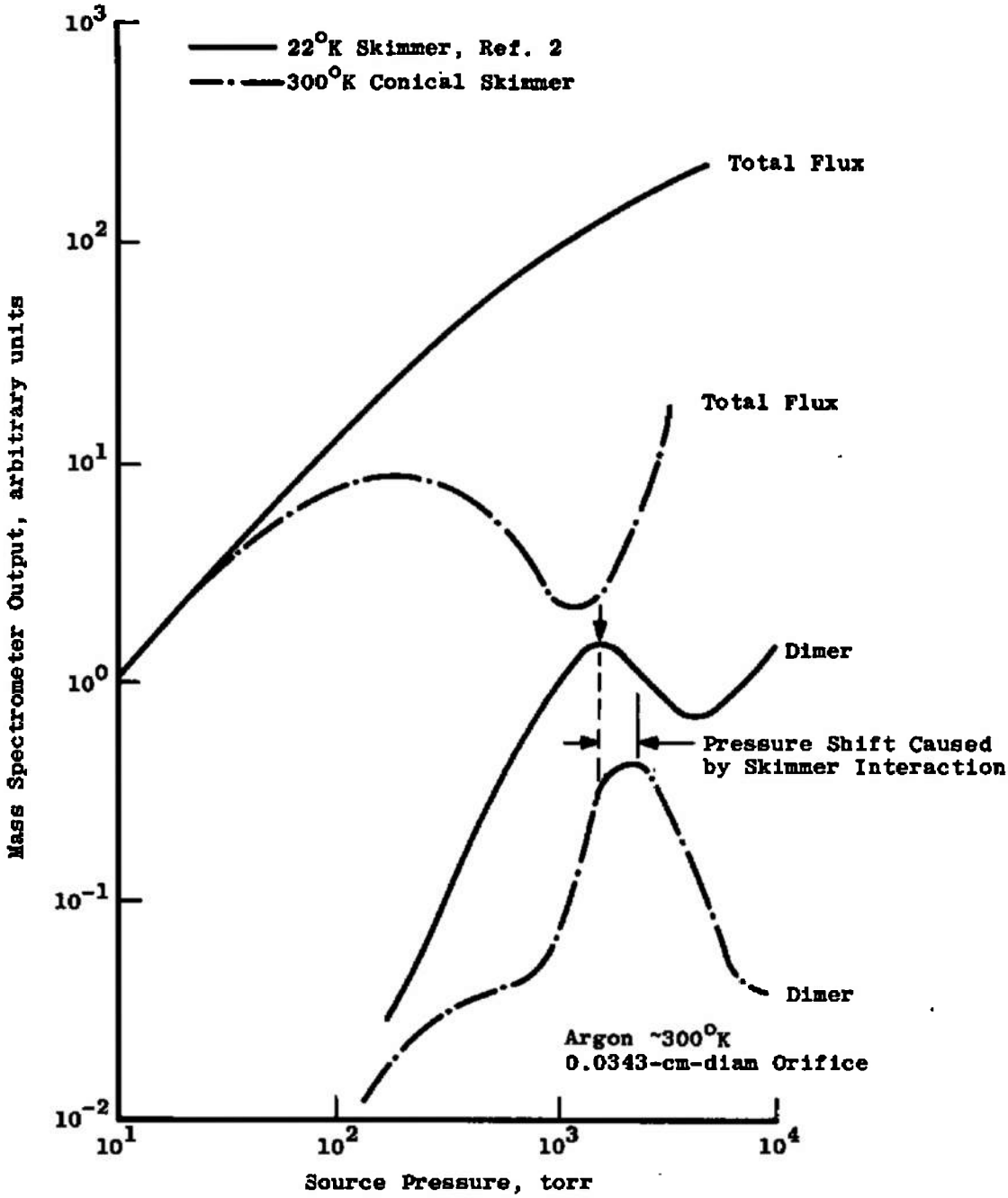

Fig. 26 Effect of Skimmer Interaction on Pressure at Which Dimer Beam Intensity Peaks

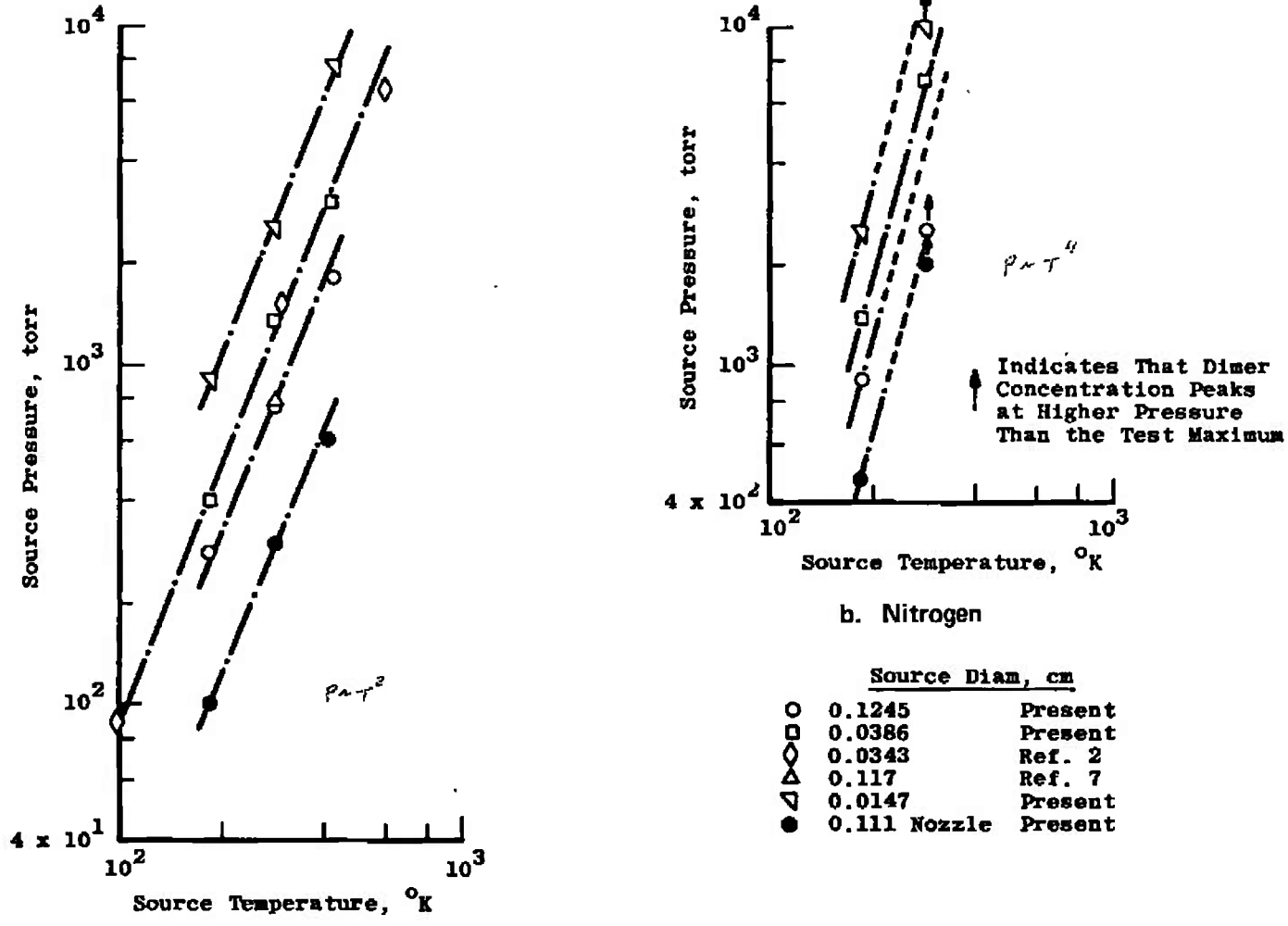

a. Argon

b. Nitrogen

Fig. 27 Pressure at Which Dimer Beam Intensity Peaks as a Function of Temperature

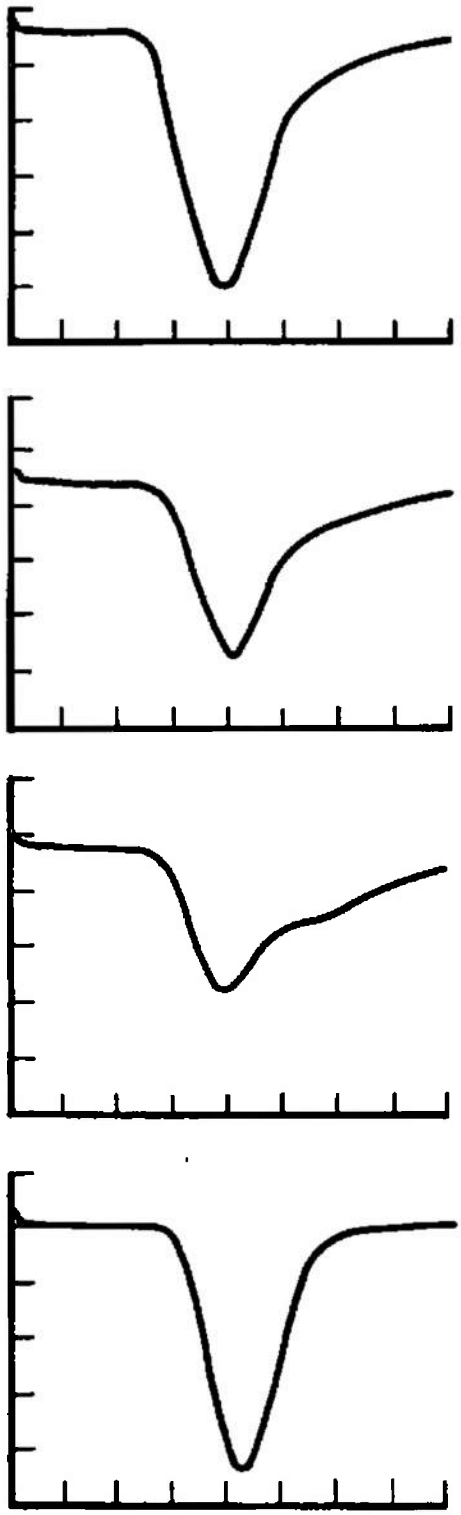

Fig. 28 Effect of Beam Scattering by Mass Spectrometer on Velocity Distribution

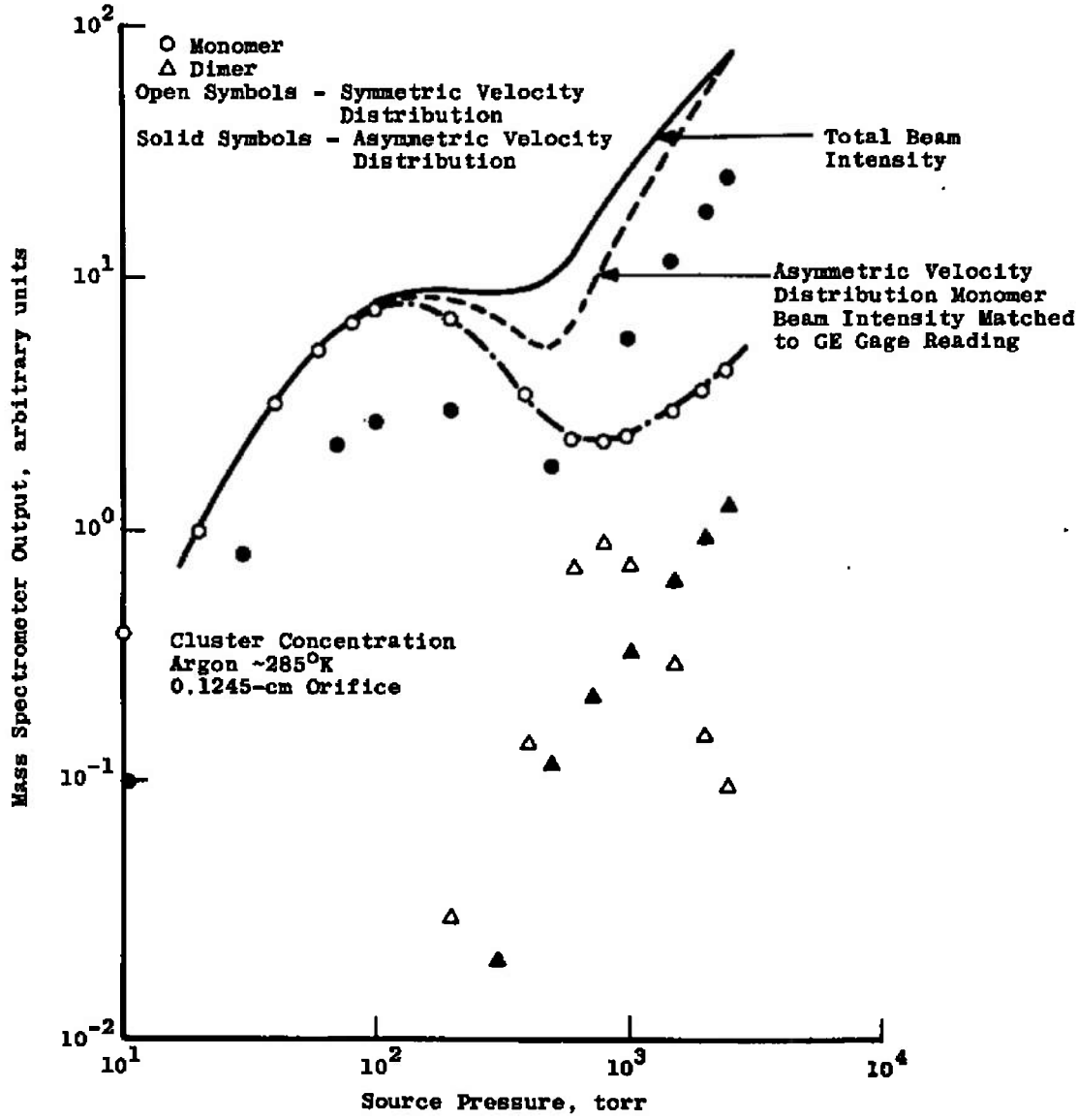

Fig. 29 Effect of Mass Spectrometer Alignment on Individual Mass Beam Intensity

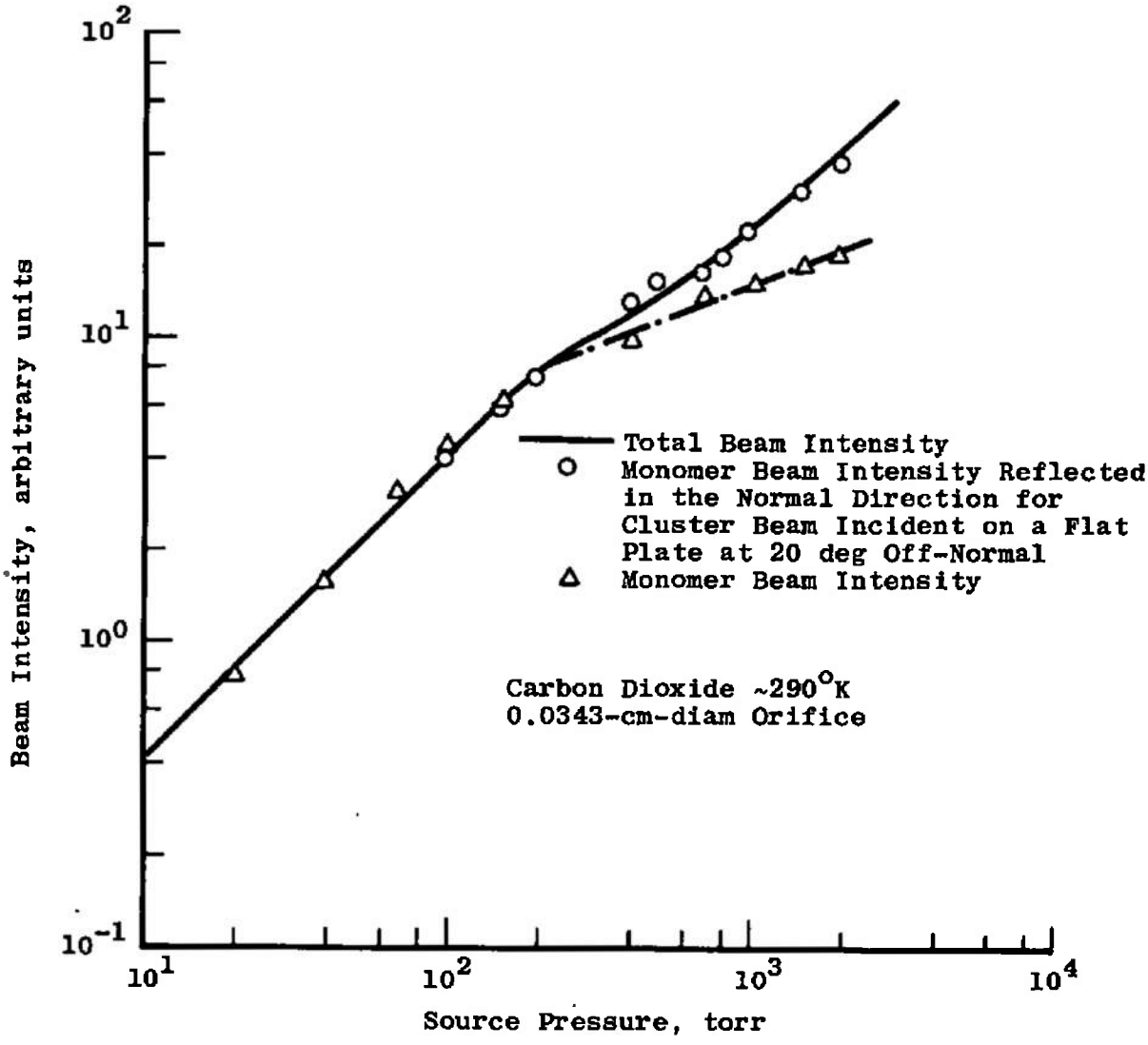

Fig. 30 Effect of Scattering on Monomer Beam Intensity

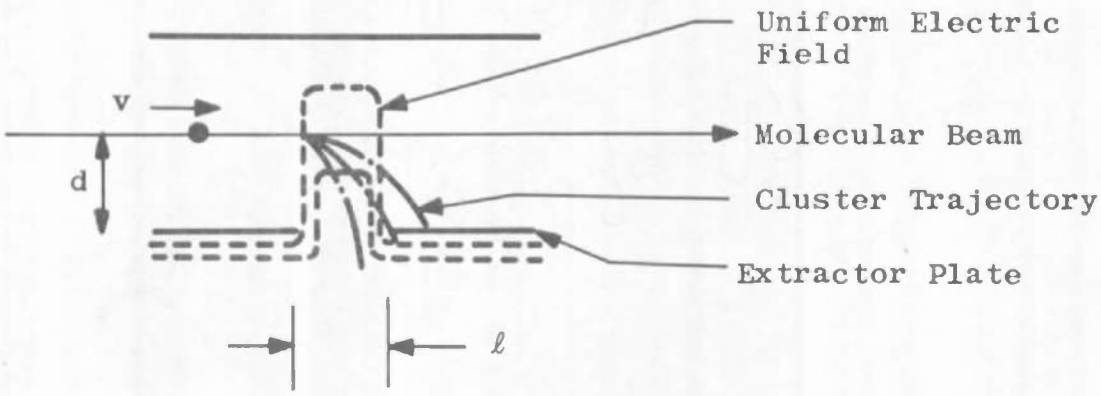

Fig. 31 Motion of a Cluster in the Electric Field of the Mass Spectrometer Head

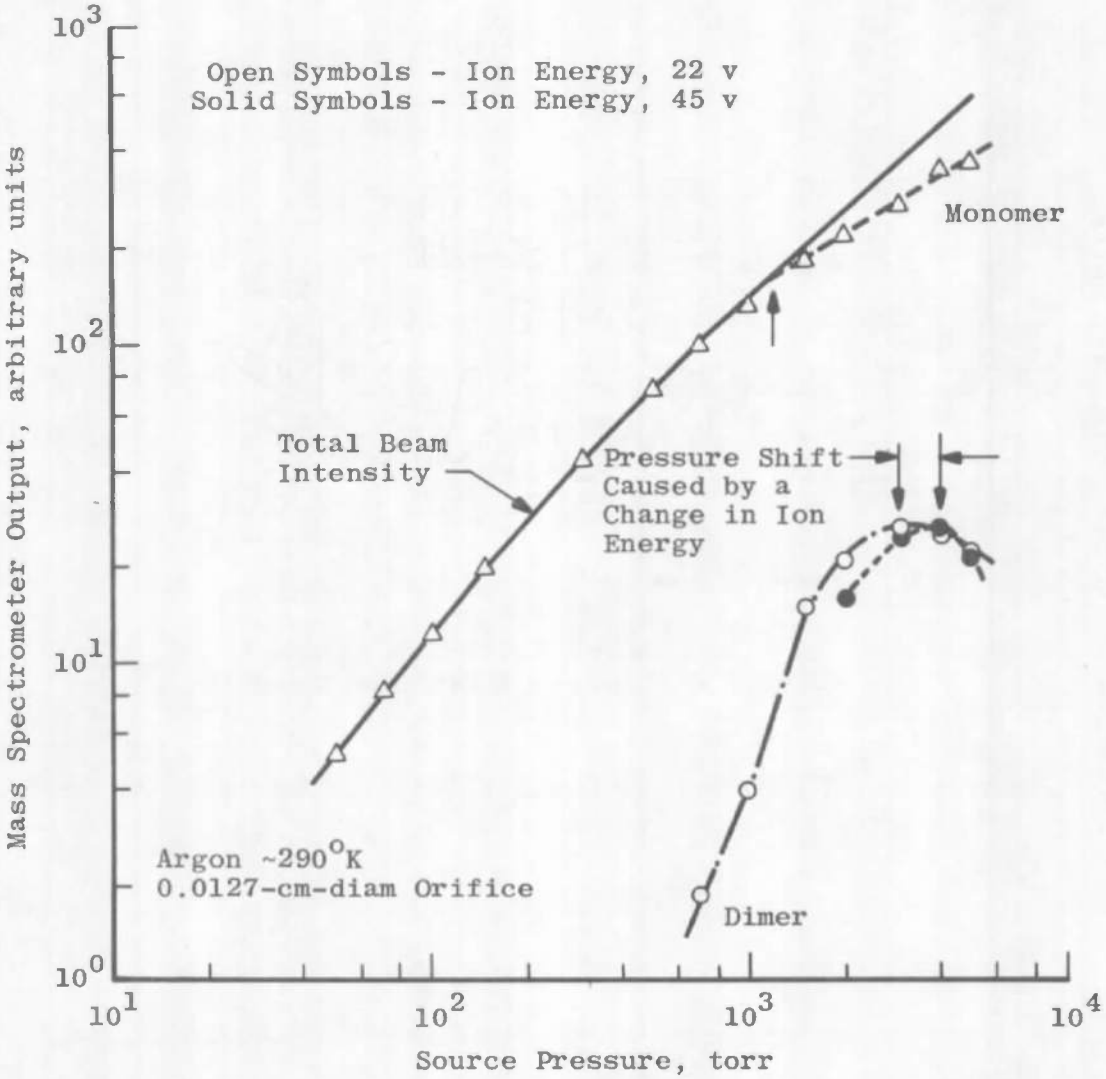

Fig. 32 Effect of Variations in Ion Energy on Individual Mass Beam Intensity

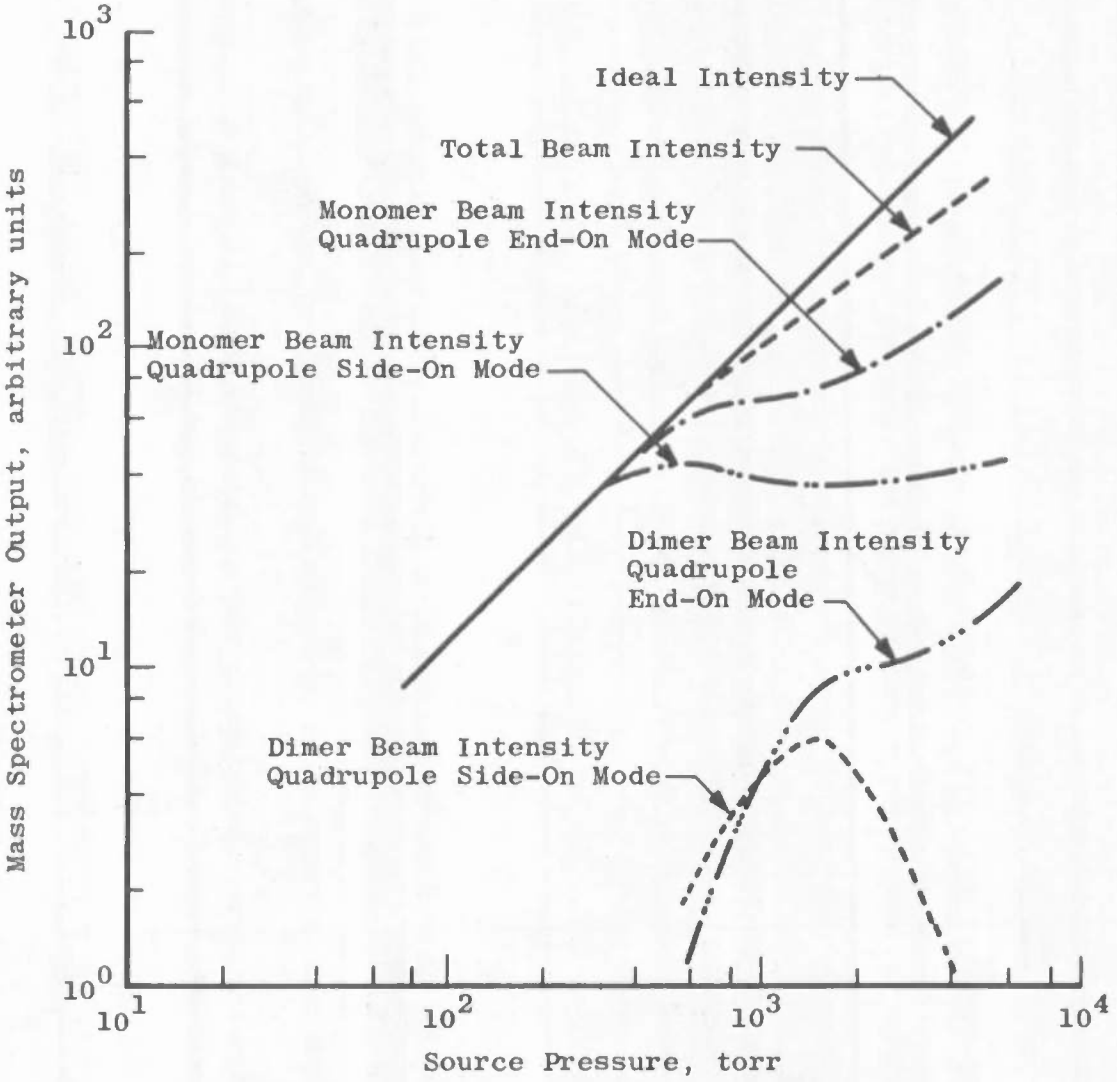

a. Argon ~ 290°K, 0.0343-cm-Diam Orifice

Fig. 33 Effect of Changes in the Mode of Cluster Ion Extraction on Individual Mass Beam Intensity

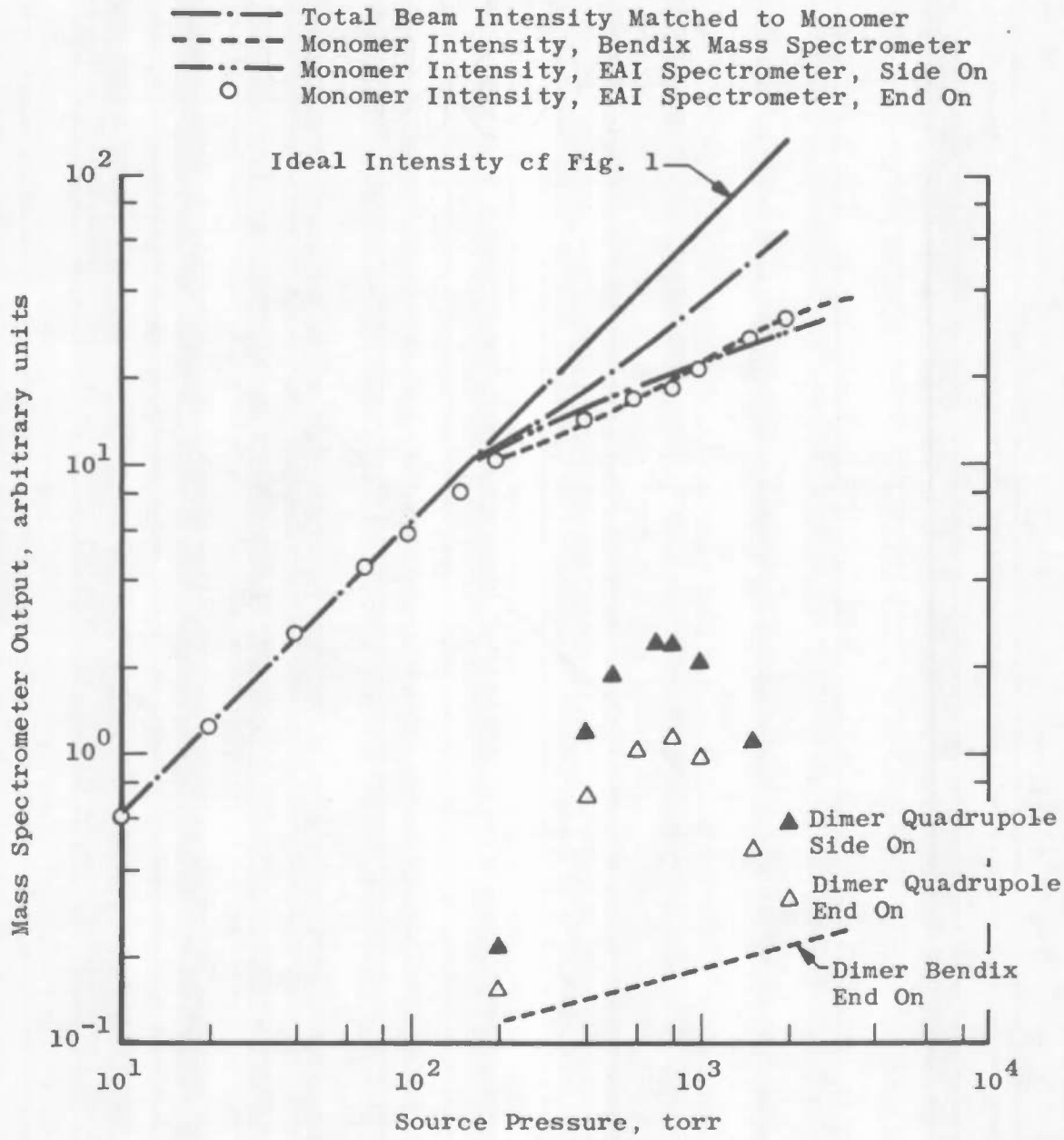

b. Carbon Dioxide ~ 290°K, 0.0343-cm-Diam Orifice
Fig. 33 Concluded

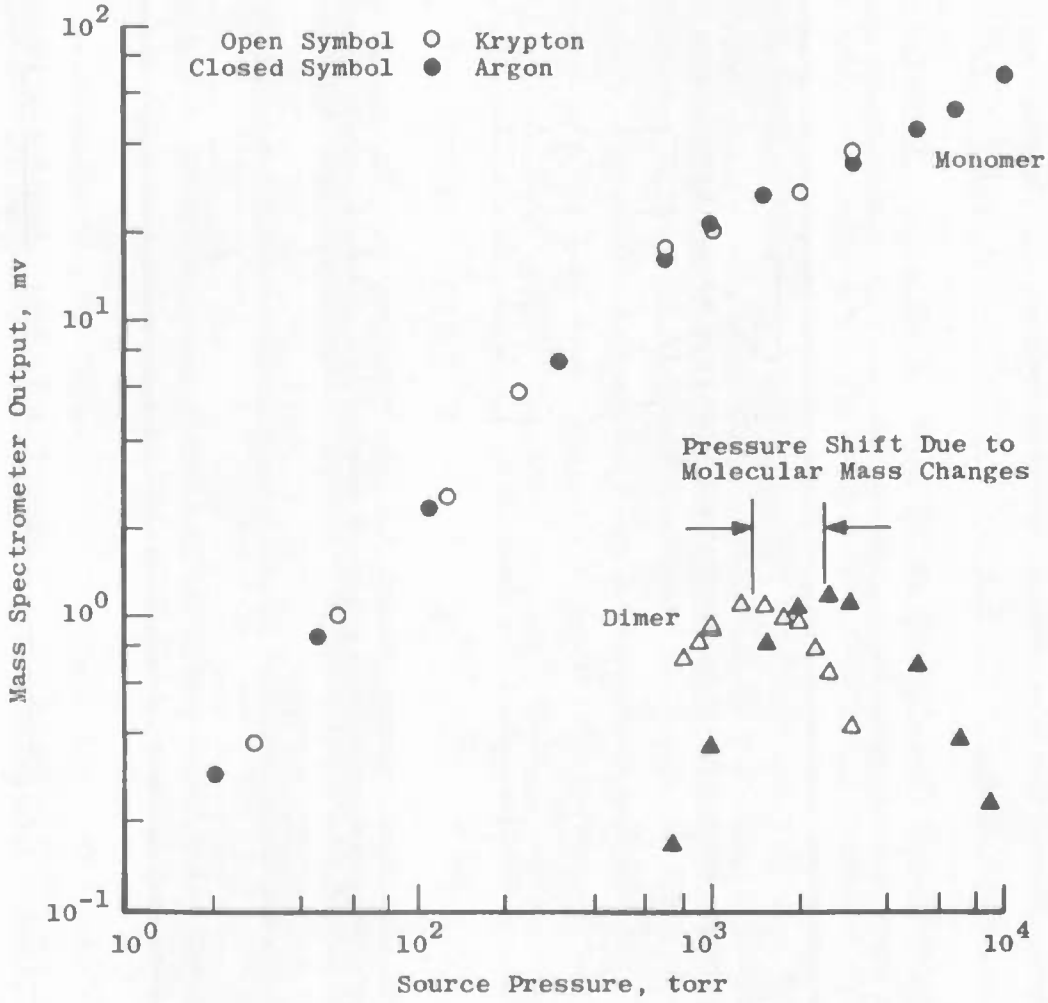

a. Krypton and Argon ~ 290°K, 0.0147-cm-Diam Orifice

Fig. 34 Individual Mass Beam Intensities for Various Gases

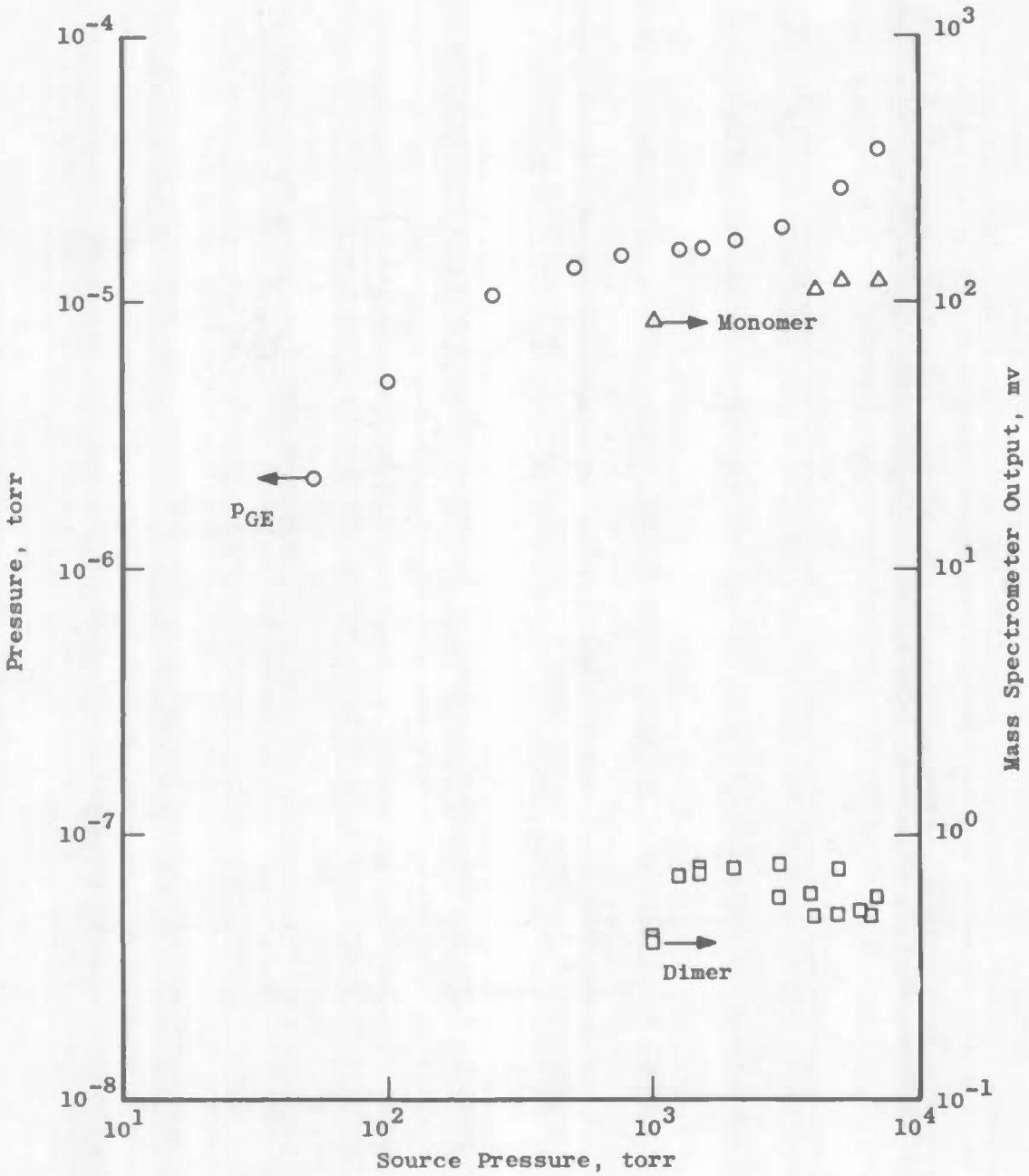

b. Nitric Oxide ~ 290°K, 0.0386-cm-Diam Orifice
Fig. 34 Continued

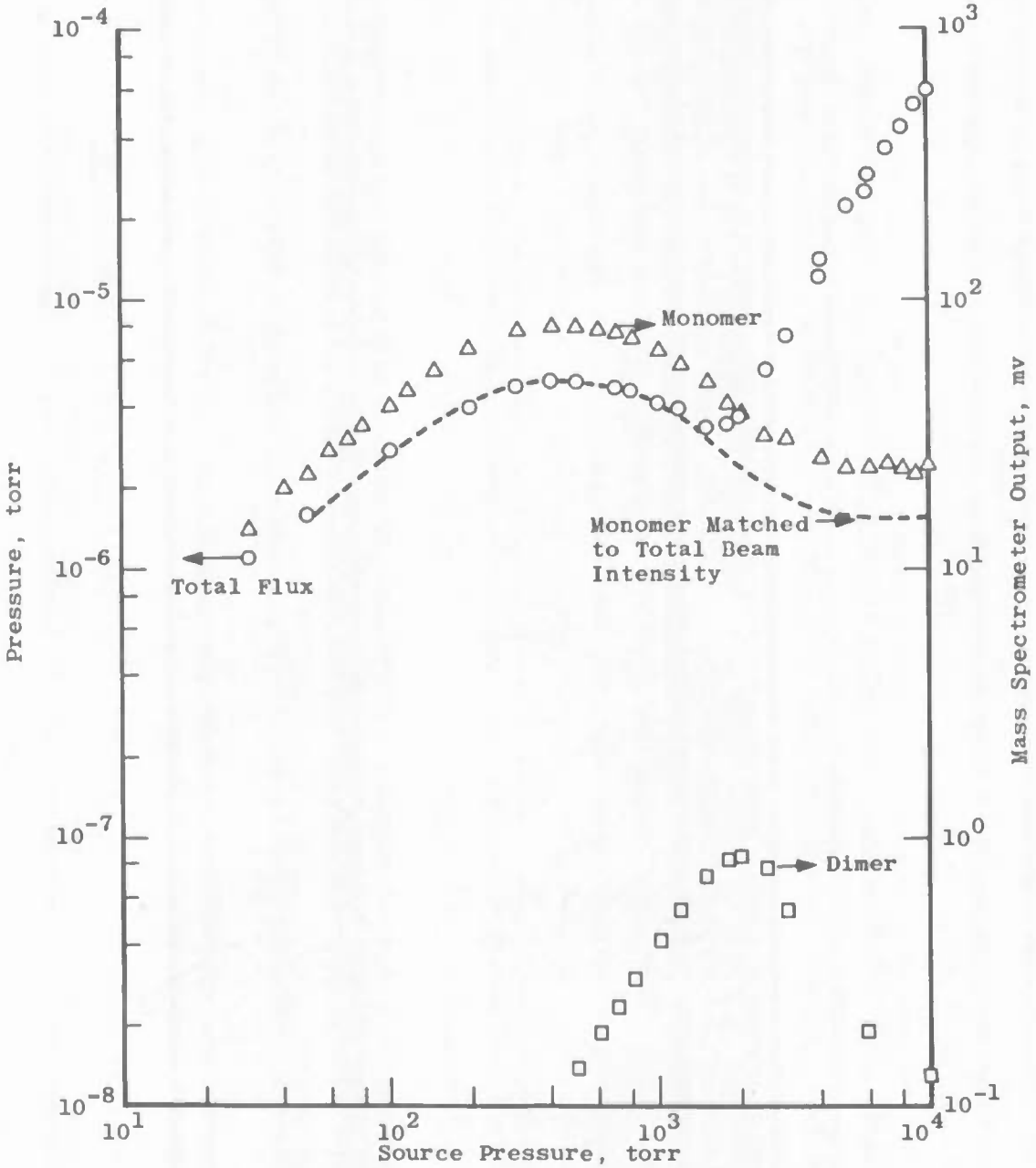

c. Nitric Oxide ~ 300°K, 0.0343-cm-Diam Orifice, Ref. 7
Fig. 34 Continued

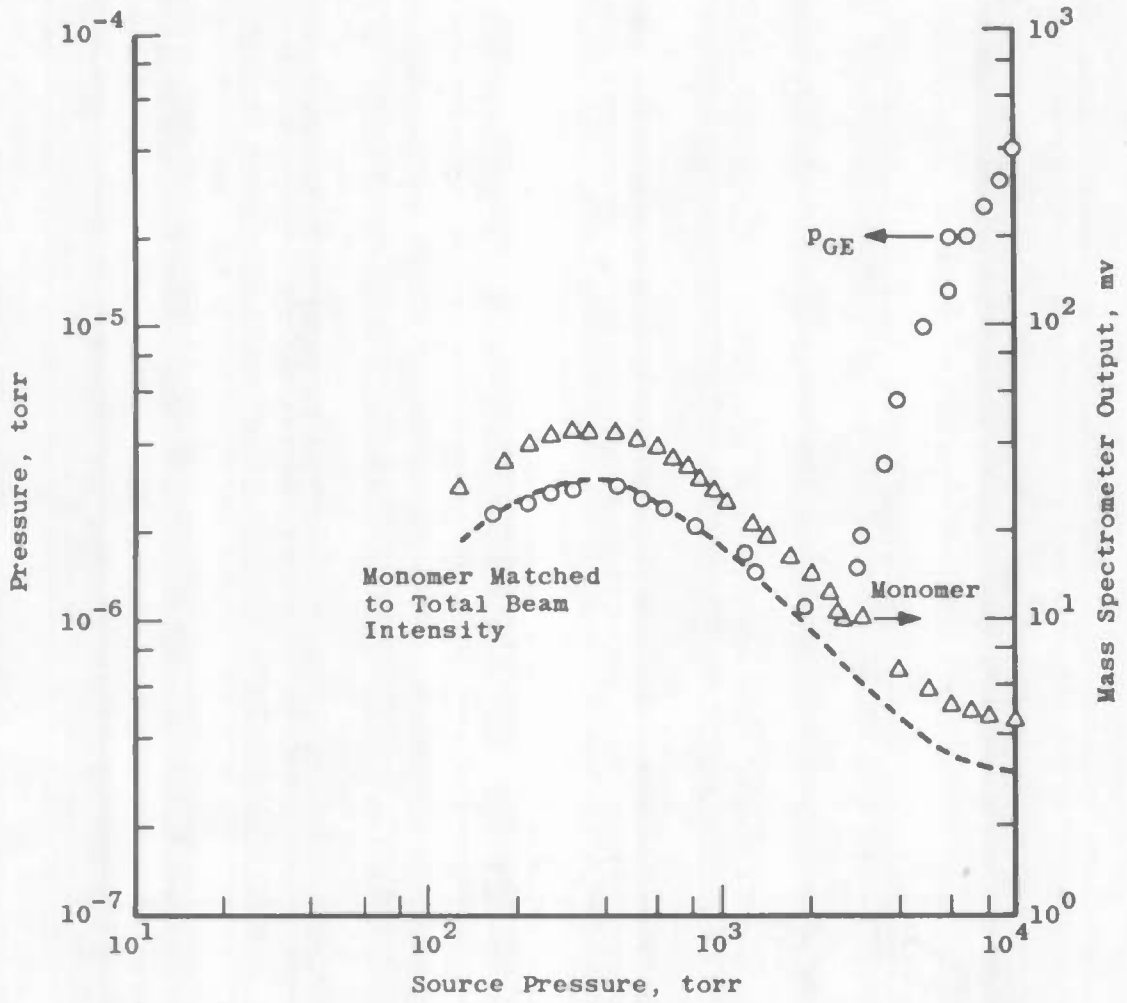

d. Nitric Oxide ~ 300°K, 0.0343-cm-Diam Orifice
Fig. 34 Continued

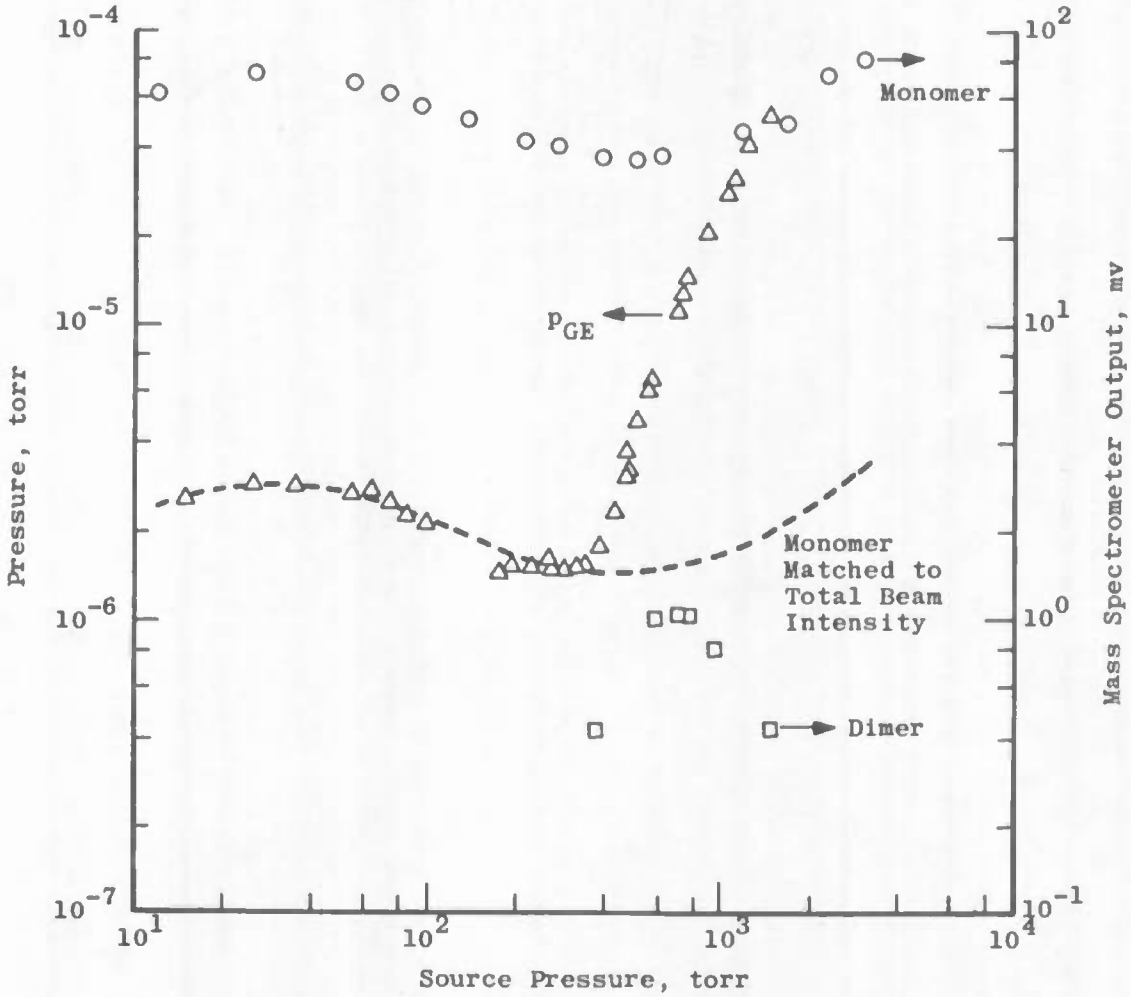

e. Nitric Oxide ~ 300°K, 0.0117-cm-Diam Orifice, Ref. 7
Fig. 34 Continued

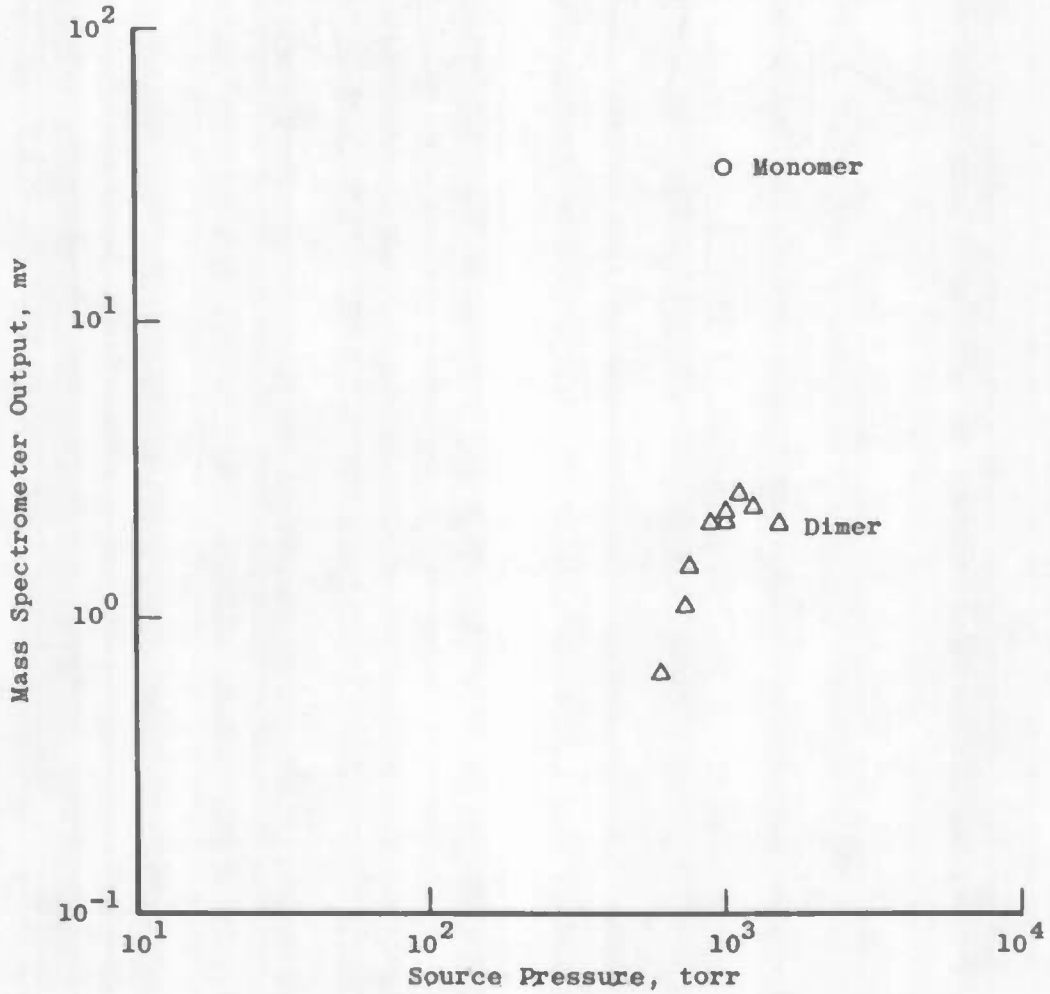

f. Sulphur Dioxide ~ 430°K, 0.0386-cm-Diam Orifice
Fig. 34 Concluded

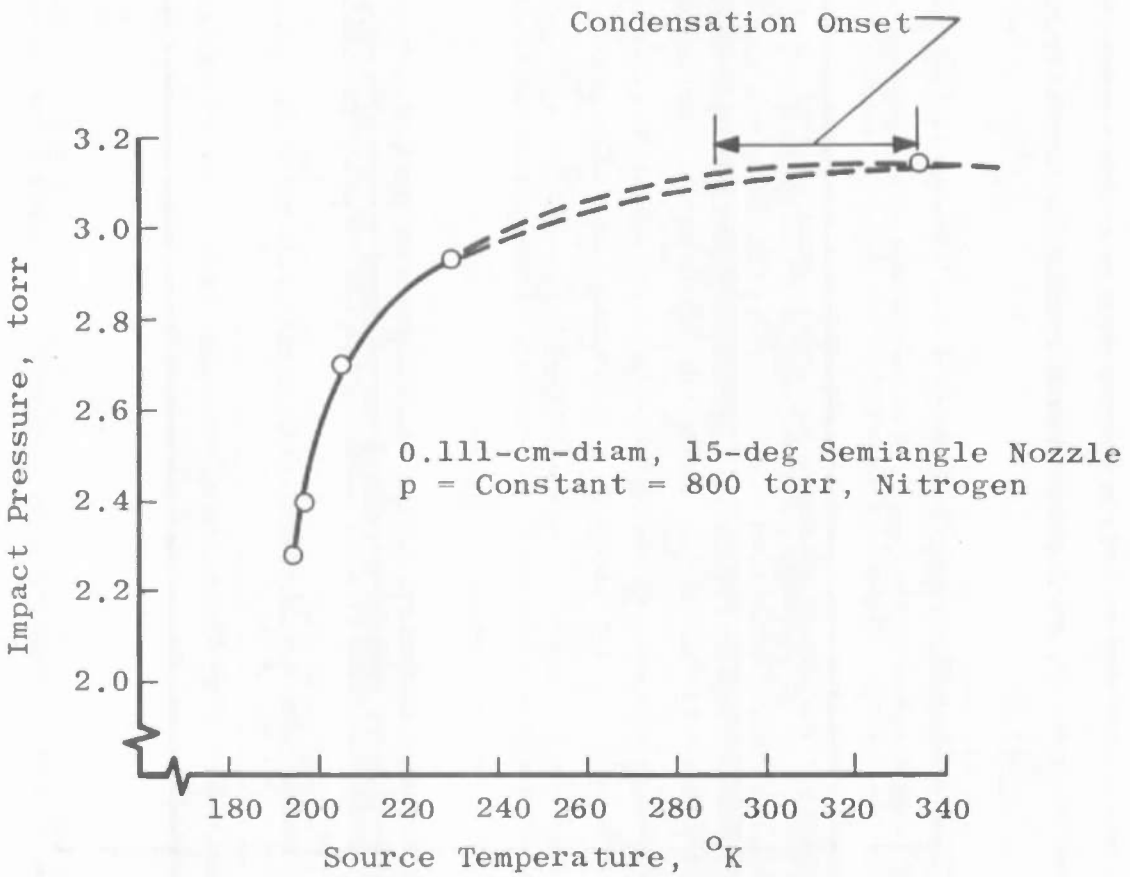

Fig. 35 Effect of Source Temperature on Impact Pressure

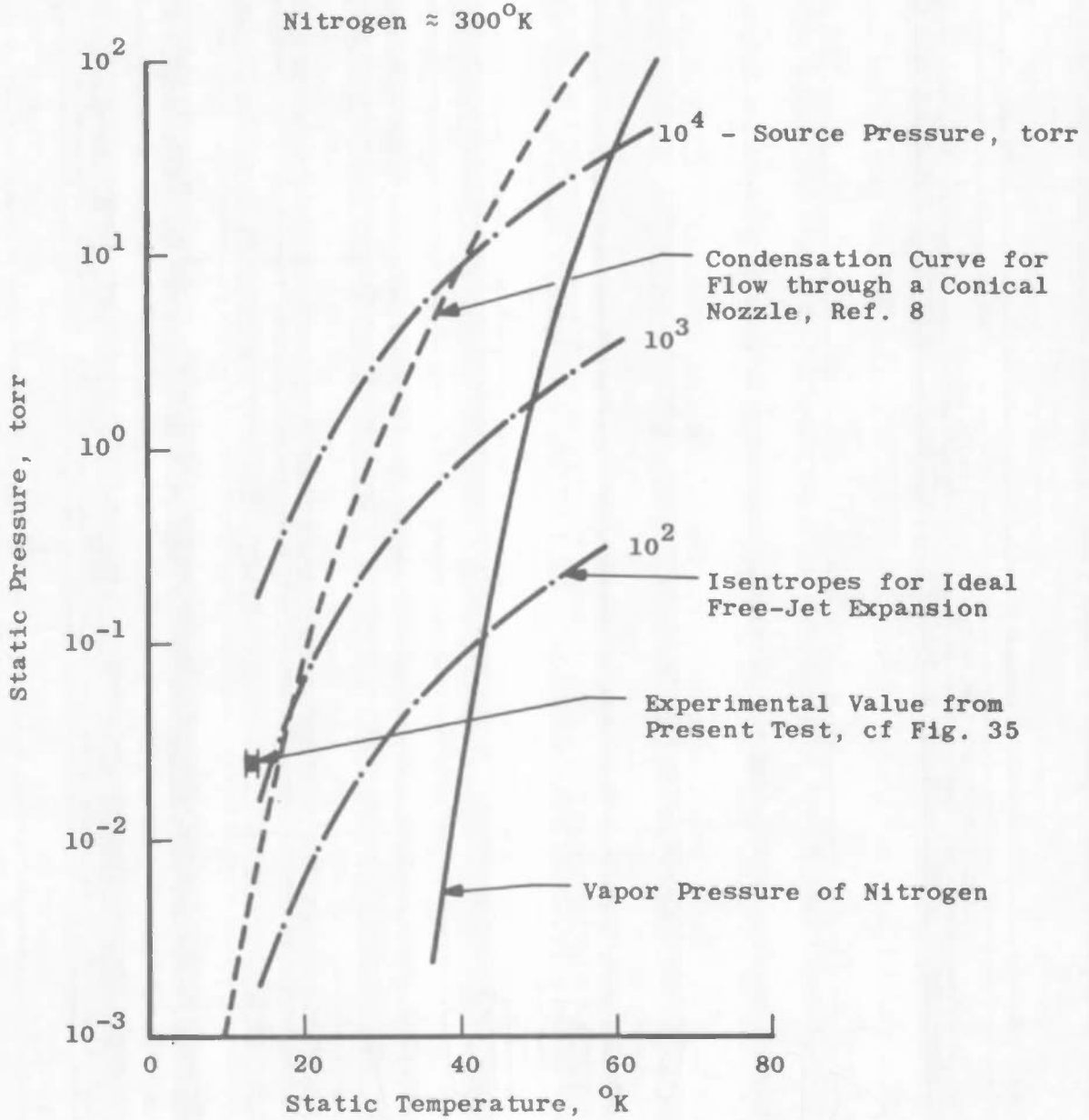

Fig. 36 Condensation in Expanding Flows

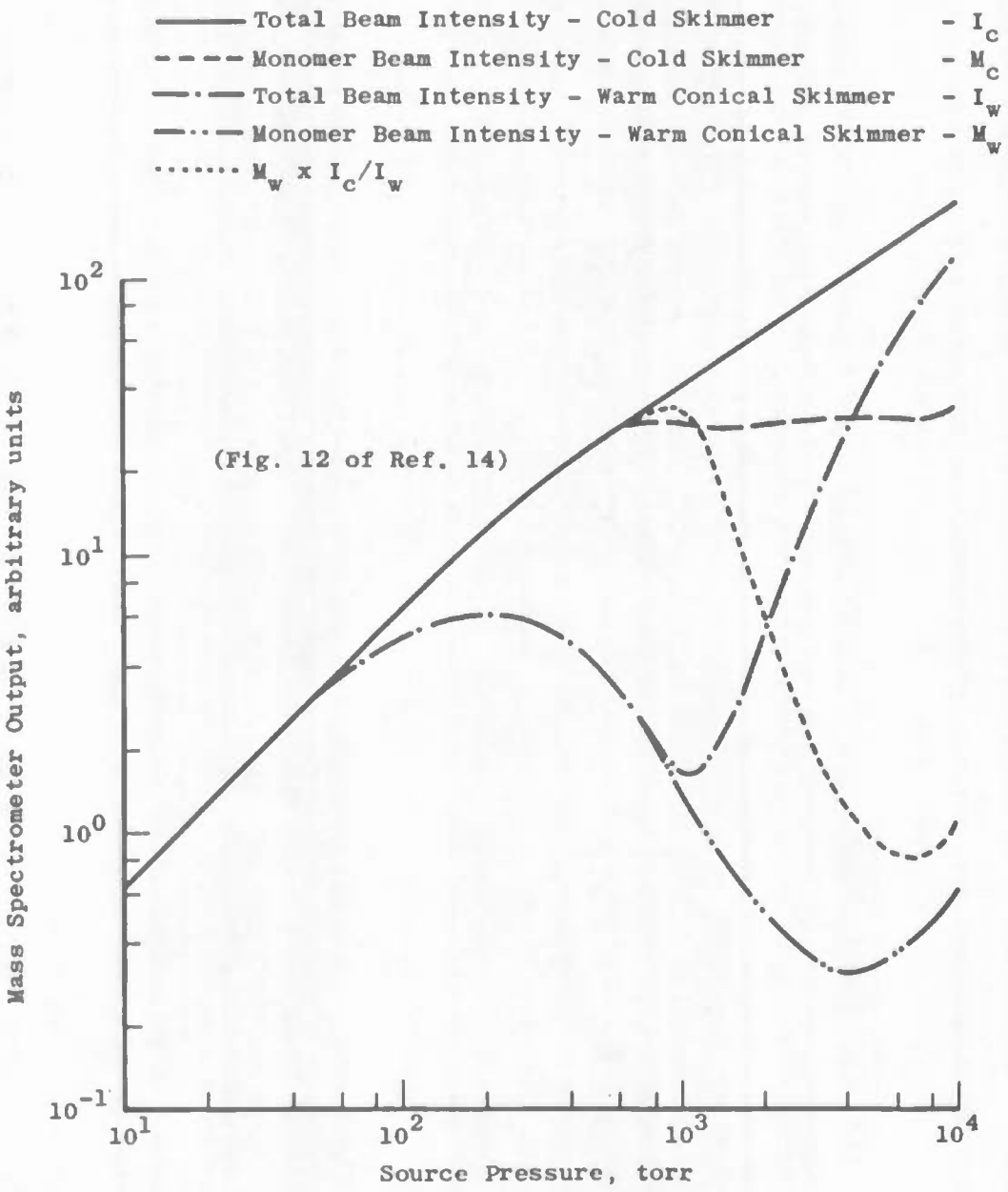

Fig. 37 Effect of Skimmer Interaction on Total and Monomen Beam Intensity

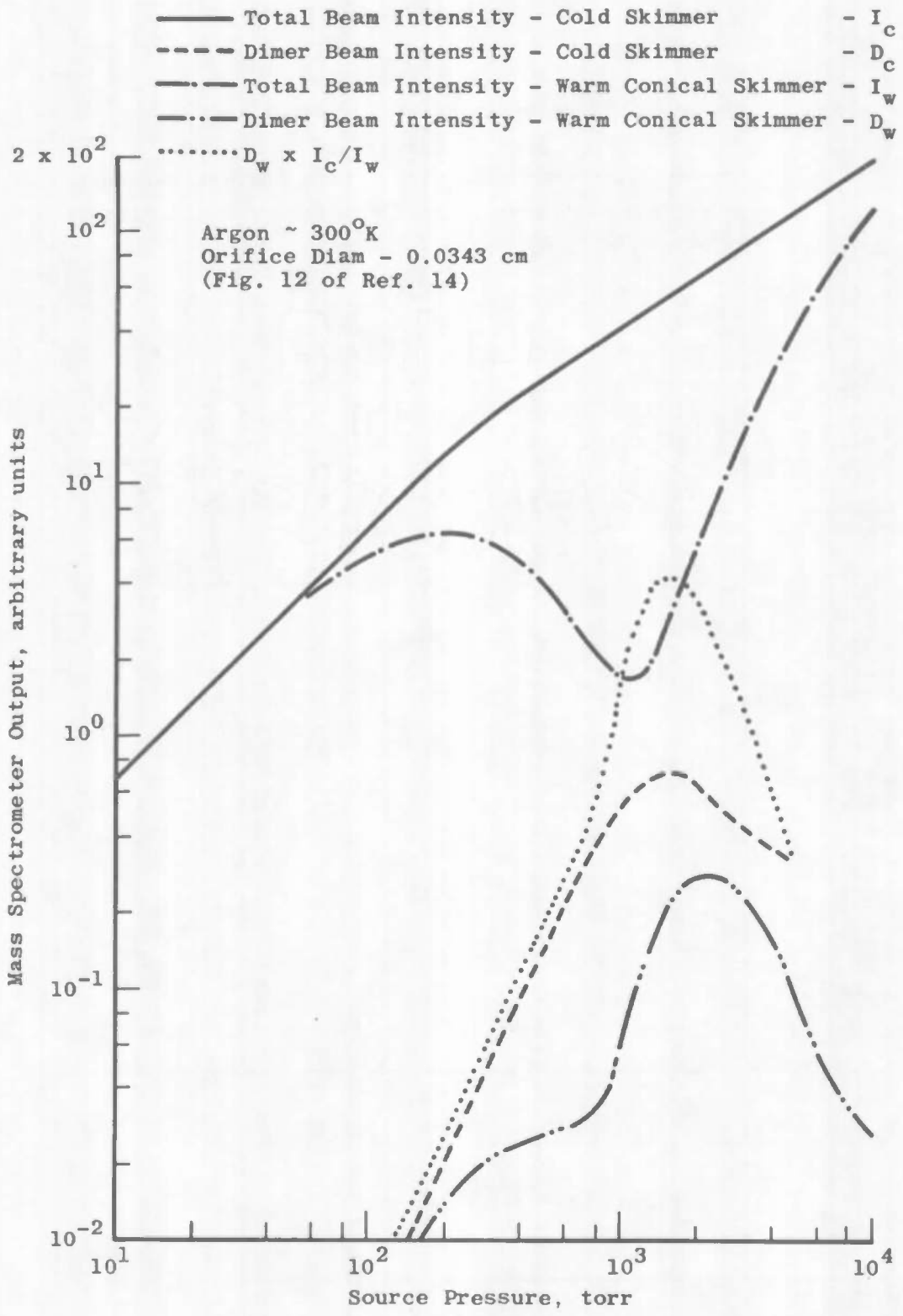

Fig. 38 Effect of Skimmer Interaction on Total and Dimer Beam Intensity

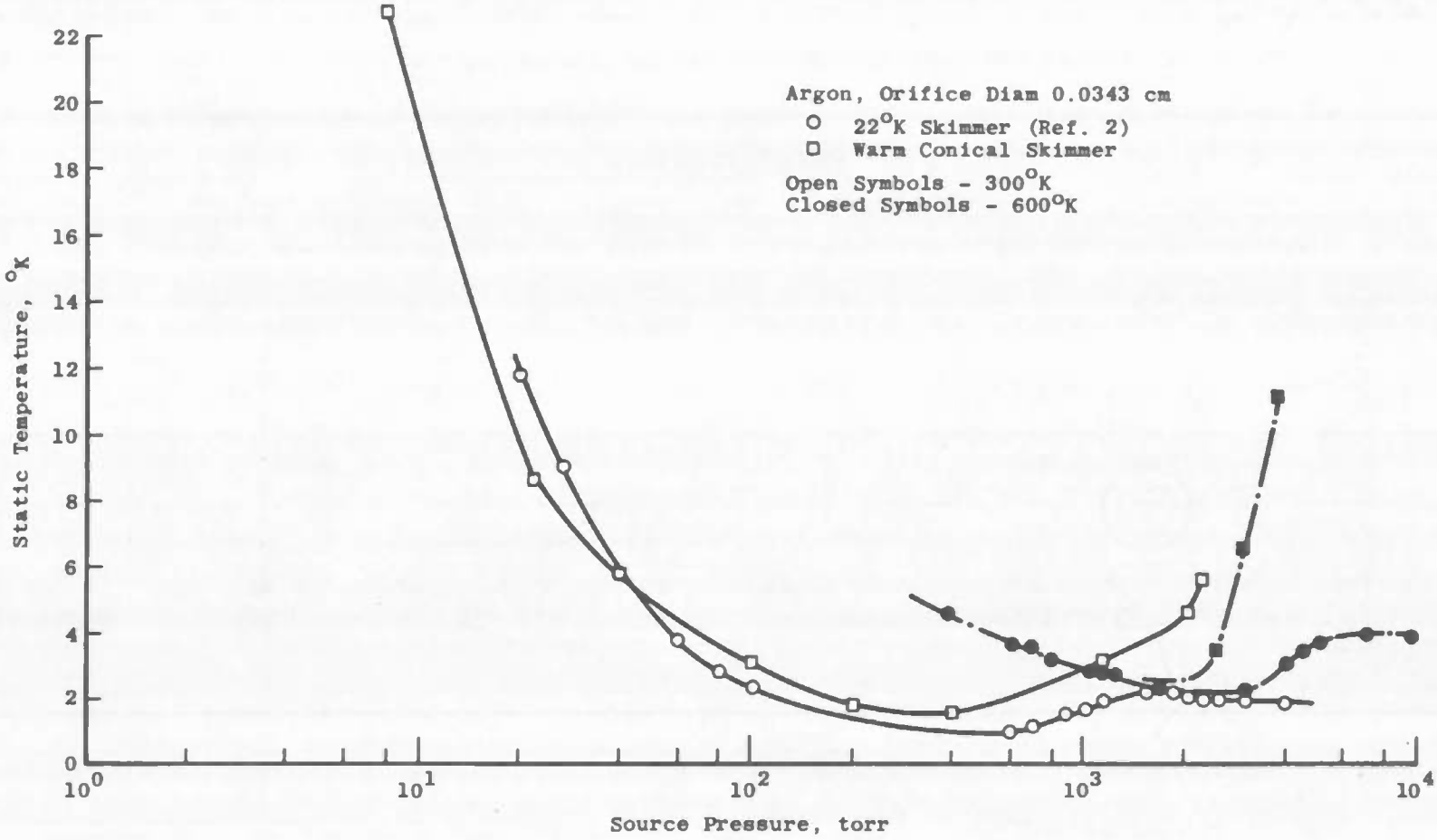

Fig. 39 Static Temperature as a Function of Source Pressure

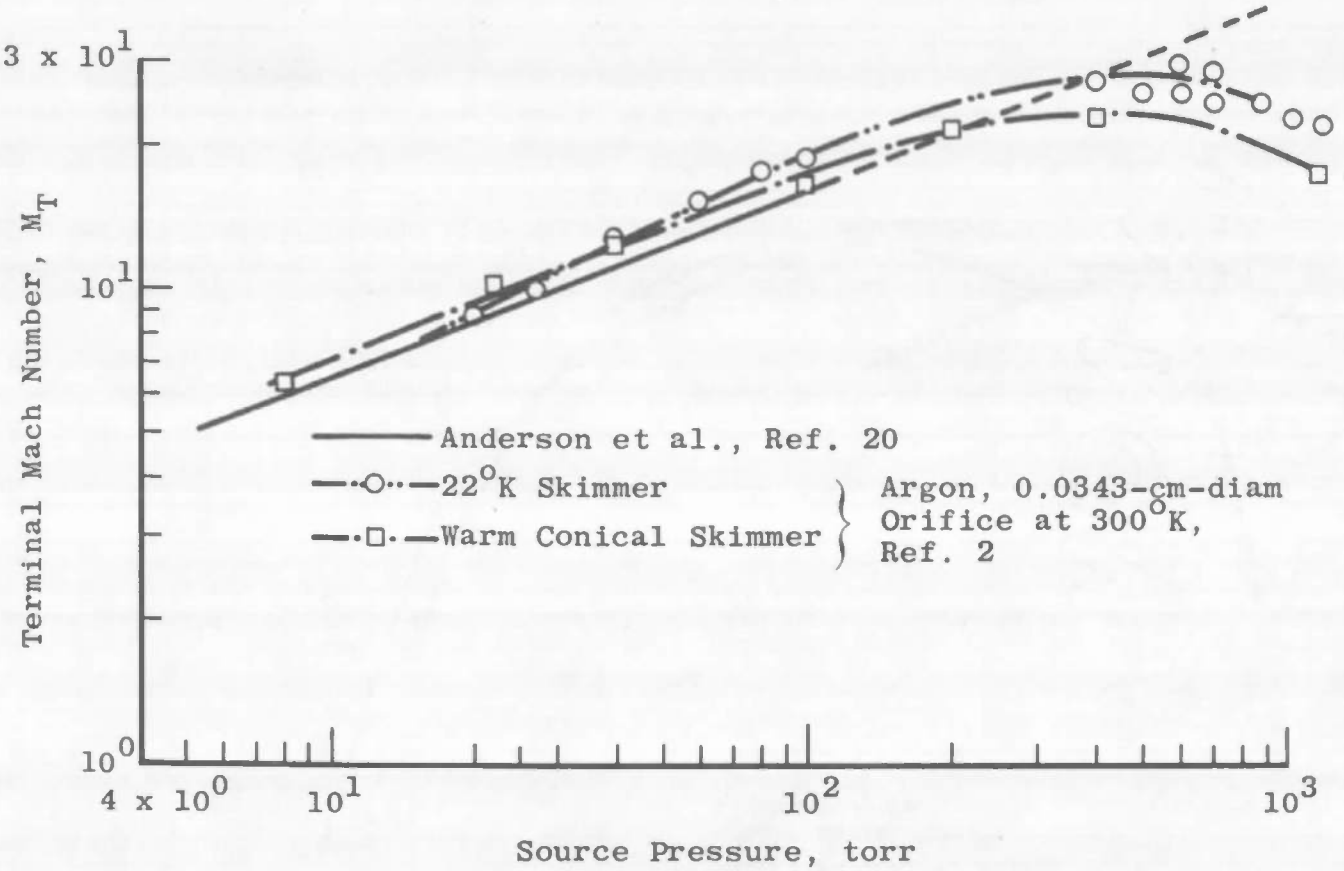

Fig. 40 Terminal Mach Number as a Function of Source Pressure

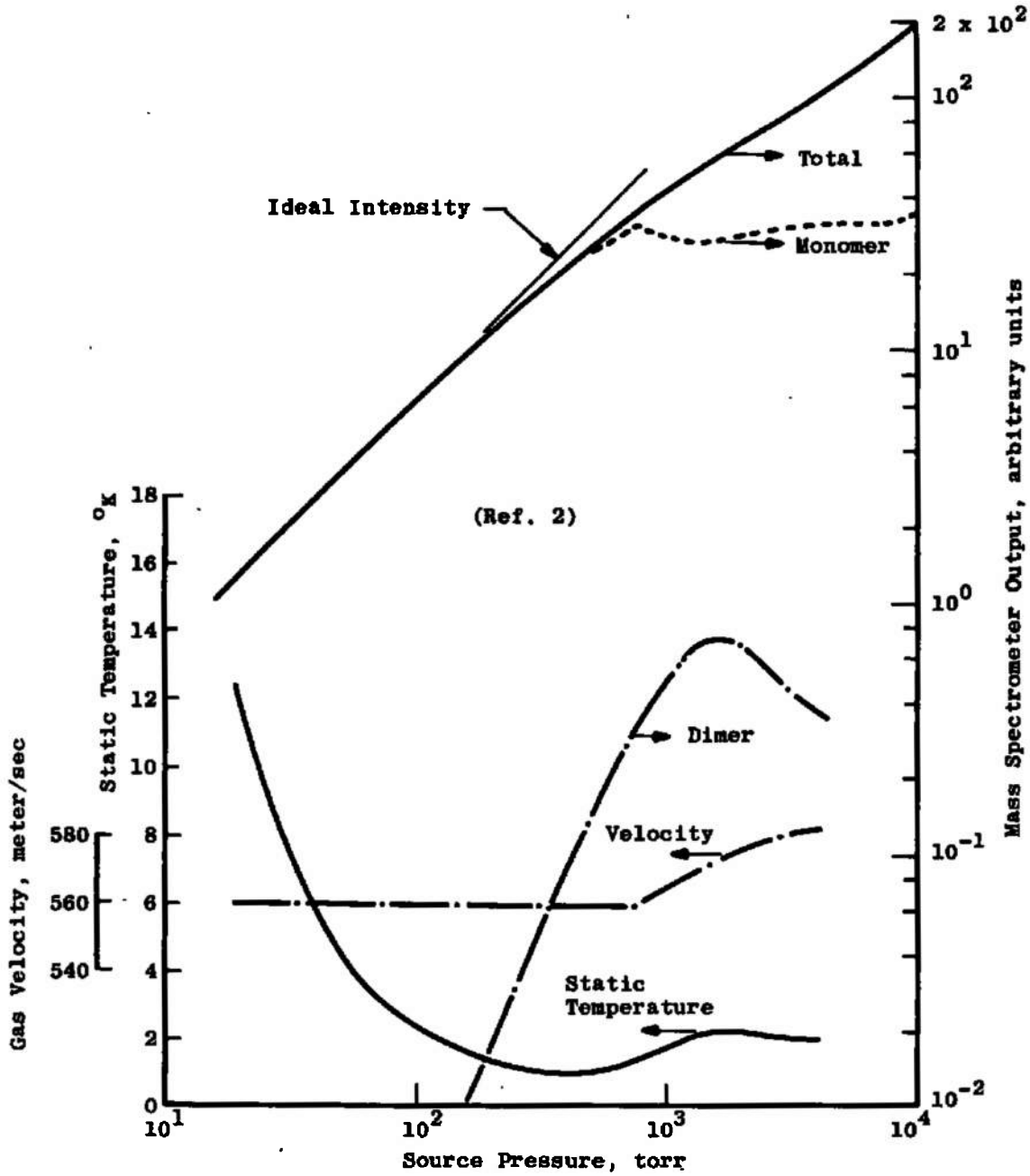

a. Argon, 0.0343-cm-Diam Orifice, 22°K Skimmer, Source Temperature ~ 300°K

Fig. 41 Comparison of the Experimental Measurements

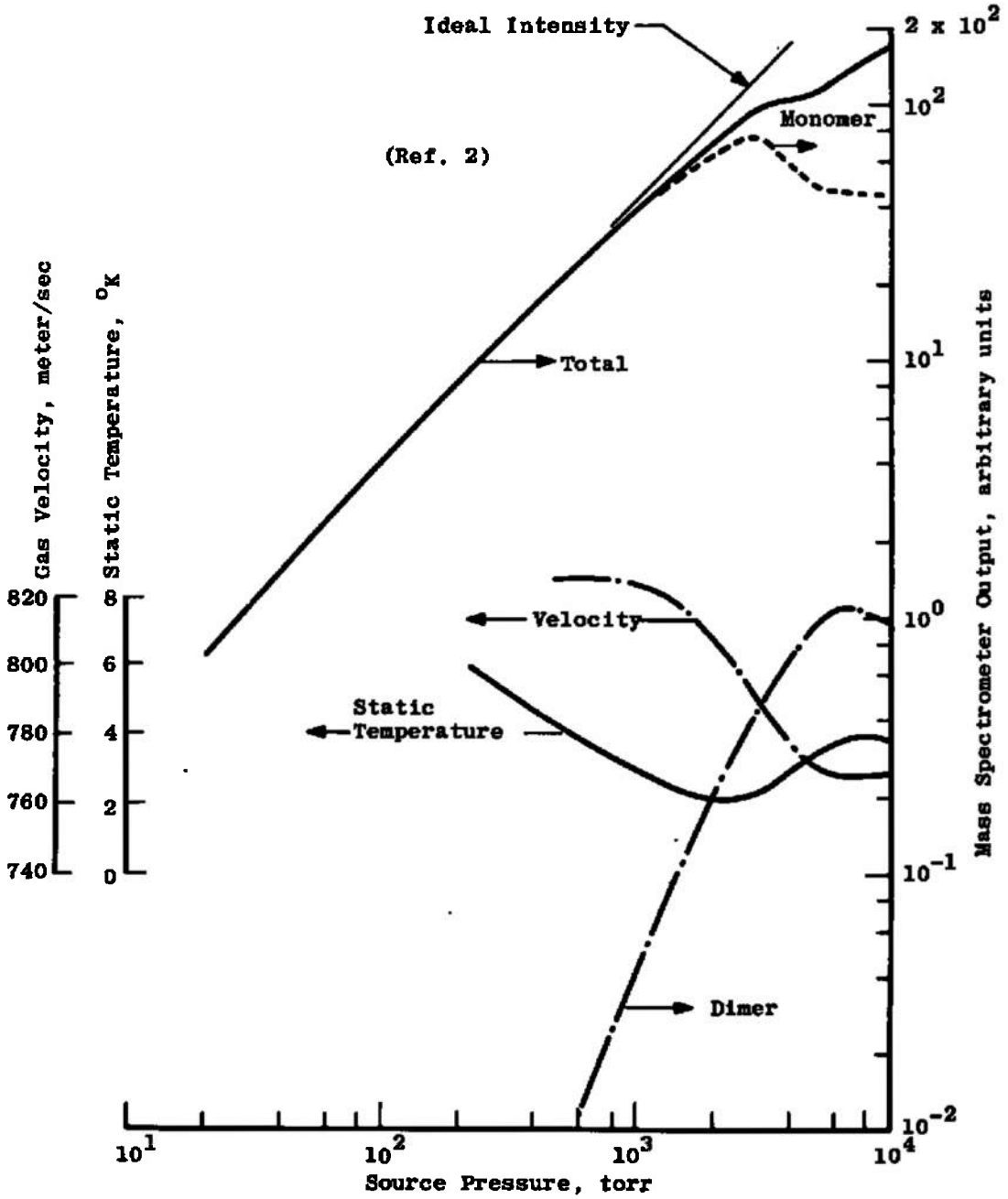

b. Argon, 0.0343-cm-Diam Orifice, 22°K Skimmer, Source Temperature ~ 600°K
Fig. 41 Concluded

UNCLASSIFIED

Security Classification

DOCUMENT CONTROL DATA - R & D

(Security classification of title, body of abstract and indexing annotation must be entered when the overall report is classified)

1. ORIGINATING ACTIVITY (Corporate author)	2a. REPORT SECURITY CLASSIFICATION
Arnold Engineering Development Center Arnold Air Force Station, Tennessee	UNCLASSIFIED
	2b. GROUP N/A

3. REPORT TITLE

CLUSTER FORMATION IN FREE-JET EXPANSIONS

4. DESCRIPTIVE NOTES (Type of report and inclusive dates)

April 1970 to April 1971 - Final Report

5. AUTHOR(S) (First name, middle initial, last name)

A. B. Bailey, M. R. Busby, and R. Dawbarn, ARO, Inc.

6. REPORT DATE	7a. TOTAL NO. OF PAGES	7b. NO. OF REFS
April 1972	127	20

8a. CONTRACT OR GRANT NO.	9a. ORIGINATOR'S REPORT NUMBER(S)
b. PROJECT NO	AEDC-TR-72-32
c. Program Element 62101F	9b. OTHER REPORT NO(S) (Any other numbers that may be assigned this report)
d.	ARO-VKF-TR-71-233

10. DISTRIBUTION STATEMENT

Approved for public release; distribution unlimited.

11 SUPPLEMENTARY NOTES	12 SPONSORING MILITARY ACTIVITY
Available in DDC	AFCRL, AFSC Bedford, Massachusetts 01731

13 ABSTRACT An aerodynamic molecular beam has been used in an attempt to develop criteria for the determination of the onset of condensation in free-jet expansions of various gases. Measurements have been made of the total, monomer, dimer, trimer, etc., beam intensity and velocity distribution as a function of source pressure for the following conditions: (1) sonic orifice diameters of 0.0147, 0.0386, and 0.1245 cm. (2) 15-deg semiangle conical nozzle with a 0.111-cm-diam throat, (3) source temperatures from 185 to 430°K, (4) source pressures ranging from 5 to 10,000 torr, (5) argon, nitrogen, nitric oxide, sulphur dioxide, carbon dioxide, and krypton, and (6) 22°K skimmer and collimator surfaces. The total and monomer beam intensities increased almost linearly with increasing source pressure up to a particular pressure. At this point the two beam intensities ceased to vary at the same rate. The pressure at which this occurred varied systematically with source temperature, pressure, and diameter according to the relation pd/T^2 = constant. For argon and nitrogen flows through sonic orifices, pd/T^2 equaled 1.7×10^{-4} and 3.6×10^{-4} torr-cm $(°K)^{-2}$, respectively.

DD FORM 1 NOV 65 1473

UNCLASSIFIED

Security Classification

14. KEY WORDS	LINK A		LINK B		LINK C	
	ROLE	WT	ROLE	WT	ROLE	WT
clump						
formations						
expansion (free-jet)						
aerodynamic						
molecular beam						
condensation						
gases						